Development of a mimotope-based synthetic peptide vaccine against HIV using plant viruses
by Uraiwan Intamaso

A dissertation submitted in partial fulfillment of the requirement for the degree of Doctor of Philosophy in Microbiology
Montana State University
© Copyright by Uraiwan Intamaso (2003)

Abstract:
Efforts to develop an HIV vaccine have been hindered by difficulties in identifying epitopes capable of inducing a broad neutralizing antibody response due to the high mutation rate and complex structure of HIV envelope glycoprotein. However, the CD4 binding site of gp120 exhibits a high degree of conservation, so epitopes at this site could potentially be used as a vaccine to induce a broad neutralizing antibody response. A random peptide phage display library was screened using monoclonal antibodies directed this site, to identify antigenic and immunogenic mimics of such epitopes of gp120. Peptides corresponding to the selected sequences plus a C-terminal cysteine were synthesized and coupled to carriers, such as the plant viruses CCMV and CPMV using heterobifunctional linkers. When these linkers were used with CCMV, low yields of conjugates and viral aggregation were obtained due to the many active lysine residues on the viral surface and the presence of excess linker. These problems were overcome by making a virus mutant with a single cysteine residue exposed on the surface of each capsid subunit (CCMV S130C). This cysteine was coupled to the peptides using a homobifunctional linkers. The peptides coupled to viral carriers and to KLH were used to immunize mice. Sera were tested for specific anti-peptide antibodies. All carrier-peptide conjugates induced anti-peptide antibodies. The amount of peptides attached to the carriers was not the only factor determining the anti-peptide antibody titers. All conjugates used were immunogenic when injected with adjuvant. However, when injected without adjuvant, CCMV S130C conjugate induced low anti-carrier antibody titers and no anti-peptide antibody titers, while KLH conjugates induced high anti-carrier antibody titers and low anti-peptide antibody titers. Anti-gp120 antibody titers were detected in sera from mice immunized with the virus-peptide conjugates but not in mice immunized with virus alone. However, sera from mice immunized with irrelevant peptide conjugates showed some anti-gp120 cross-reactivity. None of the sera showed binding to gp120 on HIV-infected cells or neutralizing activity. These results indicated that the peptides acted as antigenic mimics when screened but lost their mimicry when coupled to carriers.

DEVELOPMENT OF A MIMOTOPE-BASED SYNTHETIC PEPTIDE VACCINE AGAINST HIV USING PLANT VIRUSES

By

Uraiwan Intamaso

A dissertation submitted in partial fulfillment
of the requirement for the degree

of

Doctor of Philosophy

in

Microbiology

MONTANA STATE UNIVERSITY
Bozeman, Montana

May 2003

D378
In88

APPROVAL

of a dissertation submitted by

Uraiwan Intamaso

This dissertation has been read by each member of the dissertation committee and has been found to be satisfactory regarding content, English usage, format, citations, bibliographic style, and consistency, and is ready for submission to the College of Graduate Studies

Dr. Martin Teintze _____ 5/27/03
(Signature) Date

Approved for the Department of Microbiology

Dr.Tim Ford _____ 5/28/03
(Signature) Date

Approved for the College of Graduate Studies

Dr. Bruce McLeod Bruce R. McLeod 6-3-03
(Signature) Date

STATEMENT OF PERMISSION TO USE

In presenting this dissertation in partial fulfillment of the requirements for a doctoral degree at Montana State University, I agree that the Library shall make it available to borrowers under rules of the Library. I further agree that copying of this dissertation is allowable only for scholarly purposes, consistent with "fair use" as prescribed in the U.S. Copyright Law. Requests for extensive copying or reproduction of this dissertation should be referred to Bell & Howell Information and Learning, 300 North Zeeb Road, Ann Arbor, Michigan 48106, to whom I have granted "the exclusive right to reproduce and distribute my dissertation in and from microfilm along with the non-exclusive right to reproduce and distribute my abstract in any format in whole or in part."

Signature Uraiwan Intamaso

Date 6/2/04

ACKNOWLEDGMENTS

I would like to thank Dr. Martin Teintze who has been very invaluable to me. Not only with the research but also he has given me with the advice in the way of life. Thus only "thank you" doesn't express my gratitude to him. As a foreign student who has problems in English communication he has been very patient with me and helped me feel more comfortable speaking English. Moreover he also widened my attitude about understanding people who are different from me in terms of culture, religion and etc. I won't leave my good memories about him here but will bring them back with me forever. I would like to thank Dr. Seth Pincus who helped me understand that I can study English along with Science. Thus, I learned English any way I could and made me more comfortable with English. Moreover, thanks for his kindness and sincerity for helping me in research. Also, I would like thank Dr. Mark Young who gave me a chance to learn techniques in his lab which inspired me to learn more about viruses. I would like to thank Dr. Royce Wilkinson for his help with instrumentation. I also thank Wan for helping with some experiments and personal things. I would like to thank friends in Thailand who have never left me alone here, especially Dr. Siritida Porntosapon, Nong and Pom. Finally, I would like to thank my parents for their unconditional love and patience, most of all, for their confidence in their daughter and let me do what I really want to do.

TABLE OF CONTENTS

1. INTRODUCTION AND REVIEW OF HIV 1

Introduction 1
AIDS 2
Genetic Diversity 3
Superinfection 4
Viral Entry 5
Synthesis and Assembly of Envelope Glycoproteins 6
The Structure of Gp120 Glycoprotein 7
CD4-Binding Site 10
Coreceptor Binding Site 10
The Immnue Response to HIV in Infected Individuals 11
Cell-Mediated Immune Response 12
Humoral Immune Response 13
Gp120 Glycoprotein as an Antigen and Immunogen 14
Subunit Vaccine Strategies to Block Viral Entry 16
Recombinant Proteins 16
Peptide Vaccines 18
The Prime-Boost Strategy 19
The Structural Differences between Primary Isolates and TCLA 20
Statement of Problem 22

2. PEPTIDE-CARRIER CONJUGATES 25

Introduction 25
Cowpea Chlorotic Mottle Virus (CCMV) 26
Cowpea Mosaic Virus (CPMV) 30
Expression of CCMV Capsids in *Pichia Pastoris* 31
Conjugation of Peptides to Carrier Proteins 34
Crosslinking Reagents 36
Bismaleimidohexane (BMH) 38
N-Succinimidyl 3-(2-Pyridyldithio) Propionate (SPDP) 39
Sulfosuccinimidyl 4-(*N* Maleimidomethy) Cyclohexane-1-Carboxylate (Sulfo-SMCC) 40

3. MATERIALS AND METHODS 41

In Vitro Site Directed Mutagenesis 41
Insertion of the Gp120 Loops into the CCMV Coat Protein 43

Insertion of Gp120 Residues 419-444 into the CCMV Coat Protein 44
Insertion into the Yeast Vector pPICZA 45
In Vitro RNA Transcription of CCMV cDNA
and Plant Inoculation 46
RNA Isolation 48
DNA Sequencing 48
Electron Microscope 49
Reverse Transcription-Polymerase Chain Reaction
Amplification 49
Preparation of *Pichia* for Electroporation 50
Electroporation 51
Direct PCR Screening of *Pichia* Clones 52
Small-Scale Expression Screening of Recombinant *Pichia* 52
Medium Scale Expression of Recombinant *Pichia* 53
Extraction of Recombinant Coat Protein from
the Yeast Cell Pellet 54
Dot Blots for Small Scale Expression Screening 55
SDS-PAGE and Western Blot Analysis 56
Enzyme-Linked Immunosorbent Assay (ELISA) 57
Silver Staining 58
Sypro Ruby Staining 59
BCA Protein Assay 59
CCMV-Peptide Conjugates 60
CCMV-SPDP Linker 60
CPMV-SulfoSMCC Linker. 61
S130C K42R BMH Linker 61
KLH or OVA-Conjugate Peptides 62
Peptide Kinetic Assay 63
Immunization of Mice with Conjugates 63
Reverse Phase High Performance Liquid Chromatography (HPLC) 64

4. RESULTS 65

Genetic Manipulation of CCMV Coat Proteins.. 65
CCMV-Peptide Conjugates with SPDP 68
Kinetics of Peptide Reaction with SPDP 72
CPMV-Peptide Conjugates with Sulfo-SMCC 72
Immunogenicity of Peptides in CCMV Conjugate-Immunized Mice 78
Immunogenicity of Peptides in CPMV Conjugate-Immunized Mice 85
Cysteine Mutants of CCMV 92
Expression Screening of CCMV Mutants 96
Coupling the Peptide to Mutant CCMV Using
a Homobifunctional Linker 100
Comparison of Coupling to S130C between 44F.C and 19A.C 104

HPLC Purification of Peptide-Linker Conjugates 104
Immunization of Mice with CCMV S130C-Peptide Conjugates 107
Immunization with KLH-44 and KLH-19 112
Isotyping of Sera from mice Immunized with
CCMV, CPMV, and KLH Conjugates 118
Immunization of Mice Using Conjugates without an Adjuvant 126
Isotyping of Sera from Mice Immunized without an Adjuvant 126
Anti-Gp120 Antibodies 132

5. SUMMARY AND DISCUSSION 146

Summary and Discussion. 146
Future Directions 157

REFERENCES CITED 160

LIST OF FIGURES

Figure		Page
1	Structure of the HIV-1 gp120	9
2.1	Ribbon diagram of the CCMV coat protein subunit	29
2.2	Structure of CCMV virion showing residues changed to Cys on the capsid surface	37
3.1	Schematic of gp120 structure	42
4.1.	Silver stained gel of CCMV-peptide conjugates using SPDP	70
4.2	Western blot analysis of CCMV-44F.C conjugation using SPDP	71
4.3.	Western blot analysis of CCMV-19 A.C conjugation using SPDP	73
4.4.	Peptide kinetics	74
4.5.	Silver stained gel of CPMV-44F.C conjugated using sulfo-SMCC	76
4.6.	Western blot of CPMV-44F.C conjugated using sulfo-SMCC	77
4.7.	Silver stained gel of CPMV-19A.C conjugated using sulfo-SMCC	79
4.8.	Western blot of CPMV-19A.C conjugated using sulfo-SMCC	80
4.9.	Comparison of the amount of peptides coupled to virus coat protein evaluated by ELISA	81
4.10.	Anti-peptide activity of the first bleed sera from CCMV-44F.C immunized mice by ELISA	82

4.11. Anti-peptide activity of the second sera from CCMV-44F.C immunized mice by ELISA....83

4.12 Anti-carrier activity of sera from CCMV-44F.C immunized mice....84

4.13. Anti-peptide activity of the first bleed sera from CCMV-19A.C immunized mice by ELISA....86

4.14 Anti-peptide activity of the second bleed sera from CCMV-19A.C immunized mice by ELISA....87

4.15 Anti-carrier activity of the second bleed sera from CCMV-19A.C immunized mice....88

4.16 Anti-peptide activity of the first bleed sera from CPMV-44F.C immunized mice by ELISA....89

4.17 Anti-peptide activity of the second bleed sera from CPMV-44F.C immunized mice by ELISA....90

4.18 Anti-peptide activity of the first bleed sera from CPMV-19A.C immunized mice by ELISA....91

4.19 Anti-peptide activity of the second bleed sera from CPMV-19A.C immunized mice by ELISA....93

4.20 Anti-carrier activity of sera from CPMV-44F.C immunized mice....94

4.21 Anti-carrier activity of sera from CPMV-19A.C immunized mice....95

4.22 Direct PCR screening of *Pichia* clones....97

4.23 Expression screening by dot blot analysis....98

4.24 Electron micrograph of S130C....99

4.25 Comparison of the amount of peptides coupled to virus mutants evaluated by ELSA....101

4.26 Sypro ruby staining of virus mutant conjugates....102

4.27 Fluorescense intensity of sypro ruby gel staining of S130C-44F.C 103

4.28 Sypro ruby staining of S130C-44F.C and S130C-19A.C conjugates 105

4.29 Reverse-phase HPLC chromatography 106

4.30 MALDI-TOF mass spectroscopy of the HPLC-purified fraction eluted at a retention time of 18 minutes 108

4.31 Sypro ruby staining of S130C-44F.C conjugate after HPLC purification of excess BMH 109

4.32 Anti-peptide activity of the first bleed sera from S130C-44F.C immunized mice by ELISA 110

4.33 Anti-peptide activity of the second bleed sera from S130C-44F.C immunized mice by ELISA 111

4.34 Anti-peptide activity of the first bleed sera from S130C-19A.C immunized mice by ELISA 113

4.35 Anti-peptide activity of the second bleed sera from S130C-19A.C immunized mice by ELISA 114

4.36 Anti-carrier activity of sera from S130C-44F.C immunized mice 115

4.37 Anti-carrier activity of sera from S130C-19A.C immunized mice 116

4.38 Anti-peptide activity of the first bleed sera from KLH-44F.C immunized mice by ELISA 117

4.39 Anti-peptide activity of the second bleed sera from KLH-44F.C immunized mice by ELISA 119

4.40 Anti-carrier activity of sera from KLH-44F.C immunized mice 120

4.41 Anti-peptide activity of the first bleed sera from KLH-19A.C immunized mice by ELISA 121

4.42 Anti-peptide activity of the second bleed sera from KLH-19A.C immunized mice by ELISA 122

4.43 Isotyping determination of IgG in mice immunized with CCMV-44F.C conjugate in the presence CFA..... 123

4.44 Isotyping determination of IgG in mice immunized with KLH-44F.C conjugate in the presence CFA 124

4.45 Isotyping determination of IgG in mice immunized with CPMV-44F.C conjugate in the presence CFA..... 125

4.46 Anti-peptide activity in the third bleed sera from KLH-44F.C immunized mice without CFA 127

4.47 Anti-carrier activity of the third bleed sera from KLH-44F.C immunized mice without CFA 128

4.48 Anti-peptide activity of the third bleed sera from S130C-44F.C immunized mice without CFA..... 129

4.49 Anti-carrier activity of the third bleed sera from S130C-44F.C immunized mice without CFA..... 130

4.50 Isotyping determination of IgG in mice immunized with KLH-44F.C conjugate without CFA..... 131

4.51 Isotyping determination of IgG in mice immunized with S130C-44F.C conjugate without CFA..... 133

4.52 Detection of anti-gp160IIIB antibodies in sera from CPMV-44F.C immunized mice 134

4.53 Detection of anti-gp120 antibodies in sera from CPMV-44F.C immunized mice 135

4.54 Detection of anti-gp160IIIB antibodies in sera from CPMV-19A.C immunized mice 136

4.55 Detection of anti-gp120 antibodies in sera from CPMV-19A.C immunized mice..... 137

4.56 Detection of anti-gp160IIIB antibodies in sera from KLH-44F.C immunized mice..... 138

4.57 Detection of anti-gp120 antibodies in sera from KLH-44F.C immunized mice 139

4.58 Detection of anti-gp160IIIB antibodies in sera from KLH-19A.C immunized mice 140

4.59 Detection of anti-gp120 antibodies in sera from KLH-19A.C immunized mice 141

4.60 Detection of anti-gp120 antibodies in sera from S130C-44F.C immunized mice 143

4.61 Detection of anti-gp120 antibodies in sera from S130C-19A.C immunized mice 144

4.62 Comparison of anti-gp120 antibody level in mice immunized with various virus conjugates 145

ABSTRACT

Efforts to develop an HIV vaccine have been hindered by difficulties in identifying epitopes capable of inducing a broad neutralizing antibody response due to the high mutation rate and complex structure of HIV envelope glycoprotein. However, the CD4 binding site of gp120 exhibits a high degree of conservation, so epitopes at this site could potentially be used as a vaccine to induce a broad neutralizing antibody response. A random peptide phage display library was screened using monoclonal antibodies directed this site, to identify antigenic and immunogenic mimics of such epitopes of gp120. Peptides corresponding to the selected sequences plus a C-terminal cysteine were synthesized and coupled to carriers, such as the plant viruses CCMV and CPMV using heterobifunctional linkers. When these linkers were used with CCMV, low yields of conjugates and viral aggregation were obtained due to the many active lysine residues on the viral surface and the presence of excess linker. These problems were overcome by making a virus mutant with a single cysteine residue exposed on the surface of each capsid subunit (CCMV S130C). This cysteine was coupled to the peptides using a homobifunctional linkers. The peptides coupled to viral carriers and to KLH were used to immunize mice. Sera were tested for specific anti-peptide antibodies. All carrier-peptide conjugates induced anti-peptide antibodies. The amount of peptides attached to the carriers was not the only factor determining the anti-peptide antibody titers. All conjugates used were immunogenic when injected with adjuvant. However, when injected without adjuvant, CCMV S130C conjugate induced low anti-carrier antibody titers and no anti-peptide antibody titers, while KLH conjugates induced high anti-carrier antibody titers and low anti-peptide antibody titers. Anti-gp120 antibody titers were detected in sera from mice immunized with the virus-peptide conjugates but not in mice immunized with virus alone. However, sera from mice immunized with irrelevant peptide conjugates showed some anti-gp120 cross-reactivity. None of the sera showed binding to gp120 on HIV-infected cells or neutralizing activity. These results indicated that the peptides acted as antigenic mimics when screened but lost their mimicry when coupled to carriers.

CHAPTER ONE

INTRODUCTION AND REVIEW OF HIV

Introduction

The human immunodeficiency virus (HIV) is the etiologic agent of acquired immunodeficiency syndrome (AIDS) in humans, which is spreading unabated in many parts of the world. The highest rate of HIV infection is found in sub-Saharan Africa where the lifetime risk of death from AIDS is 40-50% and life expectancy is reduced by up to 30 years (1).

Although the current generation of antiviral drugs has succeeded in fighting against AIDS, most HIV-infected individuals will never benefit from these therapeutic agents due to lack of access and/or the prohibited costs of these drugs. The AIDS epidemic is concentrated in regions of the world where insufficient financial resources prevent access to these drugs. Even in wealthy countries where these therapeutic agents are available, concerns have been raised regarding poor tolerance of the drugs and the long-term toxicity of therapeutic combinations. The ultimate solution for containment of the AIDS epidemic will require the development of a vaccine strategy. Almost all vaccines in use today are based on either a) killed or attenuated virus b) recombinant coat proteins. Neither of these approaches has been successful against HIV. Thus, it seems that the development of a vaccine against HIV will be more difficult than originally anticipated.

AIDS

Acquired immune deficiency syndrome (AIDS) is the syndrome resulting from the destruction of $CD4^+$ lymphocytes by HIV. The course of HIV-1 infection is characterized by a biphasic viremia. Following the dissemination and propagation of HIV-1 in the lymphoid tissues during primary infection, engagement of the host antiviral immune response coincides with a fall in the plasma virus load to a set-point level (2). Uncontrolled viral replication during primary HIV-1 infection initially leads to activation of a marked cell-mediated immune response, which is later accompanied by the development of a humoral immune response (3). Elevated levels of immune markers decline as the disease enters the chronic phase (4). Although the hallmark of HIV-1 infection and AIDS is immunodeficiency resulting from functional and numeric loss of $CD4^+$T lymphocytes, there is a heightened state of systemic immune activation throughout the course of chronic HIV-1 infection (5, 6, 7). The immune activation resulting from the presence of opportunistic infections, other inflammatory stimuli, or the antigenic stimulus of HIV-1 infection itself may provide an immunological environment that actually drives viral replication and disease progression in HIV infected persons (8). Immune activation has been a key theme in therapeutic approaches to the control of HIV replication and elimination of infection. However, the ability of HIV to replicate persistently in infected individuals and avoid immune surveillance has been one of major obstacles to achieving a therapeutic cure for HIV-infected persons (9).

Genetic Diversity

The hallmark of HIV is its extensive genetic diversity. Heterogeneity in nucleic acid sequences is the result of the error-prone viral reverse-transcriptase (RT) enzyme as well as the high rate of virion production. Their heterogeneity allows for quick adaptation of viruses to environmental selection pressures.

HIV can be divided into two types: HIV-1 and HIV-2, which represent independent crossovers of simian retroviruses into humans (10). There are three branches in the phylogenetic tree of HIV-1 sequences, which constitute the M (main), N (new or non-M, non-O), and O (outlier) groups (11). Among these, group M viruses are the variants of HIV-1 responsible for more than 99% of infections worldwide. The M-group viruses have been divided into distinct genetic subtypes or clades, which are defined as groups of viruses that more closely resemble each other than other subtypes, across the whole genome (12). Using this definition, there are currently nine circulating genetic subtypes (A, B, C, D, F, G, H, J, and K) within group M. The viruses originally identified as subtypes E and I are now considered intersubtype recombinants. The prevalence of intersubtype recombination strains is increasing and creates even more HIV-1 antigenic diversity. Several recombinant viruses have now spread epidemically to establish distinct lineages. These are referred to as circulating recombinant forms (CRFs), nine of which have presently been identified (13). CRFs have a designation that includes the letters of the parent genetic subtypes (e.g., CRF01_AE) and in CRFs derived by recombination of more than three subtypes,

the letters are replaced by cpx (complex), e.g., subtypes E and I are now termed CRF01_AE and CRF04_cpx, respectively (12). Currently, strains belonging to the same subtype can differ by up to 20% in their envelope proteins, and differences between subtypes can be up to 35% (14). Moreover, this diversity is continually growing.

Globally, subtypes A and C account for most current infections followed by subtype B and the intersubtype recombinants CRF01_AE and CRF02_AG. Subtype C is currently infecting more people worldwide than any other and is common in Southern Africa and India. Subtype B is dominant in Europe, the Americas and Australia. Subtypes A and D infect large numbers of people in central and eastern Africa. In western Africa, an intersubtype recombinant, CRF02_AG, is the dominant virus type. CRF01_AE (which was previously referred to as subtype E) is the most prevalent virus in southern Asia. As HIV-1 continues to spread globally, the geographical restrictions are increasingly breaking down (11).

Superinfection.

Superinfection occurs when a cell becomes infected by at least two genetically distinct HIV virions, which may be of the same subtype or of different subtypes. HIV may increase its potential evolutionary success through recombination (15). During HIV recombination, the viral transcriptase (RT) enzyme responsible for reverse transcription of RNA into cDNA can switch from one viral RNA template to another, creating a new virion that is a chimera of the

parental virions (i.e. CRF). *In vitro* experiments have demonstrated that HIV-1 undergoes 2-3 recombination events per genome per replication cycle (16). The high rate of recombination allows HIV to evolve due to the introduction of a large number of genetic changes. Such changes can alter cell tropism, envelope serotypes, viral pathogenicity, antiretroviral drug susceptibility, and disease progression.

Viral Entry

HIV, like all retroviruses, is surrounded by an envelope consisting of a host cell lipid bilayer and virus-encoded envelope glycoproteins, organized into spikes on its surface, that are essential for viral entry into target cells. These envelope spikes consist of trimers of the surface glycoprotein (gp120), which contains the binding domains for cellular receptors, attached to trimers of the transmembrane glycoprotein (gp41) that anchor the spike into the viral membrane (17, 18).

To initiate a new infection, nascent particles need to encounter a potential target cell that expresses the appropriate receptor structures. In the case of HIV, these are the CD4 molecule, found principally on T lymphocytes, macrophages and dendritic cells, and certain members of the chemokine receptor family, which are termed coreceptors. Initially, the specific CD4 binding domain of gp120 attaches with high affinity to the N-terminal membrane-distal domain of CD4. Binding to CD4 induces a conformational change that exposes the chemokine

receptor-binding domain of gp120, allowing it to bind the chemokine coreceptor. Following coreceptor binding, a more dramatic conformational change exposes the gp41 portion of the envelope previously buried in the interior of the complex. This transient species, termed prehairpin intermediate, is formed by folding of the N-terminal trimeric coiled coil, leading to the insertion of the N-terminal hydrophobic fusion peptide region into the target membrane. This prehairpin intermediate then collapses to form a six helix-bundle structure in which the C-terminal regions pack into the hydrophobic grooves of the N-terminal coiled-coil trimer in an antiparallel manner. The formation of this "trimer of hairpins" structure brings the viral and cellular membranes into close apposition, allowing them to fuse and causing release of the viral capsid into the cytoplasm (19, 20). Following virus entry, subsequent intracellular events (e.g., nucleocapsid uncoating and reverse transcription) take place, allowing virus replication in acutely infected cells.

Synthesis and Assembly of Envelope Glycoproteins

In the infected cell, the HIV-1 envelope protein is initially produced as an approximately 845- to 870-amino acid precursor in the rough endoplasmic reticulum. Asparagine-linked, high-mannose sugar chains are added to form the gp160 glycoprotein. Gp160 trimers are assembled and subsequently transported into the Golgi apparatus, where cleavage by a cellular protease generates the mature envelope glycoproteins: gp120 and gp41. The gp120 and gp41

glycoproteins are maintained in the assembled trimer by noncovalent, somewhat labile interactions between the gp41 ectodomain and a discontinuous structure composed of NH_2- and COOH-terminal gp120 sequences. When they reach the infected cell surface, gp120 and the ectodomain of gp41 are exposed on budding virus particles, whereas the membrane-spanning anchor and the long cytoplasmic tail of gp41 are inside the cells or virions (21).

Results from electronic microscopy show that mature HIV particles are icosahedral and possess about 72 spikes forming densely arranged knobs on the viral surface. The diameter of each knob is about 14 nm and its height is 9 to 10 nm; the distance from one to another is about 21 to 22 nm (22, 23)

The Structure of Gp120 Glycoprotein

A comparison of gp120 amino acid sequences from different viral origins revealed the existence of five variable regions (V1 to V5) interspersed with five conserved regions (24). Intramolecular disulfide bonds in gp120 result in the formation of the first four variable regions into large, looplike structures that are exposed on the surface of the protein, whereas the conserved regions fold into a central core. The structure of a gp120 core, lacking V1, V2, and V3 and the COOH and NH_2 termini, as well as most of the carbohydrates, and bound to the N-terminal domain of CD4 has been solved by X-ray crystallography (25). The gp120 core forms a globular structure, consisting of 25 β-strands, five α-helices and ten loops. The structure folds to form two domains, an inner and outer

domain, and a "bridging" β-sheet in between the domains (Fig. 1). The domain names reflect the likely orientation of gp120 in the glycoprotein trimer: the inner domain orients to gp41 whereas the outer domain is mostly exposed on the surface of the trimer. The CD4 receptor-binding regions, located in a depression formed at the interface of the outer and inner domains with the bridging sheet, contain residues that are well conserved among primate immunodeficiency viruses. These regions, and also the inner domain surface, are devoid of glycosylation. Although generally well conserved compared to the five variable regions, the gp120 core also shows variability disproportionately on the surface of the outer domain proximal to the V4 and V5 region. Such variability results from the δA, δC, δD and δE surface loops and also from the N-linked glycosylation sites.

Much of the sequence of the core is highly conserved, which is likely a reflection of functional constraints. In contrast, the sequence-variable loop regions appear to be more malleable. Even under the uniform immune pressure within the same infected individual, multiple sequences of the variable loops coexist (26, 27). This indicates that there are several different structural solutions in creating viruses that replicate and resist neutralization optimally. The multiplicity of variable loop structures facilitates the emergence of neutralization-resistant viruses, thus providing greater opportunities for rapid viral adaptation to selective pressure *in vivo*.

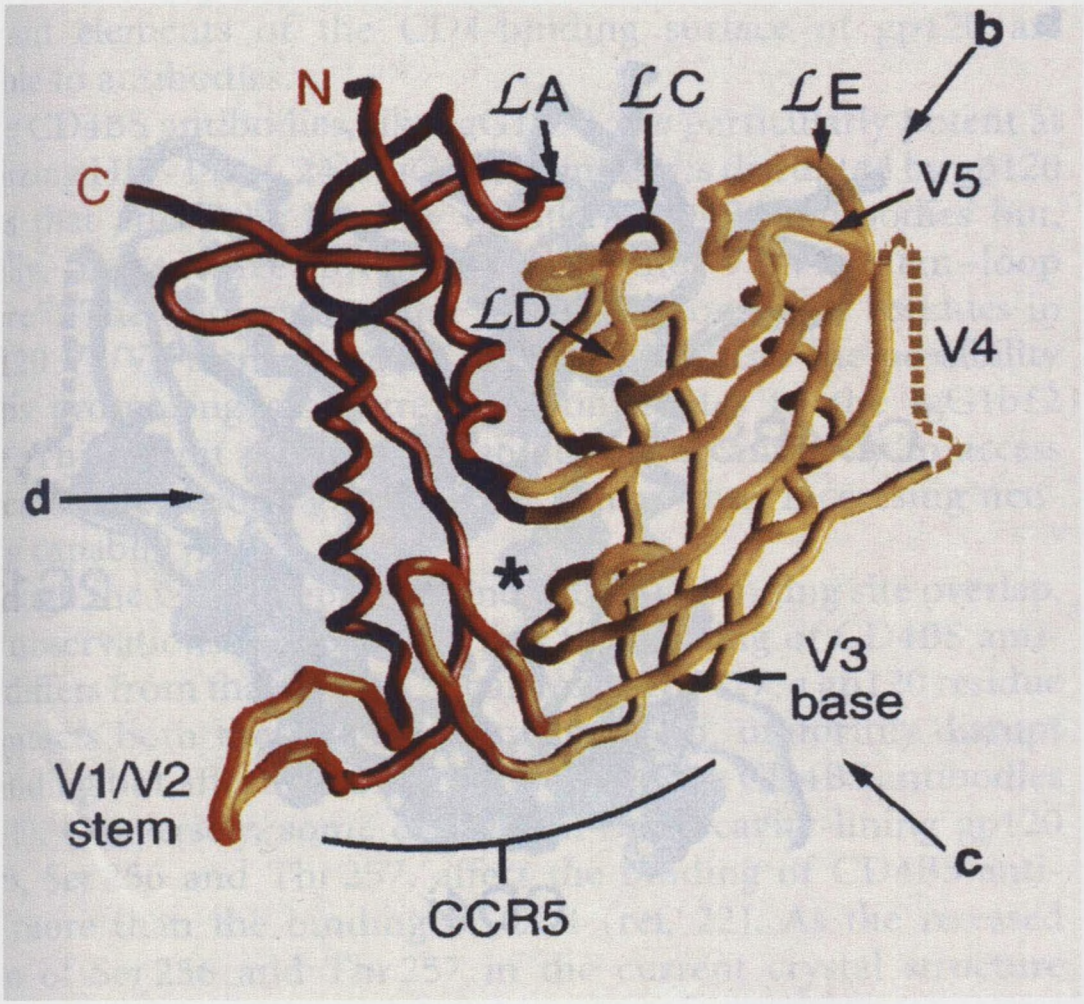


Fig 1. Structure of the HIV-1gp120 core. A Cα tracing of the gp120 core. The inner gp120 domain is shown in red and the outer domain in yellow; the bridging sheet is orange. The position of the Phe43 cavity involved in CD4 binding is indicated by an asterisk. The V4 loop was not resolved in the structure, and the V1/V2 and V3 were shortened in the "core" protein compared to the HIV sequence.

CD4-Binding Site.

CD4 binds in a recessed pocket on gp120, making extensive contact over ~800 $Å^3$ of the gp120 surface. There are two cavities at the gp120-CD4 interface. The larger cavity (about 280 $Å^3$) is shallow and filled with water molecules. It is lined with gp120 residues that do not form many direct contacts with CD4. This hydrophilic cavity is lined with variable gp120 residues. The second cavity (about 150 $Å^3$) is hydrophobic, and deeply buried within gp120. It is located at the interface between the three domains and is lined by highly conserved residues. Most important of these are Asp-368, Glu-370 and Trp-427, which surround the opening of the deep cavity and make contact mainly with Phe-43 and Arg-59 of CD4. These residues are all conserved among primate immunodeficiency viruses. Changes in these residues disrupt gp120 binding to CD4 and to certain monoclonal antibodies with epitopes at the CD4 binding site (25). When CD4 binds, its Phe-43 sidechain blocks the entrance of this cavity (28).

Coreceptor Binding Site.

The conserved region of the coreceptor binding site on gp120 is located at an approximately 90° angle to the CD4 binding site (29) and is comprised principally of the bridging sheet, with an additional part from the base of V2 loop. Importantly, exposure of this site requires that the gp120 first binds to CD4. This induces a conformational change in gp120, which enables it to interact with one of several chemokine receptors. The CC-chemokine receptor CCR5 is the major

coreceptor for macrophage-tropic (R5) strains (30, 31, 32). During the early years of infection, CCR5 is an obligate receptor, and rare individuals that are genetically deficient in CCR5 expression are relatively resistant to HIV-1 (33, 34, 35). HIV-1 isolates arising later in the course of infection often use another chemokine receptor, CXCR4. Using CXCR4, T-cell-line-tropic (X4) viruses play a role in disease progression or propagation in tissue culture (36, 37, 38, 39). Studies of chimeric envelope glycoproteins demonstrated that the V3 loop sequence of gp120 is a major determinant of which the chemokine receptor is used (40).

The Immune Response to HIV in Infected Individuals

One key factor in the rational development of a vaccine against HIV is the characterization of the immune correlates, and delineation of the specific portions of the virus that elicit this response. It has been found that a few individuals remain seronegative despite frequent HIV exposure, and a small population (~5%) of HIV-infected individuals, termed long-term non-progressors, remains asymptomatic for more than 15 years after infection. The study of these people has indicated that they show high levels of non-major histocompatibility complex (MHC)-restricted virus suppressor activity, together with strong polyepitopic cytotoxic T lymphocyte (CTL) responses and broadly reactive neutralizing antibody responses. These immune responses are able to maintain low viral loads, stable CD4+ T cells, and the structure and functional organization of lymph

nodes (41). Both neutralizing antibodies that prevent infectivity, and cytotoxic T-cells (CTL), which eliminate virus-infected cells, are considered important elements for protection against HIV infection.

Cell-Mediated Immune Response.

CTLs are known as killer T cells because they recognize, bind, and kill cells that display foreign antigens. A CTL response is highly desirable in an AIDS vaccine because CTLs can eliminate or reduce virus production by killing viral producing cells. Evidence for this protective role comes from a variety of observations. Early studies demonstrated that CD8+ T lymphocytes from HIV-1 infected individuals could suppress HIV-1 replication in autologous CD4+T lymphocytes *in vitro* (42). A temporal association was identified in HIV-1 infected patients between the appearance of virus-specific CD8+CTL in the peripheral blood and decline of primary viremia in acutely infected patients (43, 44, 45). Moreover, in those chronically infected with HIV-1, a high virus-specific CTL activity is correlated with the maintenance of low virus load and a stable clinical status (46). Since MHC class-I molecules present viral peptide fragments to CTLs, some investigators have reasoned that certain class I molecules may bind and display HIV-1 peptides more efficiently than others (47). In fact, correlations have been demonstrated between certain HLA haplotypes and the rate of clinical disease progression in HIV-1 infected individuals. HLA-B27 and HLA-B57 expression were associated with slow disease progression (48), whereas HLA-

B*3501 and HLA-Cw*04 expression were associated with rapid disease progression (49).

Whereas the CTL responses observed in chronically HIV-1-infected individuals are potent and persistent, they ultimately fail to control virus replication. The virus can escape from CTL recognition through mutation of viral epitopes (50). Furthermore, HIV has evolved mechanisms to downregulate expression of CD4 and class I MHC, cell surface proteins that are essential to CTL recognition of viral antigens on viral producer cells (51). Thus, vaccines that depend strictly on a CTL response may be countered by viral adaptations that allow the virus to evade detection by T cells.

Humoral Immune Response.

Because CTL responses alone are unlikely to provide complete protection, it will be important for an HIV vaccine to also elicit neutralizing antibodies (Abs) to the virus. Such Abs are dependent on memory B cells, a long-lived cell population that can divide and differentiate into Ab-producing plasma cells upon re-exposure to antigens, thus conferring long term protection. Another advantage of Abs is that they have the potential to inactivate the virus before it has a chance to infect the cells of the host. Antibodies may also neutralize virus indirectly by binding complement or promote antibody-directed cell-mediated cytotoxicity (ADCC), thus leading to killing of infected cells. Much of the evidence about the importance of the humoral immune response was obtained from studies in nonhuman primates. Neutralizing monoclonal antibodies (mAbs)

have been shown to confer passive protection to rhesus monkeys against challenge with a highly pathogenic SHIV (a chimeric simian-human immunodeficiency virus that expresses the envelope glycoproteins of a primary HIV-1 isolate) (52). Although it has been possible to generate antibodies against the envelope protein of HIV, such antibodies have had limited efficacy. They neutralize laboratory-adapted strains, but are not effective against primary isolates. Moreover they are often strain-specific. In natural infection, generally, primary peak viremia declines before neutralizing Abs directed against HIV envelope glycoproteins are detectable (53). HIV-infected individuals may generate potent neutralizing Ab responses to their autologous isolates, but such responses take a long time to mature. Thus, by the time such neutralizing Abs are generated, they are no longer able to suppress neutralization-escape mutants that have arisen. To develop immunogens that elicit broadly neutralizing antibodies and CTL's, the extensive genetic diversity among different strains and clades of HIV must be taken into account.

Gp120 Glycoprotein as an Antigen and Immunogen

The success of HIV in achieving persistent infections implies that the viral envelope glycoproteins have evolved to be less than ideal immunogens. The analysis of the structure of core gp120 revealed multiple potential mechanisms of immune evasion. Structures on the viral glycoprotein that are conserved among diverse viral strains are poorly exposed to the humoral immune system. Studies

of monoclonal antibody binding suggested the existence of two faces on gp120: a neutralization face and a non-neutralization face (54, 55). The non-neutralization face is buried within the gp120 trimer, but well exposed at the surface of soluble monomeric gp120. Indeed, this face induces a strong Ab response in infected individuals, but these Abs do not exhibit neutralizing activity. Spontaneous dissociation of gp120 from gp41, or release of gp120 from dying, infected cells therefore results in presentation to B cells of highly antigenic segments of molecule. However, Abs elicited to these regions are irrelevant to neutralization (56) because such Abs cannot bind the assembled, functional envelope glycoprotein complex (57).

The neutralization face induces Abs exhibiting neutralizing activity. However, to escape the Ab response, this face is relatively occluded. To replicate, HIV-1 must interact with the CD4 receptor on target cells; thus, the virus needs to keep the CD4 binding site conserved and exposed enough for receptor binding. However, at the same time, HIV must hide this region from antibodies. The first difficulty for Abs is to access the CD4 binding site recessed within the gp120 core. The Fab of an Ab molecule is wider than CD4: two Ig domains compared to one. In addition, the binding site is flanked by variable and heavily glycosylated regions (28). Since most carbohydrate moieties appear as "self" to the immune system, this may reduce the potential of these regions to serve as an immunogenic target. The large hydrophilic cavity at the CD4 binding site tolerates gp120 mutations, and this may facilitate viral escape from

anti-CD4 binding site Abs. Some of the residues of gp120 contact CD4 through their main-chain atoms. This may allow the variation of these residues to facilitate escape from neutralizing Abs without detrimental effects on CD4 binding. However, some human monoclonal Abs characterized by mutation analysis can recognize discontinuous epitopes at the CD4 binding site, called CD4 binding epitopes (58, 59). This indicates that some broadly neutralizing Abs could access the more recessed elements of the CD4-binding pocket.

Subunit Vaccine Strategies to Block Viral Entry

The exposure of HIV envelope glycoproteins on the surface of the virions makes them prime targets for antibodies that potentially bind to the HIV envelope, thereby blocking interactions between the virus and cellular receptors, and preventing viral entry into the cells. Because protein subunits or peptides are not very immunogenic by themselves, they have to be coupled with a variety of carriers and formulated with adjuvants to increase their immunogenicity.

Recombinant Proteins.

In view of the successful use of a recombinant protein as an immunogen for eliciting protective immunity against hepatitis B virus (60,61), considerable effort has been devoted to developing a recombinant protein vaccine for HIV-1. Such recombinant proteins can be produced by expression of the viral gene encoding envelope glycoproteins in tumor cell lines or insect cells. At least 13 different monomeric gp120 and gp160 candidate vaccines have been evaluated

in prophylactic trials. Initial research focused on gp120, because it was simpler to produce and did not pose any obvious disadvantages over gp160. The first generation vaccines have been safe and immunogenic in diverse populations and have induced neutralizing Abs in almost all recipients. However, the antibodies recognized linear epitopes exposed on denatured gp120 and did not neutralize primary viral isolates (62, 63). In contrast, neutralizing Abs isolated from the serum samples of HIV-infected patients recognize primarily conformation-specific discontinuous epitopes (64). The reason for this is that the native envelope exists as a trimer rather than a monomer and the most immunogenic regions of envelope are hidden on the trimeric, virion-associated form. This observation has led to the hypothesis that viral proteins maintaining a tertiary conformation similar to the native virus may be attractive as vaccine immunogens. Thus, the use of oligomeric forms of gp120 as immunogens is one strategy to improve the quality of the neutralizing Ab response. In order to mimic the quaternary structure of envelope glycoprotein, gp120 and gp41 can be stabilized by an intermolecular disulfide bond (65). However, whether this protein will be superior to existing imunogens still awaits clinical testing.

Because gp120 is heavily glycosylated (>50% carbohydrate by weight), it has been proposed that the removal of carbohydrate moieties on gp120 may expose hidden epitopes and lead to greater immunogenicity and to the production of a better neutralizing Ab response (66). Another way to expose

hidden epitopes is through the removal of variable loops that may be shielding these regions (67).

Another strategy is based on the hypothesis that binding of gp 120 to CD4 might expose otherwise cryptic epitopes, or alter the immunogenicity of extant epitopes on gp120 that could enhance the potential for gp120 to elicit broadly cross-reactive HIV neutralizing Abs. In rhesus macaques, a gp120-CD4 complex, stabilized by covalent crosslinking, elicited Ab responses that neutralize a wide range of primary HIV isolates, regardless of the coreceptor usage or genetic subtype (68).

Peptide Vaccines.

Early exploration of peptide vaccines for preventing HIV-1 infection was based on the supposition that the V3 loop of HIV-1 was the principal neutralizing determinant of the virus and it was demonstrated that this determinant could be mimicked antigenically by synthetic peptides (69). However, it is generally agreed that peptides alone are not suitable for developing vaccines because of their poor immunogenicity. To improve their immunogenicity, peptides are conjugated with carrier proteins, such as bovine serum albumin (BSA) or keyhole limpet hemocyanin (KLH) and then used together with Freund's adjuvant or aluminium hydroxide (alum) adjuvant for immunization in mice or rabbits. An attempt was also made to design multi-epitope vaccines, comprising two or three different neutralizing epitopes for overcoming the problem of sequence diversity among HIV isolates (70).

Recently, prehairpin intermediate, a transient species formed by folding of the N-terminal trimeric coiled coil of gp41, which leads to the insertion of the N-terminal hydrophobic fusion peptide region into the target membrane, has been considered as a potential immunogenic target (71). It may be possible to trap or mimic these conformational epitopes that are transiently expressed after the binding of HIV to CD4 and prior to virus entry and incorporate them into an immunogen. Peptides corresponding to the C-terminal heptad repeat of HIV-1 gp41 (C-peptides) when added exogenously, inhibit HIV-1 entry into cells by binding to the trimeric coiled coil formed in a fusion intermediate by the N-terminal haptad repeat (N-region) of HIV-1 gp41, thereby blocking the formation of the six-helix bundle necessary for fusion between the viral and cellular membrane (72,73,74,75). Similarly, the peptides derived from the N-terminal heptad-repeat region of gp41 (N-peptides) block HIV-1 fusion by binding to the C-helix region of the gp41 intermediate (76, 77, 78) or by intercalating into the N-helix coiled-coil structure (79).

The Prime-Boost Strategy

In the absence of known immune correlates of protection, it would be most prudent to develop a vaccine that stimulates multiple components of the immune system. A combination of long-lived memory T cells, both $CD8^+$ CTLs and $CD4^+$memory helper T cells, will probably be needed for a highly effective HIV

vaccine. At the same time, a strategy to induce broadly neutralizing antibodies will be required for highly effective, long-lasting immunity.

It has been demonstrated that a recombinant protein immunogen, formulated with any available adjuvant, cannot efficiently elicit a CTL response. However, such immunogens may prove useful for eliciting neutralizing Abs and prove efficacious in combination with other vaccine strategies. Viral, bacterial, and DNA vectors induce cell-mediated immunity, whereas recombinant envelope proteins are needed to elicit significant levels of neutralizing Abs. Thus, prime-boost protocols, which consist of priming with a live virus vector (e.g. a recombinant canarypox expressing HIV proteins) followed by boosting with recombinant gp120 (80) are the only immunization schedules today that can elicit both a humoral and a cellular immune response. Moreover, a DNA prime followed by boost with both the DNA and envelope protein could be an effective vaccine strategy.

The Structural Differences between Primary Isolates and TCLA

As described above, subunit vaccines based on soluble monomeric gp120 or gp160 induce Abs that can neutralize only T cell line-adapted (TCLA) isolates but not primary isolates (62, 63). The reason for this is that the most immunogenic regions of the envelope are hidden on the trimeric, virion-associated form. Moreover, certain regions that appear to be well exposed on the envelope trimers of TCLA are poorly exposed on the primary isolates (81). In

particular, two major epitopes present on TCLA virus envelopes, the CD4 binding domain and the V3 loop, are not very accessible. Consequently, most anti-CD4 binding site Abs and anti-V3 loop Abs cannot recognize envelopes from primary isolates efficiently (82). As described above, the gp120 functions in virus entry. In order to bind a receptor, it must expose constant regions; but in order to avoid immune detection, it must hide constant regions. This functional dilemma results in viruses that are optimized differently depending on the selective conditions under which the virus grows. Under the selective pressure encountered *in vivo*, primary isolates tend to obscure epitopes and display high resistance to neutralization. The high level of glycosylation of gp120 and the occlusion by variable loops are also the reasons for the inaccessibility of epitopes on native envelope of primary isolates (83). Replacement of the V1/V2 and V3 variable loops of a TCLA with those of a neutralization-resistant primary isolate creates a virus similar to the parental primary isolate (30, 31). Moreover, the native envelope glycoproteins of primary HIV-1 isolates have weaker antigenicity than those of TCLA isolates, probably due to both a low intrinsic antigencity and a low cell surface expression level (84).

A model based on the gp120 structure has been proposed. The principal features of this model are that gp120 may have two (or more) conformational states and may alternate between them. In the closed conformation, the CD4 binding site is obscured by the V1 and V2 loops and the conserved chemokine receptor binding site is masked by the V3 loop, whereas in the open

conformation these surfaces would be exposed (81). Upon CD4 binding, gp120 may be locked into the open state. It has been speculated that primary isolates may carry a gp120 for which the closed state is more energetically favorable, so the viruses are more resistant to neutralization. On another hand, viral adaptation to cell lines may select for an envelope with a more relaxed conformation, resulting in viruses more sensitive to neutralization.

Statement of Problem

The development of an HIV vaccine has proven an enormous scientific challenge. Because HIV persists indefinitely as a proviral DNA once it has infected cells, it is almost impossible to get rid of the HIV-1 completely by CTL alone. Humoral immune responses may control the virus before HIV-1 gets the chance to enter into the cells. A promising approach for vaccine design, therefore, is targeting HIV-1 entry. Effective strategies that inhibit viral entry are now feasible, because of new understanding of the entry process and the molecular structure and biology of the virus and its cellular receptors. However, in spite of the many attempts that have been made at vaccine development, none have seemed unsuccessful. There are a number of reasons why it has been difficult, but the main reason involves the many adaptations of HIV to avoid and thwart the immune system. Indeed, simply generating Abs is no challenge. Rather, the difficulty lies in the identification of immunogens that stimulate the production of broadly neutralizing Abs. Currently, envelope glycoproteins are the

prime target because they are located on the viral surface and exposed to the immune system. However, they are not ideal immunogens because of their low immunogenicity. Moreover, HIV-1 obscures its conserved neutralizing epitopes by many mechanisms: a recessed conserved CD4 binding site, shielding by variable loops and carbohydrate, and a favorable closed conformation. The fact is, that some patients do make Abs to CD4 binding site even though it is "hidden", and therefore it is useful to study such Abs. When mAbs, which were obtained from HIV-infected patients and specifically bound to HIV gp120, were used to screen phages from random peptide phage display library the selected phage sequences could mimic the epitopes on gp120. Thus, the synthetic peptide sequences corresponding to the sequences of selected phages presumably mimic residues of gp120 which interact with the mAbs, and therefore act as "mimotopes". Using these peptides, which represent epitopes specifically bound to a mAb as antigens might elicit antibodies with similar specificity for gp120 as the original antibodies obtained from HIV-patients.

The discontinuous gp120 structures at the receptor-binding sites are a good choice for antigens because they exhibit a relatively high degree of conservation, in keeping with the minimal polymorphism in the host cell receptors. The CD4 binding site constitutes a particularly attractive target. Although it is partially masked, it appears to be accessible to Abs, more than the conserved elements of the chemokine receptor-binding site, which is only transiently exposed upon CD4 binding.

For the project described here, F105 and 5145A, two human monoclonal Abs reacting with a conformationally determined epitope at the CD4 binding site of HIV-1 strains MN, RF, IIIB, and SF2 were used to screen a random peptide phage display library. A group of residues on selected peptides could mimic conserved residues in a conformational epitope at the CD4 binding site on HIV-1 gp120. Such peptides were used as antigens, coupled with a variety of carriers and formulated with adjuvants to increase their immunogenicity. The goal was to elicit Abs that could bind gp120 and act as an immune surveillance to bind HIV-1 and interfere with its binding to CD4, before the virus has had the chance to enter into cells. To get full immune protection, it would be beneficial to use such a peptide vaccine along with a vaccine inducing cell-mediated immunity, but only the former was the object of this study.

CHAPTER TWO

PEPTIDE-CARRIER CONJUGATES

Introduction

HIV prevalence rates are greater in undeveloped and developing countries where the high cost of anti-viral drugs place them far beyond the reach of most people. Consideration of the ideal requisites of any vaccine include not only efficacy in inducing protective immunity, but also safety and low costs. Generally, synthetic peptides are insufficiently immunogenic to serve as vaccines. However, such synthetic peptides become more immunogenic when biochemically or genetically fused to a carrier molecule. Ovalbumin (OVA) and keyhole limpet hemocyanin (KLH) are widely used carrier molecules. Due to their large molecular mass and strong immunogenicity, they can impart immunogenicity to peptides that have been linked to them. Plant and animal viruses have also been developed as epitope-presentation systems. Commonly used carrier molecules are the coat protein of flock house virus (85, 86), tobacco mosaic virus (87,88), potyvirus-like particle (89, 90), potato X virus (91), and alfalfa mosaic virus (92). One approach involves the engineering of virus coat proteins to function as carrier molecules for antigentic peptides and present such immunogenic peptides to the immune system. The use of a plant virus expressing therapeutic proteins offers advantages over animal viruses, such as

increased safety and reduced costs of production. When used to infect their natural hosts, some plant viruses cause the plants to produce relatively large amounts of a desired immunogenic protein that can be easily purified from the plants. This makes plant viruses well suited as transient expression vectors. Moreover, some recombinant plant virus capsid proteins can be expressed in heterologous systems (87, 89, 90) due to their potential to self assemble. Regarding safety issues, plant viruses are not known to induce disease in mammals. For viruses transmitted mainly via mucosal surfaces such as HIV-1 (93) the vaccine should activate the mucosal-associated immunity system if administered orally or intranasally (94, 95). The possibility to carry out an oral delivery of vaccine-expressing plants would be another advantage. However, a limitation of engineering virus coat proteins as carriers is the failure of virus assembly when even moderate-sized peptides are incorporated into the coat protein. Thus, it is desirable to have information regarding the structure of the coat protein to be modified so that sites for insertion can be selected to minimize potential changes in the tertiary structure of the protein.

Cowpea Chlorotic Mottle Virus (CCMV)

CCMV is a member of the bromoviridae family (alpha virus-like superfamily) and bromovirus genus. The virus infects cowpea plants (*Vigna unguiculata* (L.) var. California Blackeye) and some tobacco plants (e.g. *Nicotiana benthamiana*), causing discoloration on the leaves. The CCMV

genome consists of three unique, single-stranded, positive-sense RNA molecules. Replication of CCMV is initiated by translation of monocistronic genomic RNAs 1 and 2, which encode proteins involved in RNA-dependent replication (96). The two gene products encoded by dicistronic genomic RNA 3, the 32 kDa-movement protein (MP) and the 20 kDa-coat protein (CP), are dispensable for replication, but are required for plant infections. The 5'-proximal gene, encoding MP, is translated directly from genomic RNA 3, whereas the 3'-proximal gene encoding CP is translated from a subgenomic RNA 4 that is generated from progeny negative-sense RNA 3 after infection (96). The CCMV RNAs are encapsidated separately into virus particles, all with similar or identical capsid structures (97). RNA 1 and RNA 2 are each packaged into separate capsids. RNA 3 and RNA 4 are co-packaged into a third particle in a 1:1 molar ratio (98). All three virions are required to establish infection of plants.

The viral capsid is composed of 180 chemically identical protein subunits (19,800 Da; 190 amino acids) which form a 286 Å° diameter icosahedral shell with T=3 quasi-symmetry (99, 100, 101). The arrangement of multiple copies of a single gene product arranged with icosahedral symmetry provides a genetically economical way to generate an envelope that can package and transport the viral genome between cells of a susceptible host and between hosts. The structure of CCMV has been determined to 3.3 Å° resolution by X-ray crystallography (102). The quaternary structure displays 32 doughnut-like capsomers consisting of 12 pentamers and 20 hexamers extending above the

protein shell. Each coat protein subunit is comprised of eight strands folded in a canonical antiparallel β-barrel: two apposed β-sheets, each with four antiparallel strands. The connections between two strands on opposite sheets are made by short loops exposed on the outside of the capsid, containing residues 59-65, 98-104, 129-134 and 161-168, respectively (Fig 2.1). If a foreign sequence were successfully incorporated into one of these loops it would result in the formation of chimeric virus particles carrying 180 copies of the peptide per virion. The C-terminal and N-terminal arms of the CP extend in opposite directions away from the β-barrel core. These extensions play a major role in forming the viral quaternary structure by tying subunits together in the whole virion.

The native CCMV virion has divalent metal ions associated with it and has a sedimentation coefficient of 88S in sucrose density gradients. CCMV is stable at pH 5.0 and low ionic strength (i<0.2). Increasing the pH to >7 and maintaining a low ionic strength (i<0.2) induces swelling of the virion by approximately 10% and changes the sedimentation coefficient to 78S. Virions can be disassociated into their coat protein and RNA components by further increasing the pH (>7.4) and ionic strength (i>1.0). However, mutation of an A to a G at position 1484 of RNA 3 (position 134 of RNA 4), which results in a lysine to arginine substitution at position 42 of the coat protein, confers a "salt stable" phenotype. Unlike the wild type virus, the K42R mutant resists disassembly at pH 7.5 and high ionic strength (i>1.0) (103). The wild-type virus can be reassembled into particles by the reverse reaction. At low pH (<5) and moderate ionic strength (i=0.2-1.0), the

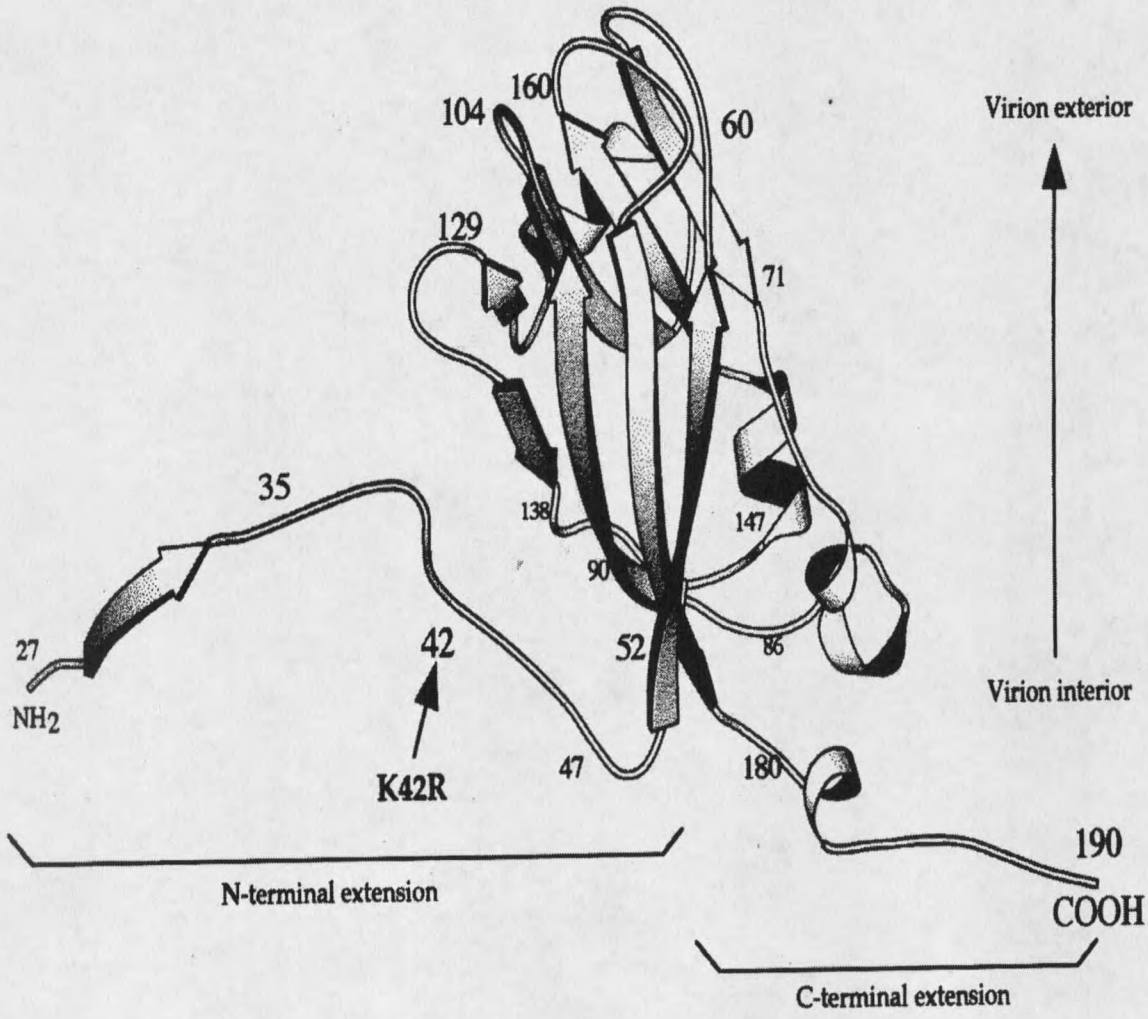


Fig 2.1 Ribbon diagram of the CCMV coat protein subunit. The N-terminal arm contains residues 1-51 (residues 1-27 are not shown). The central, eight-stranded, antiparallel, β-barrel core is formed by amino acid residues 51-179. The C-terminal arm is formed by residues 180-190.

purified coat protein spontaneously reassembles into T=3 particles even in the absence of RNA (empty particles). The CCMV coat protein can recognize its own RNA and assemble to form T=3 RNA-containing virions that are infectious and morphologically indistinguishable from native virions purified from plants (104).

In vaccine production, safety is one of the main concerns. Using viruses containing nucleic acids raises concerns about viral replication in the body. As a carrier molecule, CCMV offers an advantage in circumventing this concern. CCMV coat proteins displaying desired peptides can be expressed in a heterologous system, such as in *Escherichia coli* (97, 104) or yeast (unpublished), and subsequently assembled to form virions devoid of viral RNA under appropriate conditions.

Cowpea Mosaic Virus (CPMV)

CPMV is a member of the comovirus group of plant viruses. The virus infects legumes, such as cowpea (*Vigra unguiculata* var. blackeye). Its genome consists of two separately encapsidated positive-strand RNA molecules of 6.0-kb (RNA1) and 3.5-kb (RNA2). Both RNAs are required for plant infection. RNA 1 encodes the proteins involved in replication, whereas RNA 2 encodes proteins involved in cell-to-cell movement and encapsidation (105).

The structure of CPMV has been solved to atomic resolution (106). CPMV capsids contain 60 copies each of a large (L) and a small (S) coat protein

(CP) arranged with icosahedral symmetry. The large CP is homologous in structure to 2 small CPs that are covalently linked, thus one icosahedral asymmetric unit of the virus is comprised of three anti-parallel β-barrel structures. In total, 180 β-barrel domains comprise the pseudo T=3 structure of CPMV. The strands of the β-barrels are linked with loops of varying size and sequence. Importantly, the BC loop of the S protein is highly exposed on the capsid and shows a high degree of variability when compared in three different comovirues (107). This suggested that foreign sequences could be inserted at this site without abolishing normal virus infection. Thus, the BC loop of the S protein was selected as the insertion site. Plants infected with virus harboring epitope sequences at this site were shown to produce S protein with the antigenic properties of the inserted epitope (108,109,110). So far, more than 50 different CPMV-based chimeras have been produced. In many cases, the presence of the heterologous sequence does not affect the ability of virus to grow in plants, and yields of modified virus are similar to those obtained from plants infected with wild-type CPMV. However, for the genetic stability of chimeras, the size of insert cannot exceed 30 amino acids (109).

Expression of CCMV Capsids in *Pichia pastoris*

Pichia pastoris has been developed as a high-level expression system for recombinant proteins (111). As a eukaryote, *P. pastoris* has many advantages over *E.coli* for expression of eukaryotic proteins, such as protein processing,

protein folding, and posttranslational modification similar to those of higher eukaryotes. Moreover, it is easier, faster, and less expensive than higher eukaryotic expression systems, such as baculovirus-infected insect cells or mammalian tissue culture. As a yeast, it has the advantages of easy molecular and genetic manipulations 10 to 100-fold higher expression levels than metazoan cells. In addition, although yeasts have a majority of their N-linked glycosylations of the high mannose type, the carbohydrate chains in *Pichia* are much shorter than those in *S. cerevisiae,* and therefore more like the glycosylation of mammalian proteins.

P. pastoris is a methylotropic yeast, capable of metabolizing methanol as its sole carbon source. In the first step of this metabolism, methanol is oxidized to formaldehyde and a toxic by-product, hydrogen peroxide, by the alcohol oxidase in the presence of oxygen. To avoid hydrogen peroxide toxicity, this reaction takes place within a specialized cellular organelle, called the peroxisome, which sequesters hydrogen peroxide away from the rest of the cell. Due to the poor affinity for O_2 of alcohol oxidase, *P. pastoris* compensates for this disadvantage by producing a large amount of the enzyme under the control of a highly efficient promoter. Therefore, the promoter regulating the production of alcohol oxidase is the one used to drive heterologous protein expression in *Pichia*. Two genes in *P. pastoris* code for alcohol oxidase: AOX1 and AOX2. The AOX1 gene is responsible for the vast majority of alcohol oxidase in the cell. Under methanol induction, the AOX1 gene is expressed to very high levels,

typically more than 30% of the total protein in cells. In spite of 97% homology to AOX1, AOX2 metabolizes methanol much more slowly than AOX1. If cells lose the AOX1 gene, they lose most of the cell's alcohol oxidase activity. This results in a strain with the methanol utilization slow phenotype (Mut^s). Expression of the AOX1 gene is controlled at the level of transcription. The regulation of the AOX1 gene is a two-step process: a repression/derepression mechanism plus an induction mechanism. To optimize induction with methanol, cells first need to be grown in minimal media containing glycerol (MGY) to derepress transcription, and then subsequently grown in minimal media containing methanol (MM) to induce expression.

Heterologous genes can be introduced into *Pichia* using the pPICZA plasmids (Invitrogen, San Diego, CA). This vector contains a 5'AOX1 region that is homologous to the AOX1 locus in *Pichia*, allowing plasmid integration into chromosomal DNA via homologous recombination. High-level expression in *Pichia* is methanol-inducible under the control of *AOXI* promoter. The vector also contains two additional promoters, *PTEFI* and *PEM7*, driving Zeocin resistance gene expression in *Pichia* and *E.coli*, respectively, thereby allowing Zeocin selection in both organisms (111). Fusion proteins containing a C-terminal histidine tag can be easily purified on a Ni^{2}+ column by affinity chromatography. Moreover, a *myc* epitope preceding the polyhistidine tag permits detection of the fusion protein using anti-*myc* antibodies. Integration can only occur at the AOX1 locus. Vector linearized within the 5'AOX1 region will integrate by gene insertion

into the host 5' AOX1 region. The *Pichia* strain X-33 used has a Mut+ phenotype and is able to metabolize methanol (111). *Pichia* is capable of integrating multiple copies of transforming DNA via recombination into the genome at sites of sequence homology. The frequency of multi-copy insertion ranges from 1 to 10%, thus, many transformants must be tested for expression in order to select a clone with multiple copies of the gene and therefore a high expression level. Dot blots are used to screen multi-copy integrants using anti-CCMV polyclonal antibodies. Multi-copy integrants should show higher level of protein expression. After selecting the clones with highest expression, a 1 liter-culture is grown to isolate and characterize the desired protein.

Conjugation of Peptides to Carrier Proteins

As mentioned above, peptides are often poor immunogens but can be made highly immunogenic by coupling them to a suitable carrier molecule. All carriers used in the experiments described below were linked to the designated peptides by either a heterobifunctional linker covalently coupling amino groups on lysine sidechains of a carrier to a sulfhydryl group on the cysteine sidechain of a peptide, or a homobifunctional linker coupling between two sulfhydryl groups of cysteine sidechains on a carrier and a peptide, respectively.

Due to its many lysine sidechains (6% by mass) and large size, KLH is one of the most widely used carriers for immunization of laboratory animals. Activated by covalently coupling to sulfo-SMCC at its amino groups, a

commercially available activated KLH (Pierce Chemical Co.) has the sulfhydryl-reactive maleimide on the linker available to covalently couple to cysteine groups on another protein or peptide.

Peptides were linked to CPMV as a carrier using sulfo-SMCC. There is only one reactive lysine sidechain on the outer surface of the viral capsid per large and small subunit pair. Thus the activated virus carries 60 sulfhydryl-reactive maleimide groups on the linkers available for coupling to sulfhydryl groups on another protein or peptide. However, CCMV contains at least 6 lysine residues per coat protein subunit that appear to be accessible to a linker. Coupling the linker to CCMV with so many reactive lysine sidechains on the surface may cause unwanted reactions, such as coupling too many peptides per subunit or viral aggregation. It would be optimal if CCMV contained only one reactive lysine residue per subunit on the surface but it would be laborious to replace so many lysine residues in the CCMV sequence. Thus, rather removing lysine residues, adding a cysteine residue, where there were previously none on CCMV surface, was considered a better option. Due to concerns about viral aggregation, the introduced cysteine should not be too exposed on the surface where it would easily couple to a cysteine from another virus. The cysteine substitution should also not result in two cysteines on adjacent subunits being close enough to cause unwanted coupling between cysteines and loss of a peptide coupling sites. On the other hand, the sites should not be too buried, making them inaccessible to linker. Based on examination of the crystallographic

structure of CCMV, 3 different residues, S73, S130 and A152, were chosen for cysteine substitution by site-directed mutagenesis. When looking at the 32 doughnut-like capsomers, S73 and A152 of each CCMV coat protein subunit are located on the outside, while S130 is on the inside of doughnut shape. The closest distance to the same residue on an adjacent subunit is 20Å°, 15.44Å° and 12.97Å°, for S73, A152, and S130, respectively (Fig 2.2). The mutated CCMVs were all made in the K42R background, and are termed S73C, A152C and S130C, respectively.

Peptides were synthesized chemically corresponding to the sequences of phage selected from a random peptide phage display library using human mAbs F105 and 5145A, which recognize conformation-dependent epitopes at the CD4 binding site of HIVgp120. The synthetic peptides specifically inhibited binding of their corresponding mAbs both to the respective phage and to gp120 (J. Jacobs, unpublised). Presumably these sequences mimic residues of gp120. In order to be able to couple to a carrier with a sulfhydryl-reactive linker, a cysteine residue was added to the sequence of the synthesized peptides at the C-terminal end. This allowed the N-terminus of the attached peptides to be free, as they were on the N-terminal end of the pIII in the phage that had been selected.

Crosslinking Reagents

Crosslinking reagents contain two reactive groups, thereby providing a means of covalently linking two target molecules. In homobifunctional

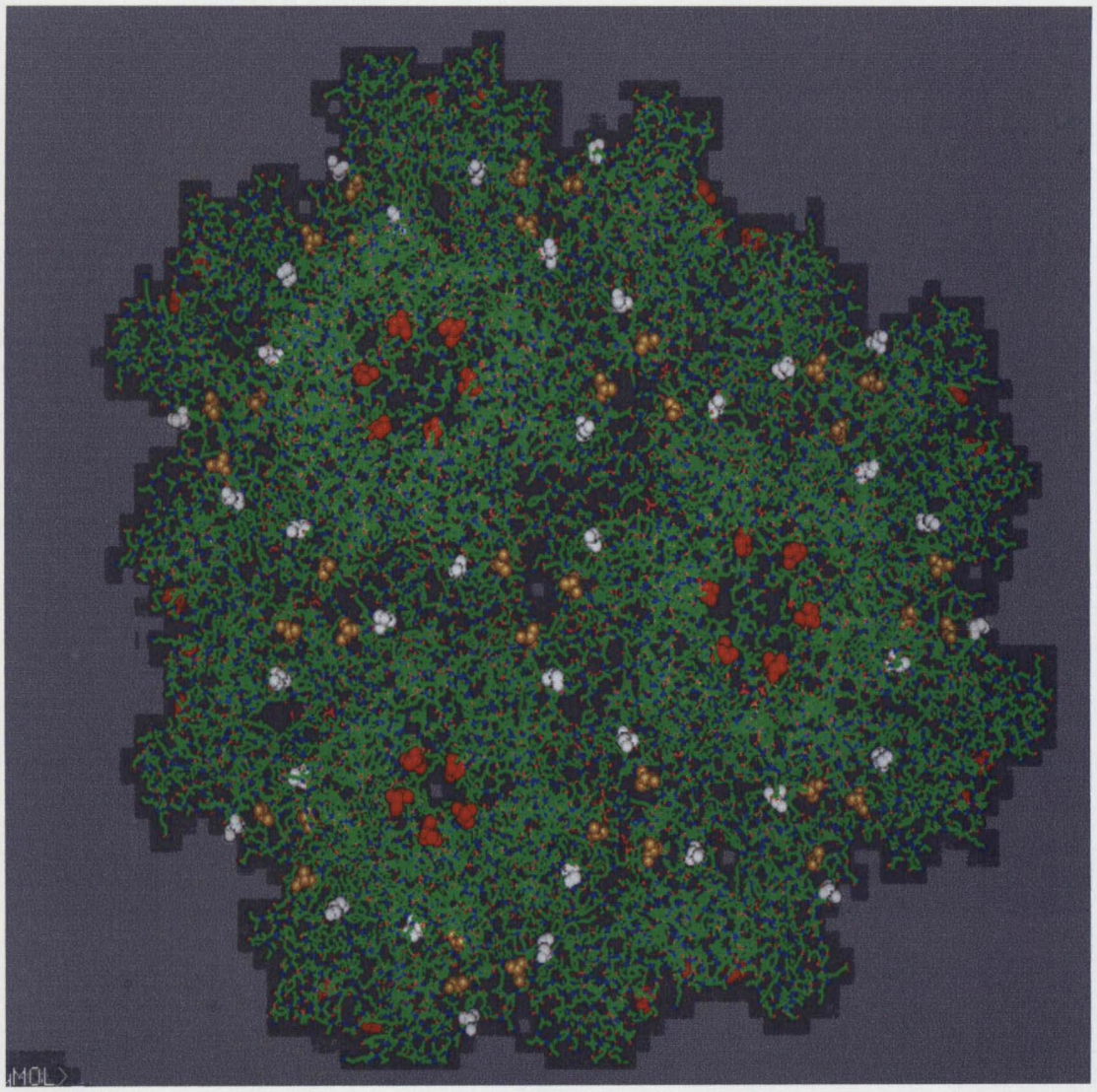


Fig 2.2. Structure of CCMV virion showing residues changed to Cys on the capsid surface: S73 (white), S130 (red), A152 (orange). Two hexamers and one petamer are shown.

crosslinking reagents, the reactive groups are identical, permitting conjugation between the same functional groups. On another hand, heterobifunctional crosslinking reagents contain dissimilar functional groups allowing the formation of crosslinks between unlike functional groups. When either of these crosslinking reagents is used to conjugate two different biomolecules, they may result in high molecular weight aggregates. Thus, the reaction needs to be controlled to optimize the stoichiometry of target molecules.

Bismaleimidohexane (BMH)

BMH is a homobifunctional crosslinker containing two maleimide groups that are selective for thiol (a.k.a. sulfhydryl) groups (-SH), such as those on cysteine residues of target molecules (112). The reaction involves addition of the thiol across the double bond of the maleimide to yield a thioether. The thioether linkage between the maleimide group and the reacted sulfhydryl is very stable and cannot be cleaved under physiological conditions. However, primary amines can react with maleimides and compete in the reaction. To have the maleimide group be more selective for sulfhydryl groups, the pH of the reaction mixture needs to be kept between 6.5 and 7.5. At pH 7, the rate of reaction of a maleimide with sulfhydryls is 1,000-fold faster than with amines ($-NH_2$). Above this pH range, the reaction rate with primary amines becomes more significant. At a pH above 8, maleimides can also be hydrolyzed to a mixture of isomeric nonreactive maleimic acids and this reaction competes significantly with thiol modification (112). A protein containing a sulfhydryl group must have it in a

reduced form to react with the maleimide: if necessary a reducing agent may be added to make sure the sulfhydryl group is reduced. However, BMH will cause virus-virus crosslinks or inter-subunit crosslinks if added in excess, so there is a need to couple to the peptide and purify first prior to coupling to the virus.

N-Succinimidyl 3-(2-Pyridyldithio) Propionate (SPDP)

SPDP is a heterobifunctional, cleavable cross-linker, containing one N-hydroxysuccinimide (NHS) group and one pyridyl disulfide. These functional groups react with primary amines and sulfhydryls, respectively. When conjugating an amine-containing protein with a sulfhydryl-containing peptide using SPDP, the amine-containing protein is first conjugated to the linker via the NHS-ester group. Amide bonds are formed, which are as stable as peptide bonds. The free sulfhydryl-containing peptide is then added to the 2-pyridyl disulfide-activated protein. A sulfhydryl exchange can occur between the peptide's –SH group and the 2-pyridyl-disulfide group. As a result of this reaction, pyridine-2-thione is released and a disulfide crosslink is formed (113). The pyridine-2-thione released after the reaction with free-sulfhydryl peptide can be measured kinetically at 343 nm to determine how well the peptide reacts with SPDP. Disulfide link between SPDP and sulfhydryl-containing peptide can be cleaved under reducing conditions (e.g. in reducing SDS-PAGE) but should be stable in the extracellular oxidizing environment *in vivo*.

Primary amines, such as ε–amino groups on lysine side chains in proteins are the principal targets for NHS-esters. The most significant factor affecting an

amine's activity is its basicity. A pH of 8.5-9.5 is usually optimal for modifying lysine residues. The rate of hydrolysis of an NHS-ester increases with pH and thereby competes with the NHS-ester acylation reaction. Hydrolysis occurs more readily in dilute protein or peptide solutions. In more concentrated solutions, the acylation reaction is favored (113).

Sulfosuccinimidyl4-(N-Maleimidomethy)Cyclohexane-1-Carboxylate(SulfoSMCC)

Sulfo-SMCC is another heterobifunctional linker, consisting of one N-hydroxysuccinimide (NHS) group and a maleimide group. These functional groups react with primary amines and sulfhydryls, respectively. Most often, the NHS reaction is first performed at pH 7-9, and then excess crosslinker is removed. Addition of free-sulfhydryl peptide allows the maleimide to react with the sulfhydryl group. Unlike SPDP, the linkage made by sulfo-SMCC to the sulfhydryl is uncleavable. Thus, addition of dithiothreitol (DTT) or other reducing agents does not cleave the peptide from the carrier protein. The only competing reaction for both the NHS group and the maleimide is hydrolysis. At high pH, maleimides may react with amines, so the reaction needs to be at pH 6.5-7.5 for the maleimide coupling reaction (114).

CHAPTER THREE

MATERIALS AND METHODS

In vitro Site Directed Mutagenesis

To insert a sequence from constant region 4 and variable region 4 (V4C4) of HIVgp120 IIIB into CCMV coat proteins, the complementary mutagenic oligodeoxynucleotides 5' TACAGCAGTGCGGCTCTCACTCGCATAAAGCAGAT AATAAATATGTGGCAGGAGGTGGGCAAGGCGATGTACGCGCCACCGATATC CGGCCAGATACGCGAGGGCGACGTCATC 3' and 5' GATGACGTCGCCCTCG CGTATCTGGCCGGATATCGGTGGCGCGTACATCGCCTTGCCCACCTCCTGC CACATATTTATTATCTGCTTTATGCGAGTGAGAGCCGCACTGCTGTA3', which contain the coding sequence for residues 419 to 444 of gp120: RIKQ FINMWQEVGKAMYAPPISGQIR (Fig 3), were used in conjunction with pCC3 (96). The oligonucleotides also contain CCMV RNA 3 nucleotides 1834-1869 and incorporate an *Eco*RV site (underlined) for screening mutant clones. This construct results in insertion of the gp120 sequence between CCMV coat protein residues 164 and 165. Each oligonucleotide primer (125 ng, 22 nM) anneals to its complementary strand of the denatured plasmid (5-50 ng) and is extended during temperature cycling by means of *Pfu* DNA polymerase (2.5 U) (Stratagene, San Diego, CA). The incorporation of the oligonucleotide primers results in a nicked mutated double stranded plasmid. This product was treated with *Dpn* I (10U) to digest nonmutated methylated and hemimethylated parental

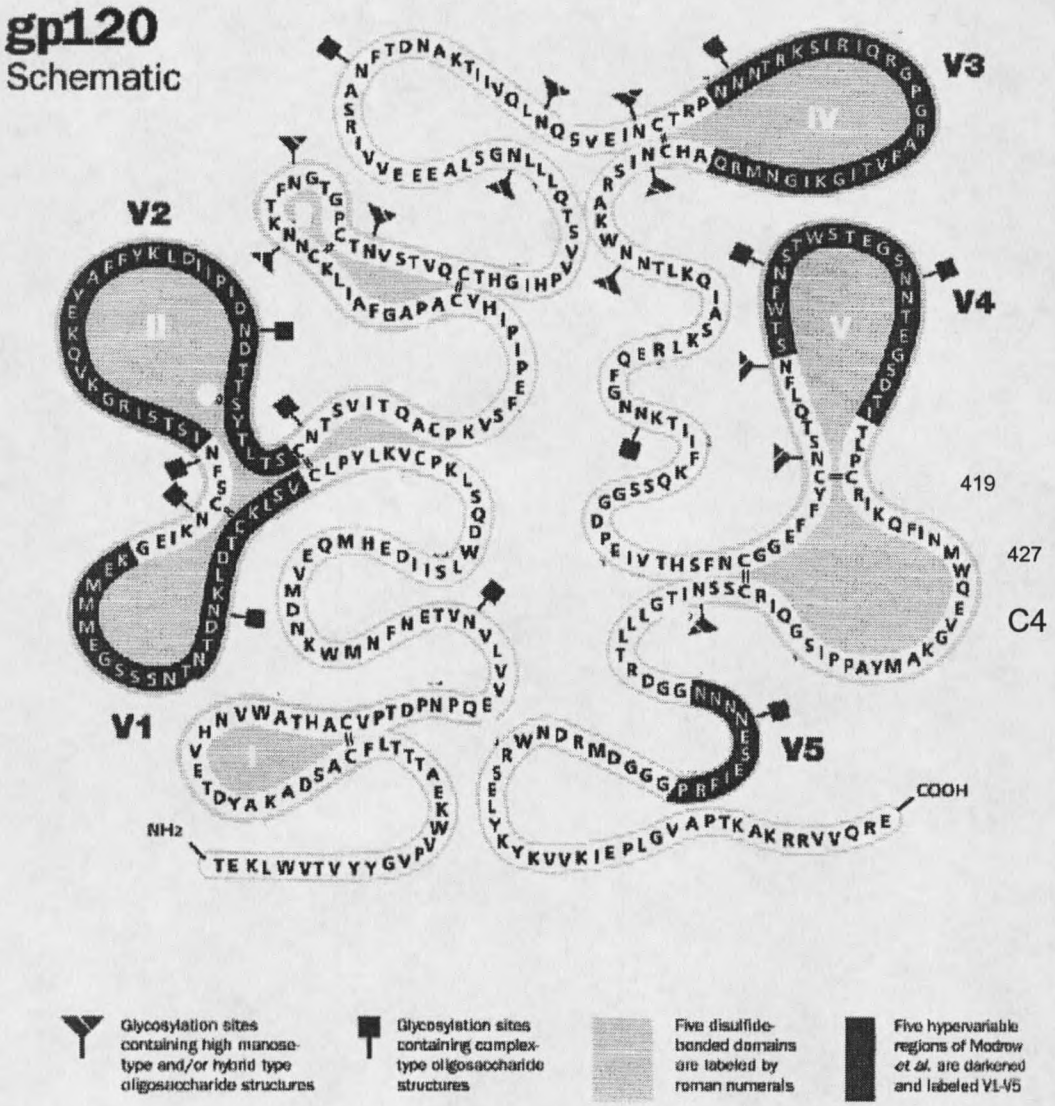


Fig 3. Amino acid schematic of gp120 structure. Figure shows the five known variable regions as well as the many glycosylation site found on gp120.

DNA. The remaining mutated nicked double stranded DNA was transformed into XL-1 Blue supercompetent cells (*Epicurian Coli* XL-1Blue, Stratagene) to repair the nicks in the mutated plasmid. Following transformation, colonies were selected on LB-ampicillin agar plates (1% tryptone, 0.5% yeast extract, 1% NaCl and 1.5% agar, pH 7.2 with ampicillin 100 μg/ml) at 37°C for 18 hrs and screened by plasmid isolation and *Eco*RV enzymatic digestion. The DNA sequences of the *Eco*RV-positive clones were confirmed using fluorescent dideoxynucleotides (Bigdye, Applied Biosystems Inc).

Insertion of Gp120 Loops into the CCMV Coat Protein

A "short loop" corresponding to residues G^{379}GEFFY^{384}GPR^{419}IKQ FINMWQEVGKAMYAPPISGQIR^{444}of HIV-1 gp120 and a long loop G^{379}GEFFYC NSTQLFNSTWFNSTWSTEGSNNTEGSDTITLPCRIKQFINMWQEVGKAMYAPP ISGQIR^{444} encompassing the V4C4 region of HIVgp120 (Fig 3) were each inserted at a *Bam*HI site introduced between codons 159 and 160 of the CCMV coat protein gene in pCC3 (provided by Mark Young, Department of Plant Sciences). The "long loop" represents a region of gp120 bounded by 2 cysteines forming a disulfide bond. The short loop was designed to eliminate the V4 loop portion between C^{355} and C^{388}, replacing it with a GP to make a reverse turn. For the short loop, oligonucleotide primers were designed as follows: 5' TCGGATCCCTGGAGGGGAATTTTTC 3' and 5' TCGGATCCCTCTAAT

TTGTCCACTGATG 3' sense and antisense, respectively. For the long loop, 5', TCGGATCCCTGGAGGAGAATTCTTCTACGGCCCATGCAGAATAAA ACA 3' was used together with the antisense strand primer used for short loop. *Bam*HI sites (underlined) were included at the ends of the oligonucleotides for cloning into the *Bam*HI site of vector. PCR was performed using HIV NL4-3 (HxB2) gp140 or gp120 DNA as templates, and the PCR products obtained were digested with *Bam*HI and ligated into the *Bam*HI-linearized vector. Following ligation and transformation into *E. coli* XLI blue or DH5α, colonies were selected on LB-ampicillin agar (100 μg/ml) at 37°C for 18 hrs and screened by PCR for the short loop or by *Sca*I enzymatic digestion for the long loop. The constructs were confirmed by sequencing the cloned plasmid DNA.

Insertion of Gp120 Residues 419-444 into the CCMV Coat Protein

Sequences at the codons for residues 63, 102, 114, and 129, located in each of the surface-exposed loops of the CCMV coat protein were mutagenized by Mark Young's group to incorporate *Bam*HI sites into pCC3. HIV gp120 residues R^{419}IKQ FINMWQEVGKAMYAPPISGQIR^{444}, from the C4/V4 region that also contacts CD4 (Fig 3), were inserted into each of the 4 CCMV loops using the complementary oligonucleotides: 5'GATCCGCATAAAGCAGATAATAAATAT GTGGCAGGAGGTGGGCAAGGCGATGTACGCGCCACCGATATCCGGCCAGA

TACGCG 3' and 5' GATCCGCGTATCTGGCCGGATATC GGTGGCGCGTACATCGCCTTGCCCACCTCCTGCCACATATTTATTATCTGC T TTATGCG3', which contain the coding sequence for the HIV gp120 fragment and an *Eco*RV site (underlined), with *Bam*HI 5' cohesive ends. Prior to ligation, oligonucleotides were 5' phosphorylated using T4 kinase and annealed to each other. The product was subsequently ligated into each of the 4 *Bam*HI-linearized vectors. Following transformation, colonies were selected on LB-ampicillin agar (100 μg/ml) at 37°C for 18 hrs and screened by PCR and *Eco*RV enzymatic digestion. The identities of the resulting clones, with the HIV insert at residues, 63, 102, 114, or 129, were confirmed by sequencing.

Insertion into the Yeast Vector pPICZA

To express the CCMV capsid proteins with HIV gp120 residues 451-466 exposed in each of 4 different loops in the yeast *Pichia pastoris*, the chimeric genes described above needed to be cloned into pPICZA. The plasmids described in the previous section were amplified by PCR with oligonucleotides 5' GATAGTAAGAATTCATGTCTACAGTCGG 3', corresponding to CCMV RNA 3 nucleotides 1346-1374 3' of the *Eco*RI restriction site (underlined), and 5' GTAACGGTCGACAGCGGGC 3', complementary to CCMV RNA3 nucleotides 1934-1953 3' to a *Sal*I site (underlined). The PCR product was digested with *Eco*RI and *Sal*I, and then ligated into *Eco*RI-*Xho*I-linearized pPICZA vector. Prior to transformation into *E. coli* DH5α or XL I blue, the ligated DNA was

digested with *Kpn*I to eliminate vectors religated without the CCMV insert. Clones were selected on low salt LB-Zeocin agar (1% tryptone, 0.5% yeast extract, 0.5% NaCl, pH7.0 with 25 μg/ml Zeocin), at 37°C for 18 hrs. The resulting clones were analyzed by *Eco*RV enzymatic digestion and confirmed by DNA sequencing.

In vitro RNA Transcription of CCMV cDNA and Plant Inoculation

RNA was synthesized *in vitro* by T7 polymerase using a T7 megascripts kit (Ambion). The plasmid templates, which contained an HIV gp120 sequence inserted into a CCMV coat protein gene downstream of a bacteriophage T7 promoter, was cut on the 3' side of the CCMV gene using *Xba*I. The digested plasmid was treated with Proteinase K and extracted with phenol/choroform prior to ethanol precipitation of the plasmid. The T7 RNA polymerase transcripts were generated and capped by incorporating cap analog ($M^7G(5')ppp(5')G$) at the 5' terminal G of the transcript during the transcription reaction (37°C for 2 hrs). After the transcription reaction was completed, DNase I was added to remove the template DNA and the reaction was terminated with ammonium acetate stop solution (provided in the kit). To analyze the yield of *in vitro* transciption products, RNA was run on an agarose gel containing formadehyde (0.6 g agarose and 31 ml H_20 melted and cooled to 55°C, then added to 10 ml 5XMOPS (10 ml 0.5 M EDTA, 20.94 g MOPS, 0.42 g sodium acetate, in 1 liter DEPC-treated water, pH7.0)) and 9 ml 37% formaldehyde to denature secondary structure in the

transcripts that may cause aberrant migration. To analyze the yield of RNA transcripts, a 2 μl aliquot of each reaction was mixed with gel loading buffer (1μl H_2O, 2 μl 37% formaldehyde, 5 μl formamide, 2 μl 5X MOPS, 1 μl 10 mg/ml ethidium bromide) and heated for 10 minutes at 65°C prior to adding 2 μl bromophenol blue. The gel was run in 1X MOPS buffer (diluted from 5X MOPS) for 30 minutes at 100 V (115). If a high yield of RNA was observed on the gel, the rest of the RNA in the Eppendorf tube was extracted with phenol/chloroform prior to the addition of a half volume of LiCl precipitation solution (provided in the kit).

CCMV wild-type RNAs 1,2, and 3 were transcribed using *Xba*I-linearlized pCC1, pCC2, pCC3, respectively (96), using the same procedure as that described for the mutant RNA3 above. A mixture of RNA1, RNA2, and RNA3 (or mutant RNA3) in a 1:1:2 molar ratio was used to inoculate cowpea plants (*Vigra unguiculata* (L.) var. California Blackeye) or *Nicotiana benthamiana* grown and maintained in a greenhouse. Inoculations were performed by applying 0.5 μg total RNA in 0.1 M phosphate buffer, pH 6.0 on a single 10-day leaf of each plant by gentle rubbing on the leaves after abrading the leaf surface with carborundum (320 grit: Fisher, Pittsburgh, PA). The infection was allowed to proceed for 14 days, after which infected and other leaves of the same plant were harvested. Leaves inoculated with phosphate buffer and with only RNA1 and RNA2 in phosphate buffer were used as negative controls.

RNA Isolation

50 μg of virus in 250 μl virus buffer (diluted from 10X virus buffer=33.33 ml 3 M NaOAc pH 4.8, 20 ml 0.5 M EDTA, 0.65 g NaN_3 in 1 liter) was added to an equal volume of 200 mM TrisHCl pH 7.5, 4% SDS, 1.6 μg/ml proteinase K in RNAse free H_2O. The mixture was heated at 55°C for 30 minutes prior to adding an equal volume of warmed phenol (65°C) for phenol extraction. After vortexing and centrifugation at 14,000 rpm for 5 minutes, the aqueous upper layer was transferred to a new Eppendorf tube. An equal volume of phenol/chloroform mixture was added to the tube and the procedure was repeated. RNA in the aqueous layer was precipitated with an equal volume of isopropanol in the presence of 1/10 volume of 3 M ammonium acetate at -20°C for 1 hr. The RNA pellet was collected after centrifugation at 14,000 rpm for 20 minutes and subsequently washed with 70% ethanol. The pellet was air-dried and finally resuspended in RNAse-free H_2O prior to analysis on a denaturing gel as described above.

DNA Sequencing

All mutant CCMV gene constructs were sequenced to verify the mutations. Briefly outlined, 500 ng of plasmid DNA or 20 ng of PCR product and 1 μl of primer at 5 pmol/μl were included in the reaction (total of 20 μl) containing 4 μl of 5X sequencing buffer and 4 μl of the ABI Prism Big Dye Terminator Cycle

Sequencing Ready Reaction kit (PE Applied Biosystems) for use with the ABI Prism 310 DNA sequencer. First, DNA was amplified on a Perkin Elmer 2400 thermocycler using the following program: 96°C for 10 seconds, 50°C for 5 seconds and 60°C for 4 minutes for 25 cycles. Once the sequencing reaction was complete, amplified DNA was precipitated by adding 80 μl of 75% isopropanol and incubating at room temperature for 15 minutes. The pellet was collected after centrifugation at 5,000 rpm for 30 minutes. The remaining isopropanol was drained out prior to adding loading buffer and loading the sample into sequencing machine as described by the manufacturer (PE Applied Biosystems).

Electron Microscopy

Viral assembly was examined on Leo 912 LB transmission electron microscope. Samples were absorbed to carbon-coated grids and negatively stained with 1% uranyl acetate. A total magnification of 50,000x was used.

Reverse Trancription-Polymerase Chain Reaction Amplification

RNA extracted from inoculated and other leaves from the same plant was used as a template for RT-PCR of the coat protein coding sequence to monitor viral RNA expression. The oligodeoxynucleotide 5' GTAACGGTCGACA GCGGGC 3' complementary to CCMV RNA3 nucleotides 1934-1953 with a unique *Sal*I site (underlined) was used to prime cDNA synthesis. First strand

cDNA was synthesized with avian myeloblastosis virus reverse transcriptase. Second strand cDNA synthesis and PCR amplification was performed with the above primer in combination with a second oligonucleotide, 5' GATAGTAAGTCGACATGTCTACAGTCGG 3' that corresponds to RNA 3 nucleotides 1346-1374 with a *Sal*I site (underlined), using DNA polymerase from *Thermus flavus*. 10 pg-1 ug total RNA template and 50 pmol of each primer were used per reaction according to the instruction of manufacturer, (Promega, Medison, WI). For a negative control, sterile nuclease-free water was substituted for the RNA template in the reaction.

Preparation of *Pichia* for Electroporation

Pichia pastoris wild-type (strain X-33) was grown in 5 ml YPD medium (1% yeast extract, 2% peptone, 2% glucose) at 30°C overnight. The next day, 0.1-0.5 ml culture was transferred into 500 ml fresh YPD medium and grown overnight until OD_{600}=1.3-1.5. The cells were centrifuged at 3,000 rpm for 5 minutes at 4°C and the pellet was gently resuspended with 100 ml cold sterile water and subsequently treated with 0.389 g dithiothreitol (25mM final concentration) at room temperature for 10 minutes. The cells were centrifuged at 3,000 rpm for 5 minutes at 4°C and 100 ml cold electroporation buffer (10 mM Tris-HCl pH 7.5, 270 mM sucrose and 1 mM $MgCl_2$) was added to resuspend the pellet. Two centrifugations at 5,000 rpm for 5 minutes were done to wash the

cells. Finally, the pellet (approximately $5x10^7$ cells) was resuspended in 1-2 ml cold electroporation buffer and the cells were kept on ice for immediately use.

Electroporation

E. coli cells containing pPICZA plasmid constructs were grown in 50 ml low salt LB with Zeocin (25 μg/ml) at 37°C overnight. Plasmid DNA was extracted using a BioRad kit as described in the instructions of manufacturer (BioRad) and digested with *Bst*XI, a unique restriction site in the 5' *AOX*I region. After phenol/choloroform extraction and ethanol precipitation, linearized plasmid DNA was resuspended in a small volume of water to get a concentration of approximately 5-10 μg/μl. 1-2 μl of DNA sample was mixed gently with 40 μl of the competent cells and electroporated in a 0.2 cm electroporation cuvette. The micropulser (BioRad) was preprogrammed for *Pichia* (yeast settings) at 1 pulse of 2 kV. After electroporation, 1 ml ice-cold YPD medium was immediately added to the cuvette and the diluted cells were gently transferred to a sterile tube and kept on ice for 5 minutes. Thereafter, cells were incubated at 30°C for 4-5 hrs without shaking prior to plating on YPDS agar (YPD plus 1M sorbitol) with 100 μg/ml Zeocin. The plate was incubated at 30°C for 48-72 hrs until colonies were seen. The linearized vector and water were used as positive control and negative controls, respectively.

Direct PCR Screening of *Pichia* Clones

A single colony was resuspended in 10 μl of water. 5 μl of a 5 U/μl solution of lyticase (Sigma) was added to the cells and the mixture was incubated at 30°C for 30 minutes. Subsequently, the mixture was frozen at -80°C for 10 minutes and then thrawed at room temperature while setting up the PCR reaction (116). Primers 5' GACTGGTTCCAATTGACAAGC 3' and 5' GCAAATGGCAT TCTGACATCC 3' were used in the PCR reaction and the parameters of thermocycler were set as described in the manufacturer's instructions for the "EasySelect™ *Pichia* Expression Kit" (Invitrogen) (111). A negative control PCR was performed by substituting DNA with water and vector-integrated *Pichia* chromosomal DNA was used a positive control. A 10 μl aliquot of the 50 μl PCR reaction was analyzed by 0.8% agarose gel electrophoresis and compared with positive and negative controls. The mutant clones with HIV inserts were seen as band mobility shifts compared to the positive control. The mutations were confirmed with *Eco*RV enzymatic digestion and DNA sequencing. For single point mutations, the mutant clones were seen as the same molecular weight as the control and those clones were verified by DNA sequencing.

Small-Scale Expression Screening of Recombinant *Pichia*

A single colony of *Pichia* was inoculated into 1 ml of MGY medium (1.34% YNB, 1% glycerol and 0.4 μg/ml biotin) and incubated in a 30°C shaking incubator until OD_{600} reached 2-6. After centrifugation at 5,000 rpm for 5

minutes, the cell pellet was collected and resuspended with 1 ml of MM medium (1.34% YNB, 0.4 μg/ml biotin and 0.5% methanol). For methanol induction, cells were grown for another 4 days at 30°C by adding 100% methanol every 24 hrs to a final concentration of 0.5%. Finally, cells were collected after centrifugation at 5,000 rpm for 5 minutes and resuspended in 20 μl of 2xSDS buffer (100 mM sodium phosphate buffer pH 7.2, 1% SDS, 10% glycerol, 0.001% bromophenol blue, and 5% β-mercaptoethanol. To break the cells, a small amount of 0.5 mm glass beads was added and the mixture was alternately vortexed for 5 minutes, and kept on ice for 5 minutes. The procedure was repeated 4-5 times. After centrifugation at 14,000 rpm for 5 minutes, the supernatant was harvested for dot blot and western blot assays. For these analyses, the supernatant was heated at 90°C for 5 minutes and loaded on a 12 % SDS-PAGE gel or spotted on a polyvinylidene difluoride (PVDF) membrane pretreated with 100% methanol for 15 minutes and water for 2 minutes as recommended by the manufacturer (Millipore, MA).

Medium Scale Expression of Recombinant *Pichia*

A single colony of *Pichia* was inoculated in 25 ml of MGY and incubated in a 30°C shaking incubator until the culture reached OD_{600}= 2-6. Cells were harvested by centrifugation at 5,000 rpm for 5 minutes. 20 ml of MM medium was added to resuspend the cell pellet prior to transferring the resuspended cells to 1-liter of MM medium in 2-liter flask. The culture was placed in a 30°C

incubator shaker to continue growth for another 4 days. To maintain induction, 100% methanol was added to a final concentration of 0.5% methanol every 24 hrs. The cells were harvested by centrifugation at 5,000 rpm for 5 minutes.

Extraction of Recombinant Coat Protein from the Yeast Cell Pellet

The cell pellet from a 1-liter culture was resuspended with homogenization buffer (66.7 ml 3 M NaOAc, pH 4.8, 20 ml 0.5 M EDTA, 1.98 g ascorbic acid in 1 liter) in a 1:2 ratio of cell pellet (g) to homogenization buffer (ml). 0.5 g glass beads was added to allow breaking the yeast cells by alternately vortexing for 5 minutes and leaving on ice for 5 minutes (repeated 5 times). A 0.5 ml aliquot of crude lysate was saved for dot blot analysis as a pellet and a supernatant after bead beating. The rest of the crude lysate was centrifuged at 15,000 rpm for 30 minutes and then the supernatant was ultra-centrifuged at 25,000 rpm for 2 hrs in a Beckman 50Ti rotor. After centrifugation, the supernatant was saved and the pellet was resuspended with 2 ml virus buffer. 2 μl of the resuspension was saved for dot blot analysis and the rest was used to purify the recombinant coat protein by banding in 39% CsCl gradients formed at 38,000 rpm for 20 hrs in a VTi65 rotor. The white bands of coat protein in the CsCl gradient were visualized and collected under a flashlight in a dark room. Prior to examining the empty virions by EM, the protein was dialyzed against 2-3 changes of PBS (11.5 g Na_2HPO_4, 2.96 g NaH_2PO_4, 5.84 g NaCl in 1 liter) in a cold room. Aliquots of the pellets and supernatants collected along the procedure were analyzed by dot

blot. The concentration of recombinant coat protein was assayed using BCA (Pierce, IL).

Dot Blots for Small Scale Expression Screening

A 2 μl aliquot of protein solutions boiled in SDS sample buffer (at least 1 μg/ml) was spotted on a methanol-pretreated polyvinylidene difluoride (PVDF) membrane. The membrane was blocked with "blotto" (1xPBS+0.1% Tween-20+5% dry skim milk), shaking on a platform for at least 30 minutes at room temperature. The blocking solution was discarded and the membrane was washed with new buffer (1xPBS+0.1% tween20) on the platform for 10 minutes. The buffer was replaced twice, shaking on the platform for 5 minutes each time. After the old buffer was discarded, the primary antibody (1:5000 dilution of 1 mg/ml polyclonal rabbit anti-CCMV) was added in new buffer (10 ml per 15x15-cm^2 membrane). The membrane was incubated with primary antibody, shaking gently on the platform for 2-3 hrs. A washing step was performed prior to adding a 1:1000 dilution of 1 mg/ml alkaline phosphatase (AP)-conjugated goat anti-rabbit secondary antibody (Zymed) in sufficient new buffer to cover the membrane, shaking gently on the platform for at least an hour. A washing step was performed and the membrane was drained of the buffer. For AP detection, 66 μl of NBT stock solution (0.5 g of NBT in 10 ml of 70% dimethylformamide) was added in 10 ml of AP buffer (100 mM NaCl, 5 mM $MgCl_2$, 100 mM Tris, pH 9.5). After mixing, 33 μl of BCIP stock solution (0.5 g of BCIP (disodium salt) in

10 ml of 100% dimethyformamide) was added and the mixture was poured on top of the membrane. The signal was allowed to develop for at least 30 minutes until dark purple bands were seen. The membrane was washed in water to stop the reaction.

SDS-PAGE and Western Blot Analysis

For Western blots, protein solutions boiled in SDS sample buffer were separated on 12 or 15% (w/v) SDS-PAGE gels in the Laemmli running buffer (50 mM Tris, 100 mM glycine, 0.1% SDS) (117). The proteins were then transferred electrophoretically onto methanol-treated polyvinylidene difluoride (PVDF) membranes in cold transfer buffer (25 mM Tris, 192 mM glycine, and 10% methanol) at 200 milliamps for 2-3 hrs. Membranes were saturated in PBS buffer with 0.1% Tween 20 containing 5% dry skim milk for at least 30 minutes before incubation with a primary polyclonal Ab (1:5000 dilution of 1 mg/ml rabbit anti-CCMV or 1:3,000 dilution of mouse anti-KLH-44F.C or anti-KLH-19A.C). Bound antibodies were detected with alkaline phosphatase (AP)-conjugated goat anti-rabbit secondary antibody for anti-CCMV detection as described for the dot blot analysis or a 1:1,000 dilution of 1 mg/ml alkaline phosphatase (AP)-labeled goat anti-mouse secondary antibody (Zymed) for anti-44F.C and anti-19A.C detection. AP detection was done as described in the previous section.

Enzyme-Linked Immunosorbent Assay (ELISA)

ELISA assays were performed following the description of Harlow *et al* (111). Plates were coated with 0.1 μg of antigens (except 0.5 μg of CCMV or CPMV) and each well was loaded with 100 μl of solutions (except 200 μl of blocking solution). Sera were screened for anti-peptide 44F.C or anti-peptide 19A.C activity on plates coated with 0.1 μg of ovalbumin conjugated to the same peptide (OVA-44 or OVA-19, respectively) in PBS at 4°C overnight. The coating solution was discarded and the plate was blocked with blocking solution (10 g bovine serum albumin, 0.1 g sodium azide in 1 liter PBS) for 6-8 hrs at room temperature. After blocking, the plate was washed 4-5 times with PBS containing 0.1% Tween 20. Sera were diluted 1:1,000; 1:5,000, 1:10,000 and 1:20,000 in blocking solution prior to addition into wells. The plate was incubated at 4°C overnight and then washed 4-5 times with the same buffer. A 1:1000 dilution of 1 mg/ml AP-labeled goat anti-mouse antibodies (Zymed) was added into the wells. After incubation for 4 hrs at room temperature, the plate was washed prior to detection using *p*-nitrophenol phosphate (PNPP) (Sigma) as a substrate (1 tablet of 10 mg in 10 ml of 10 mM diethanolamine, pH 9.5 containing 0.5 mM $MgCl_2$). Positives appeared bright yellow and the signal was read at 405 nm kinetically every 10 minutes for 50 minutes with a plate reader (Tecan Safire, with Xflouro 4 software). OD405 values that were greater than twice the background obtained from sera binding to wells coated with unconjugated ovalbumin (usually >0.16) were considered positive. For the anti-HIV gp120 or gp160 titer assay, 1:300 or

1:1000 dilutions of sera were added to plates coated with 0.1 μg of HIV gp160IIIB or HIV-1Bal gp120. The procedure was performed as described above. 1D6, a mouse mAb specific to gp120, was used as a positive control and pre-immune sera with the same dilutions were used as negative controls.

For isotype determination, 1:200 and 1:600 dilutions of sera were added to wells coated with 0.1 μg OVA-44. 100 μl each of 1:1,000 diluted IgG1, IgG2a, IgG2b, and IgG3 (Sigma) were added to wells after washing out the sera. 100 μl of 1:8,000 diluted AP-labeled rabbit anti-goat IgG was added as a secondary antibody. Detection was performed as described above.

Silver Staining

After running, SDS-PAGE gels were placed in a container containing 5 gel volumes of PAGE gel fixer (50% methanol, 12% acetic acid), and shaken for 40 minutes at room temperature. The solution was discarded and then the gel was washed 3 times with 50% ethanol, each time shaking for 20 minutes. After the last ethanol was discarded, the gel was washed with 2% sodium thiosulfate for 1 minute. After rinsing with water for 2-3 times, Silver nitrate solution (0.25 g $AgNO_3$ and 125 μl 40% formaldehyde in 125 ml water) was added to stain the gel for 20 minutes in dark. The gel was washed with water prior to adding developing solution (60 g sodium carbonate, 1 ml of 40% formaldehyde, 30 ml of 2% sodium thiosulfate in 1 liter) and incubating on a shaker at room temperature

until protein bands were seen. The reaction was stopped with destaining solution (1% glycerol, 10% acetic acid).

Sypro Ruby Staining

A 8x10 cm gel was placed in a plastic container containing a washing/fixing buffer (10% methanol and 7% acetic acid) at least 1-2 hrs. The buffer was discarded and drained of the remaining buffer prior to adding 50 ml Sypro Ruby staining reagent (BioRad) and shaking on a platform for at least 3 hrs or up to overnight in a container covered with aluminium foil. The gel was destained with 2 changes of the washing/fixing buffers, shaking on the platform for 2-3 hrs or until ready to image by Molecular Imager^{TM} FX.

BCA Protein Assay

The protein assay was based on bicinchoninic acid (BCA) for the colorimetic detection and quantitation of total protein. The purple-colored product exhibited a strong absorbance at OD_{562} that was nearly linear with increasing protein concentration in a range of 20-2,000 μg/ml. Protein concentration was determined based on a standard curve of known concentrations of bovine serum albumin. The procedure was described in the instructions of the manufacturer (Pierce, IL).

CCMV-Peptide Conjugates

CCMV-SPDP Linker

CCMV contains 180 coat protein subunits and each has a molecular weight of 20,000 daltons. 0.25 mg CCMV (salt stable) virus in 500 μl virus buffer, pH 4.8 was dialyzed twice for 30 minutes in reaction buffer (20 mM NaH_2PO_4, 0.15 M NaCl, 5 mM EDTA, pH 7.5). A 5 molar excess of SPDP (Pierce, IL) in DMSO was added to react with ε–amino groups on lysine side chains of the virus coat protein. To control the reaction, pH was maintained at 7.5 by addition of 1 M $NaHCO_3$, pH 9.5. The virus-linker reaction was incubated for an hour at room temperature on a shaking platform. The reaction was stopped with freshly prepared 1.5 M hydroxylamine, pH 8.5 (2% final concentration) and subsequently dialyzed in reaction buffer (20 mM NaH_2PO_4, 0.15 M NaCl, 5 mM EDTA, pH 6.5). Peptide containing a free sulfhydryl group (10 molar excess over viral subunit) was added and incubated at room temperature for 1 hr. The product was then run on a 12.5% SDS-PAGE gel and analyzed by silver staining and Western blotting. Compared to the unconjugated coat protein, the conjugates exhibited a molecular weight shift on the gel. For Western blot analysis, 1:3,000 diluted anti-KLH-44 or anti-KLH-19 was used as the primary antibody and a 1:1000 dilution of 1 mg/ml AP-labeled goat anti-mouse antibody was used as the secondary antibody. Prior to inoculating mice, the conjugates were dialyzed against PBS at 4°C.

CPMV-SulfoSMCC Linker

2 mg of CPMV in 500 µl PBS, pH 7 was incubated at room temperature for 4 hrs with a 20X molar excess of sulfoSMCC (Pierce), over subunit pairs. CPMV virions contain 60 copies each of a large and a small coat protein subunit with molecular weights of 42 kD and 23 kD, respectively. There is only one reactive lysine side chain on the outer surface of the viral capsid per subunit pair. The excess sulfo-SMCC was then removed on a PD10 desalting column (Pharmacia), equilibrated with PBS, pH 7. Approximately 14-15 fractions of 1 ml each were collected. OD was measured at 280 nm for all fractions and graphed. Fractions of the first peak exhibiting high OD_{280} were pooled and then run through a desalting Biogel P-6 (BioRad) column equilibrated with PBS. Fractions were collected and OD_{260} measured. Beer's law was used to calculate the concentration of virus, using an extinction coefficient of 8 $cm^{-1}M^{-1}$. A 60-fold molar excess of free sulfhydryl-containing peptide was added to the sulfoSMCC-linked virus, and the reaction was incubated at 4°C overnight. The excess peptide was removed by washing through a YM-50 centricon membrane with PBS twice at 6,000 rpm for 5 minutes. The retentate was collected and analyzed as described above. Prior to injecting mice, the conjugates were dialyzed against PBS at 4°C.

S130C K42R-BMH Linker

10 mM bismaleimidohexane (Pierce, IL) in DMSO was mixed with 10 mM free sulfhydryl-containing peptide in a 2:1 molar ratio and incubated with shaking

at 4°C for an hour. The conjugate was purified by reverse-phase HPLC to remove excess peptide and BMH. Fractions exhibiting high OD_{230} were analyzed by MALDI-TOF mass spectroscopy after mixing the sample with an equal volume of a saturated solution of α-cyano 4-hydroxycinnamic acid (ACHA) in 50% acetonitrile. The fraction containing a dominant peak with a molecular weight of 1321 was selected as the peptide-BMH conjugate and lyophilized overnight.

0.5 ml of 1 mg/ml mutant CCMV containing an engineered cysteine at residue 130 (S130C) was treated with 1 mM freshly dissolved TCEP for an hour at room temperature. The lyophilized peptide-BMH conjugate was dissolved in reaction buffer (20 mM NaH_2PO_4, 0.15 M NaCl, 5 mM EDTA, pH 7) and added to TCEP-treated virus at a ratio of 5 moles conjugate per mole coat protein subunit. The pH was adjusted to 7 prior to incubating at 4°C for 2 hrs with shaking. The reaction was quenched by adding 1 M cysteine hydrochloride freshly dissolved in reaction buffer (25 mM final concentration), and incubated at room temperature for 30 minutes. All substances were dissolved in reaction buffer, unless otherwise indicated. The conjugates were analyzed by SDS-PAGE and Western blots, as described above. Prior to injecting mice, the conjugates were dialyzed against PBS at 4°C.

KLH or OVA-Conjugated Peptides

600 μg of 10 mg/ml KLH or ovalbumin conjugated to sulfoSMCC (Imject, Pierce, IL) was mixed with 300 μg of 1 mg/ml freshly dissolved free sulfhydryl-containing peptide in reaction buffer (20 mM NaH_2PO_4, 0.15 M NaCl, 5 mM

EDTA, pH 7). The mixture was incubated for 2 hrs at room temperature. For peptide linked to KLH, the conjugates were dialyzed against PBS at 4°C prior to inoculating mice.

Peptide Kinetic Assay

The ability of peptides 44F.C and 19 A.C to react with the SPDP linker was measured using a kinetic assay. 100 μl 0.8 mg/ml peptide (or DTT used as a positive control) was incubated with 40 μl 0.5 mg/ml SPDP in a total volume of 200 μl 1xPBS pH 7.5. The 2-pyridyl-disulfide group on the linker reacts with the thiol group on the peptide or DTT and releases the pyridyl-2-thione group, which can be quantified by measuring the absorbance at 343 nm. The amount of the pyridyl-2-thione was monitored before adding the peptide or DTT and then every 2 minutes up to 24 minutes. In the experiment, the linker alone in the PBS buffer was used as a negative control and the buffer alone was used as a blank to subtract the background.

Immunization of Mice with Conjugates

3 mice per group of five-week-old CD1 mice were immunized by subcutaneous (s.c) injection with 50 μl of 50 μg conjugate mixed with an equal volume of Complete Freunds's Adjuvant (CFA) at week 0 and boosted with 25 μg in Incomplete Freunds at week 5, 6, and 7 by intraperitoneal (i.p.) injection. Sera were obtained by bleeding on day 0 and 7-10 days after each boost. For

injection without an adjuvant, inoculations were performed i.p., except that two additional boosts were performed subcutaneously.

Animal handling and maintenance were performed according to the principles and guidelines for the use of animals in research, testing, and education prepared by the Ad Hoc Committee on Animal Research (New York Academy of Sciences, New York, N.Y.)

Reverse Phase High Performance Liquid Chromatography (HPLC)

BMH-linked peptides were purified by reverse phase HPLC, using a C4 semiprep column equilibrated in 0.1% TFA, 10% acetonitrile at a flow rate of 5 ml/min. Sample was injected prior to eluting with a gradient of 10-90% acetonitrile in 0.1% TFA at a flow rate of 3 ml/min. The absorbance at 230 mm was used for detection of peptide dimer, BMH-peptide conjugate, and free BMH with retention times of approximately 16.5, 18, and 23 minutes, respectively.

CHAPTER FOUR

RESULTS

Genetic Manipulation of CCMV Coat Proteins

The sequences from conserved region 4 and variable region 4 (V4C4) of HIV gp120 were incorporated into the CCMV coat protein gene. Since these regions contain parts of the CD4 binding site which are conserved among HIV-1 strains, presentation of these epitopes to the immune system on the CCMV coat protein could potentially elicit antibodies that recognize the CD4 binding site and neutralize a broad range of HIV strains. In order to produce virus chimeras, different regions of HIV gp120 were inserted into each of the 4 surface-exposed loops of the CCMV coat protein as described in Materials and Methods. The cowpea leaves inoculated with RNA constructs that had HIV sequences inserted at codon 102 showed what appeared to be local CCMV lesions on inoculated leaves within 14 days, whereas the other constructs did not show any evidences of viral infection. RT-PCR analysis of RNA isolated from inoculated leaves revealed a band with the expected size (≈600 bp) for the chimeric gene (data not shown). However, accumulation of recombinant coat proteins could not be detected by ELISA, and Western blot analysis, using polyclonal anti-CCMV antibodies. Virions could not be detected by EM. These results indicated that recombinant CCMV coat proteins were not assembled into virions in cowpea

plants. To confirm this assumption, sap of inoculated leaves was re-inoculated into cowpea and also benthamiana plants (another host for CCMV), and the inoculated leaves were analyzed by RT-PCR, EM, Western blotting and ELISA. Neither recombinant coat proteins nor virions were detectable in any leaves analyzed.

Since chimeric CCMV coat protein molecules could not be assembled into viral particles in plants, the production of viral coat capsids in heterologous systems was examined. Previous work by the Young lab had shown that viral particles assembled *in vitro* from coat proteins expressed in *E. coli* are indistinguishable from plant-purified particles (97), and expression of the coat protein in the yeast *Pichia pastoris* resulted in assembly of viral particles *in vivo* that were also identical to virions from plants, except that they did not contain the viral genomic RNA. In order to introduce foreign genes into *Pichia*, the chimeric CCMV coat protein gene previously assembled in the pCC3 vector had to be cloned into a yeast vector, pPICZA, prior to electroporation into yeast cells. This vector integrates into the *Pichia* chromosomal DNA by homologous recombination. High expression integrants containing multiple copies of the inserted gene were chosen based on dot blot analyses from 1-ml culture using polyclonal anti-CCMV antibodies (data not shown). The presence of the HIV peptide in the coat proteins produced by these clones was checked by looking for gel mobility shifts on Western blot analyses using polyclonal anti-CCMV antibodies and by PCR amplification of the *Pichia* chromosomal DNA.

Compared to the wild-type coat protein and the wild-type *Pichia* chromosomal DNA used as controls for the former and latter analysis, the selected transformants exhibited the expected molecular weight shifts (data not shown), showing that transformants contained the HIV insert. To confirm these results, their PCR products were verified by DNA sequencing. All transformants showed the correct insert sequence (data not shown). These recombinant *Pichia* clones were grown in 1-liter cultures and expression of the desired recombinant coat protein was checked again as described above. Examination of the virus particles isolated from these cultures by EM showed a few intact virions. The cultures of these constructs were further scaled up in 4-liter fermenter batches. After breaking the yeast cells using a bead beater, samples of pellets and supernatants were collected at each step of the process and analyzed on dot blots using polyclonal anti-CCMV antibodies to determine how much of the protein was contained in each fraction. The extraction process was performed in parallel with a culture expressing wild-type CCMV coat protein as a control. Unlike the control, most of the chimeric proteins remained in the first (low speed) pellet and only a small amount was present in the supernatant after bead beating. Various kinds of detergents and sonication were used in attempts to increase the yield of recombinant proteins in the supernatant, but to no avail. The final amount of chimeric coat protein in the supernatant after harvesting by ultra-centrifugation at 25,000 rpm for 2 hrs was approximately 50-100 nanograms per 1 kilogram of yeast cells, as estimated by SDS-PAGE and silver staining. A

few virion-like particles were detected by EM, but most were not the proper size and shape for T=3 virus capsids. Additional chimeric gene constructs, with HIV gp120 residues 451-466, were inserted into each of the 4 loops of the CCMV coat protein independently were also expressed in *Pichia*, but none of them produced any significantly yield of viral particles; neither did CCMV chimeras with short peptides being expressed by the Young lab (pep11, an 8-residue laminin sequence) nor the Pincus lab (S9, a 9-residue phage display peptide). We therefore abandoned this approach and tried chemically coupling the peptides to intact viral capsids.

CCMV-Peptide Conjugates with SPDP

Salt stable (K42R) CCMV capsids isolated from *Pichia* were used to make peptide conjugates. Peptide 44F.C or 19A.C was coupled to amino groups on surface-exposed lysine side chains of the CCMV coat protein using SPDP. The presence of the peptide attached on the coat protein was analyzed by SDS-PAGE and silver staining, which showed the peptide-coupled coat protein bands migrating slower than the corresponding uncoupled protein band. (Fig. 4.1 lanes 3 and 4, compared to lanes 1 and 6). The same shift was also observed using an irrelevant peptide, S9, of the same length (Fig. 4.1, lane 5). Moreover, there was an additional faint slower migrating band observed after coupling with peptides 44F.C and S9 (Fig. 4.1, lanes 3 and 5), indicating that there may have been more than 1 peptide attached to some of the coat protein subunits. Of the

3 peptides used, peptide 19A.C seemed to couple the least on the coat protein (Fig. 4.1, lane 4). Although SPDP linked cysteine groups on the peptides to amino groups on the virus, it also caused unwanted reactions where virus subunits were linked to each other causing formation of dimers and multimers, which were seen as very slow migrating bands after adding only the linker to the virus (Fig. 4.1, lane 2), as well as in lanes 3-5 after subsequently adding the peptide.

The presence of a peptide on the coat protein was verified by Western blot analysis. Using anti-KLH-44F.C serum, 4 bands were seen: 2 bands migrated the same as the uncoupled coat protein bands and the other 2 migrated slower (Fig 4.2, lane 5). Although some nonspecific binding of serum was observed in the uncoupled control (lane 6), the intensity of bands 2 and 3 (from the bottom) were stronger. This indicated that peptide 44F.C coupled to the coat protein caused the molecular weight shift. Additionally, a strong signal was also detected in the dimer band. The link between SPDP and the peptides is cleavable by DTT or other reducing agents capable of reducing S-S bonds at pH 7-9. Therefore, beta-mercaptoethanol (β-ME) was added to the conjugate samples to confirm the presence of the peptide on the coat protein. After adding the reducing agent, peptide 44F.C was not detected in the conjugates (Fig. 4.2, lane 2). However, β-ME did not release peptide 44F.C coupled to maleimide-activated OVA as a control (Fig. 4.2, lane1) because the maleimide-cysteine link cannot be cleaved by reducing agents.

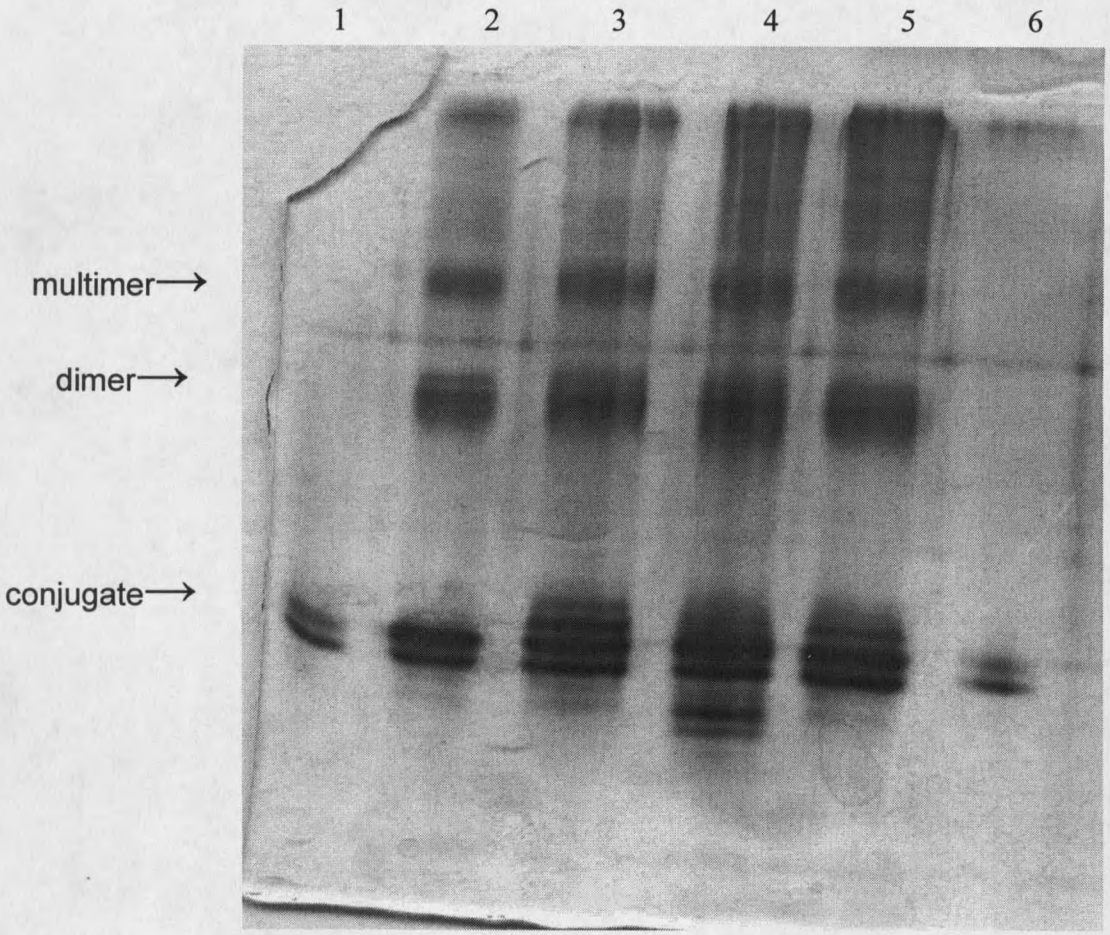


Fig 4.1. Silver stained gel of CCMV-peptide conjugates using SPDP. Proteins were separated on a 12.5% SDS-PAGE gel, and stained with silver nitrate solution. The presence of conjugate, dimer and mulitmer are indicated by arrows. Lane 1 and 6, unconjugated protein; lane 2, CCMV coat protein incubated with SPDP alone; lane 3, CCMV-44F.C-conjugate; lane 4, CCMV-19A.C-conjugate; lane 5, coat protein conjugated with an irrelevant peptide, S9.

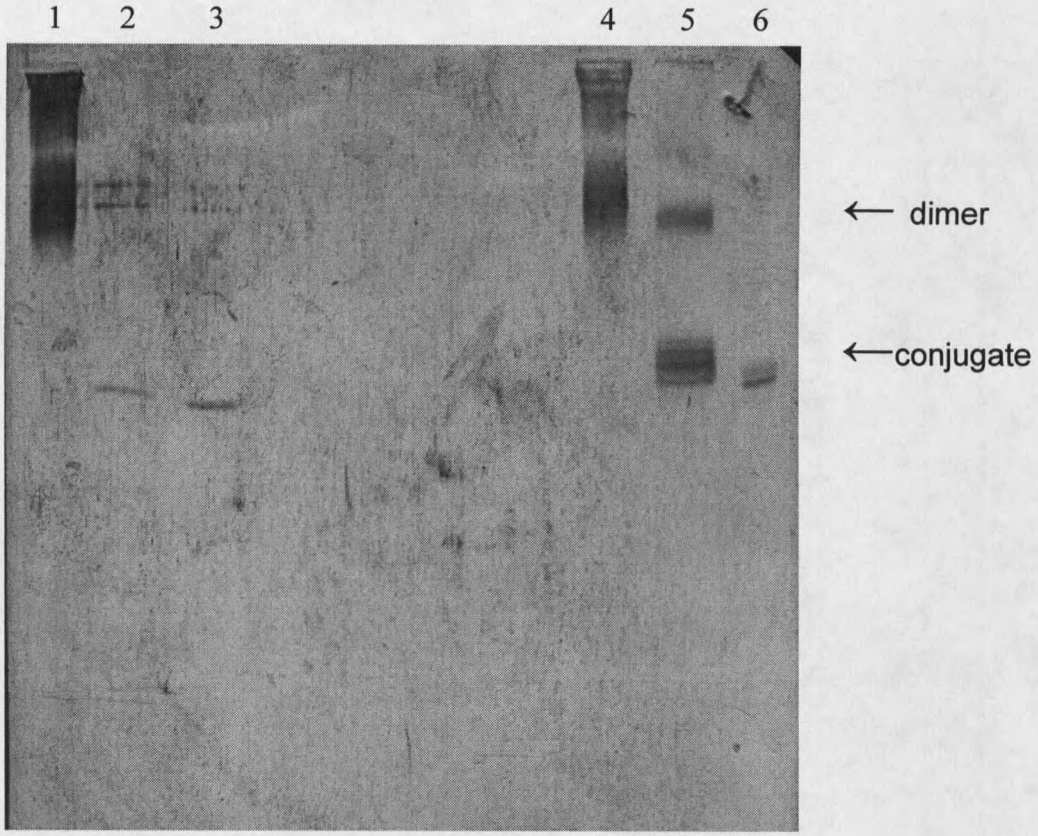


Fig 4.2. Western blot analysis of CCMV-44F.C conjugation using SPDP. Proteins were separated on a 12.5% SDS-PAGE gel and transferred to a PVDF membrane. The membrane was incubated with mouse anti-KLH-44F.C serum, followed by alkaline phosphatase (AP)-labeled goat anti-mouse IgG. The presence of peptide is indicated by arrows. Lane 1-3 reducing conditions; lane1, OVA-44F.C conjugate used as a positive control; lane 2, CCMV-44.C conjugate; lane 3, Unconjugated coat protein. These lanes were replicated in lane 4-6 under non-reducing condition.

The Western blot analyses of CCMV-19A.C using anti-KLH-19A.C polyclonal antibody showed similar results to that of CCMV-44F.C. As compared to the uncoupled coat protein (Fig. 4.3, lane 1), the peptide 19A.C was detected on the CCMV-19A.C conjugate run in lanes 2 and 3. In lane 3, with more protein loaded, an additional fast migrating band and the virus dimer band were also detected.

Kinetics of Peptide Reaction with SPDP

Since peptide 19A.C coupled the least to the coat protein, a kinetic assay was used to determine how well the peptide 19A.C reacted with the linker compared to peptide 44F.C. The extent of peptide coupling to SPDP can be measured by the amount of pyridine-2-thione released when SPDP couples to the peptide due to its absorbance at 343 nm. The graph in Figure 4.4 showed that peptide 19A.C reacted with the SPDP linker more rapidly than 44F.C and reached a higher steady-state level. Thus, there was nothing about peptide 19A.C that prevented its coupling to the linker, and the low yield of CCMV-19A.C conjugate must have been due to other factors.

CPMV-Peptide Conjugates with Sulfo-SMCC

Using SPDP to couple the peptide to CCMV caused unwanted aggregation and low yields of conjugates, so another linker, sulfo-SMCC, was also tried. Like SPDP, sulfo-SMCC is a heterobifunctional linker that linked

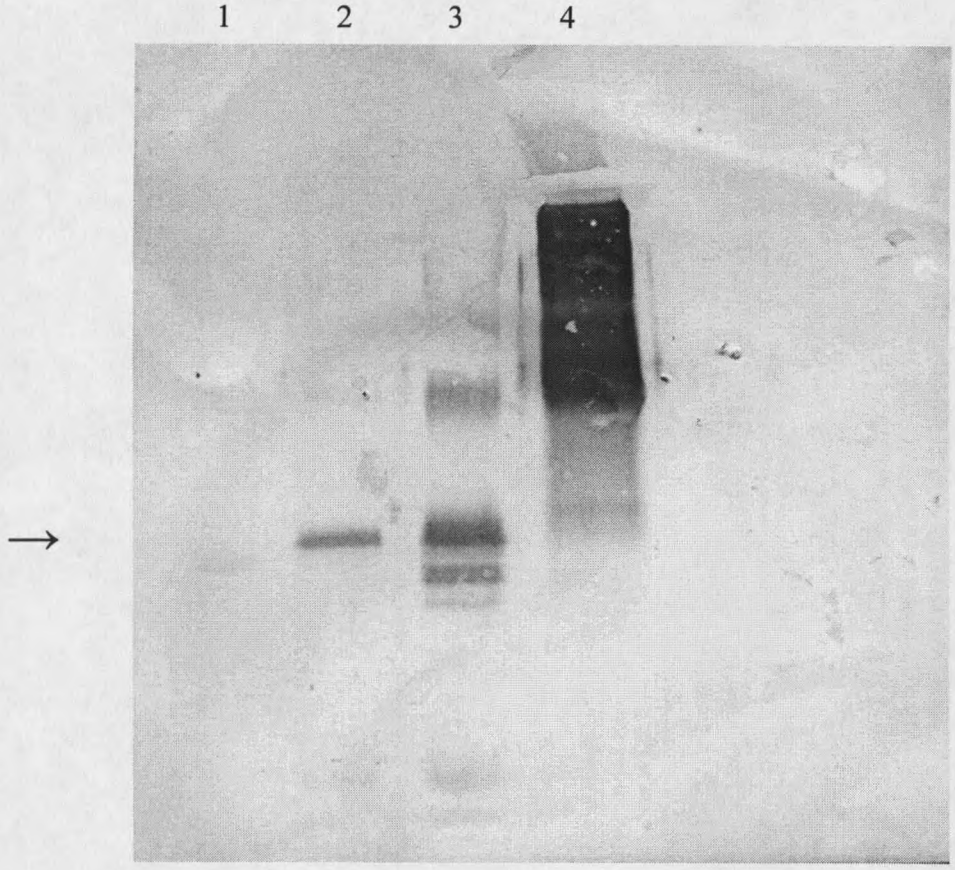


Fig 4.3. Western blot analysis of CCMV-19A.C conjugation using SPDP. Proteins were separated on a 12.5% SDS-PAGE gel and blotted to a PVDF membrane under non-reducing conditions. The peptide was bound with mouse anti-KLH-19A.C serum and then detected by alkaline phosphatase-labeled goat anti-mouse IgG. The presence of peptide is indicated by the arrow. Lane1, unconjugated coat protein; lane 2 and 3, different amounts of CCMV-19A.C conjugate ; lane 4, OVA-19A.C conjugate used as a positive control.

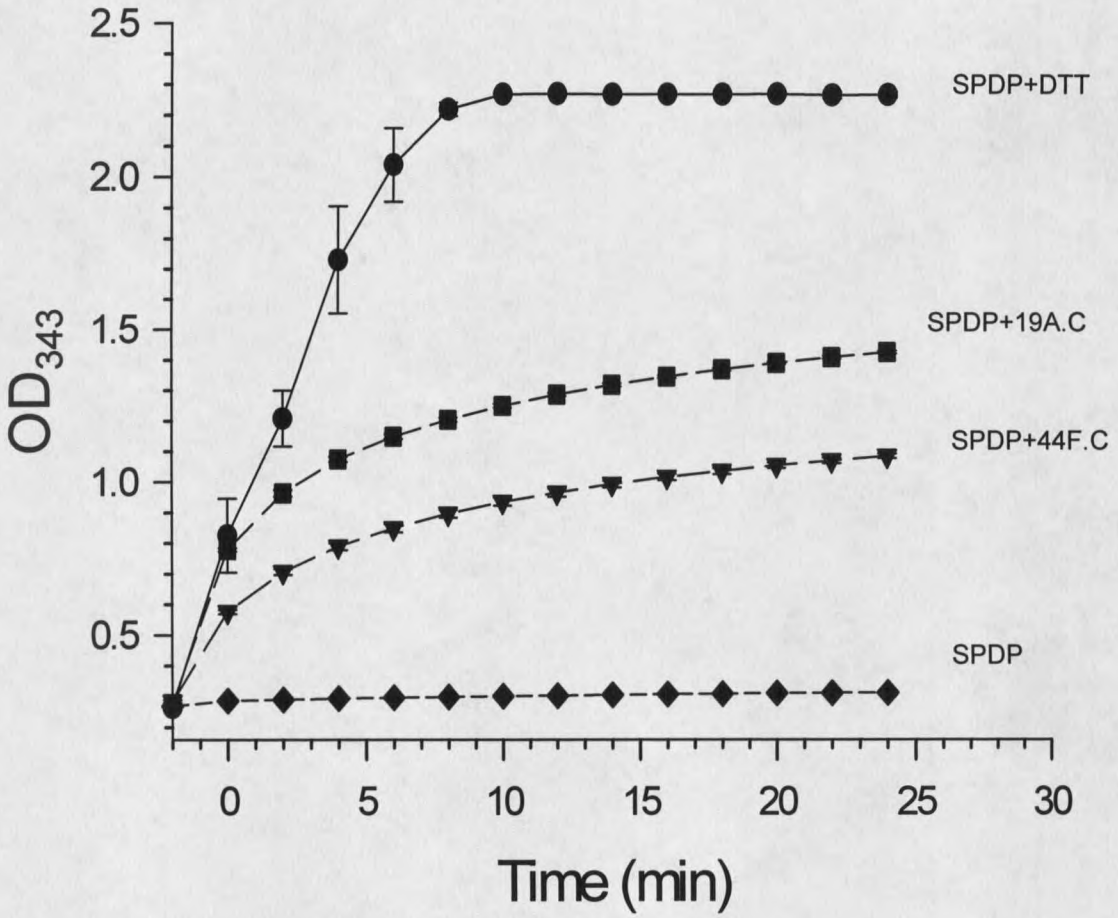


Fig 4.4. Peptide kinetics. The reaction between 2 pyridyl-disulfide group on SPDP linker and thiol group on a peptide was monitored by measuring the amount of pyridyl-2 thione group released at 343 nm before and after adding the linker. DTT was used in place of peptide as a positive control and SPDP alone was a negative control. Error bars indicate the standard deviation of the triplicate samples (for most points these are smaller than the symbols shown). Experiment was performed by R. Pomwised.

cysteine sulfhydryl groups on the peptides to amino groups on the lysine side chain of the virus. An experiment was performed to test whether sulfo-SMCC was more effective than SPDP, in terms of more coupling to CCMV subunits and less aggregation. The result, however, was a similar pattern on SDS-PAGE silver staining gel (data not shown). Therefore, another virus, CPMV, was chosen as a scaffold to attach the peptide, because CPMV contains only one reactive lysine on its surface for each asymmetric unit or 60 per virion. The hope was that the unwanted reaction causing virus aggregation might be reduced compared to CCMV. The SDS-PAGE profile of the CPMV coat protein showed that adding sulfo-SMCC alone to CPMV made the 2 small subunit bands and the one large subunit band migrate slower than unreacted coat protein bands (Fig. 4.5, lane 2 compared to lane 1). A virus dimer and multimers were also observed at this step, as had been seen for CCMV. When peptide 44F.C was added to the virus-linker mixture, the amount of lower small subunit band was dramatically reduced and the upper band of the small subunit had 3 additional bands stacking on top, suggesting that more than 1 peptide reacting with each small subunit (Fig. 4.5, lane 3). Western blot analysis using anti-KLH 44F.C antiserum revealed the presence of 44F.C peptide on the upper small subunit band and 3 additional slowly migrating bands. Moreover, the peptide was also detected on the large subunit of the virus (Fig. 4.6, lane 1). The peptide was not detected in unreacted virus or the virus-linker mixture (Fig. 4.6, lane 2 and 3). Attaching of peptide 19A.C to CPMV resulted in a similar pattern, both on silver

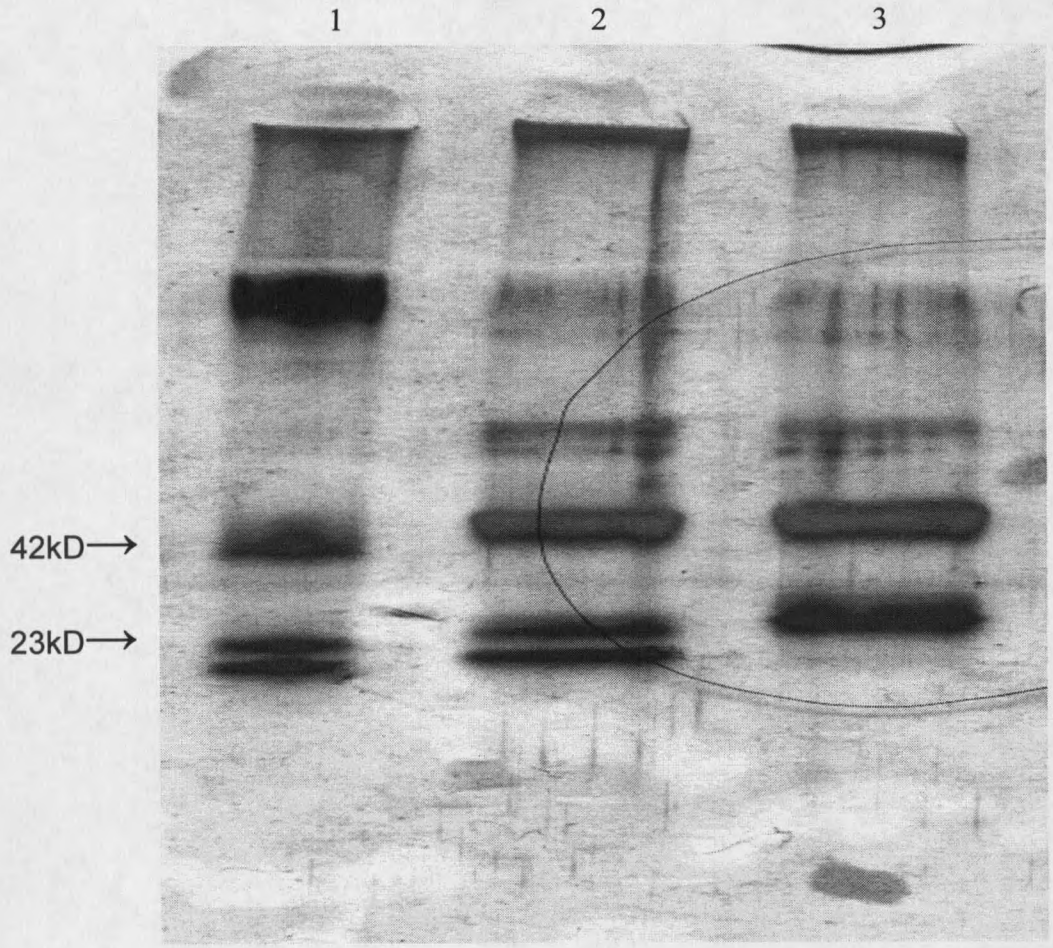


Fig 4.5. Silver stained gel of CPMV-44F.C conjugated using sulfo-SMCC. Proteins were separated on a 12.5% SDS-PAGE gel and stained with silver nitrate solution. Small and large subunits of CPMV coat protein are indicated by arrows. Lane 1, unconjugated CPMV coat proteins; lane 2, CPMV incubated with sulfo-SMCC only; lane 3, CPMV-44F.C-conjugate.

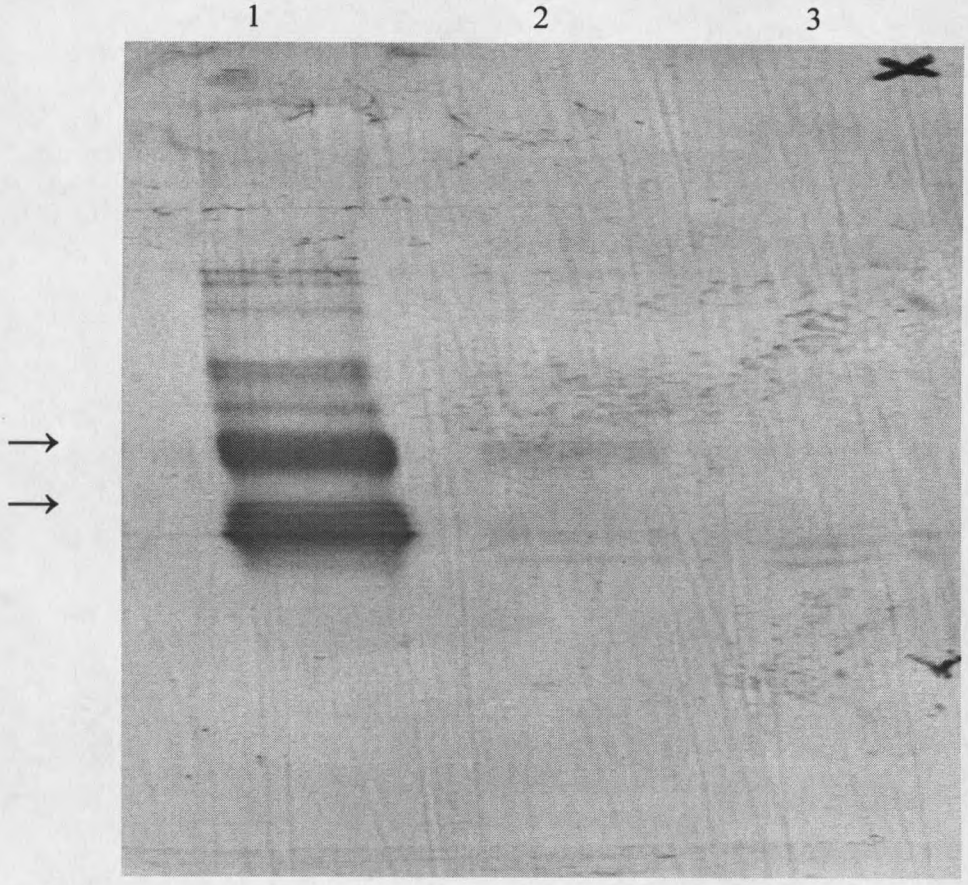


Fig 4.6. Western analysis of CPMV-44F.C conjugated using sulfo-SMCC. Proteins were separated on a 12.5% SDS-PAGE gel and blotted to a PVDF membrane. The membrane was incubated with mouse anti-KLH44F.C serum, followed by alkaline phosphatase-labeled goat anti-mouse IgG. The antibodies recognized peptide44F.C attached to the small and large subunits of the coat protein. The presences of peptides on small and large subunit are indicated by arrows. Lane1, CPMV-44F.C-conjugate; lane2, CPMV incubated with sulfo-SMCC only; lane 3, unconjugated coat protein.

staining of the SDS-PAGE gel and Western blot analysis (Fig. 4.7 and 4.8, respectively). Based on SDS-PAGE profile, both of the peptides seemed to couple more to CPMV than to CCMV. To confirm that result, the amount of the peptide on the conjugate was determined by ELISA analysis using anti-KLH44 or anti-KLH19 polyclonal antibodies for their corresponding peptides (Fig. 4.9). Comparison of the coupling yield between both virus carriers demonstrated that peptide 44F.C and 19A.C were attached to CPMV more effectively than to CCMV. In spite of the fact that CCMV should have 180 attachment sites whereas CPMV has only 60.

Immunogenicity of Peptides in CCMV Conjugate-Immunized Mice

Mice were immunized with CCMV-peptide conjugates in CFA and boosted in IFA. The sera from these mice were tested for their reactivity to the peptides by ELISA. OVA-44F.C or OVA-19A.C was coated on the wells and the binding of sera to antigen was measured using goat-anti-mouse AP conjugate. Sera from 3 mice immunized with CCMV-44F.C in the first bleed (after the first boost) had titers ranging from 1:1,000-1:10,000 (Fig. 4.10). After a second boost the titer of the sera was increased to 1:10,000-1:50,000 (Fig. 4.11). Antibodies against the carrier were also measured by coating the wells with CCMV; these titers were greater than 1:100,000 (Fig. 4.12).

In contrast, sera from mice inoculated with CCMV-19 showed great variation between the 3 mice. One of these mice seemed to have a very low

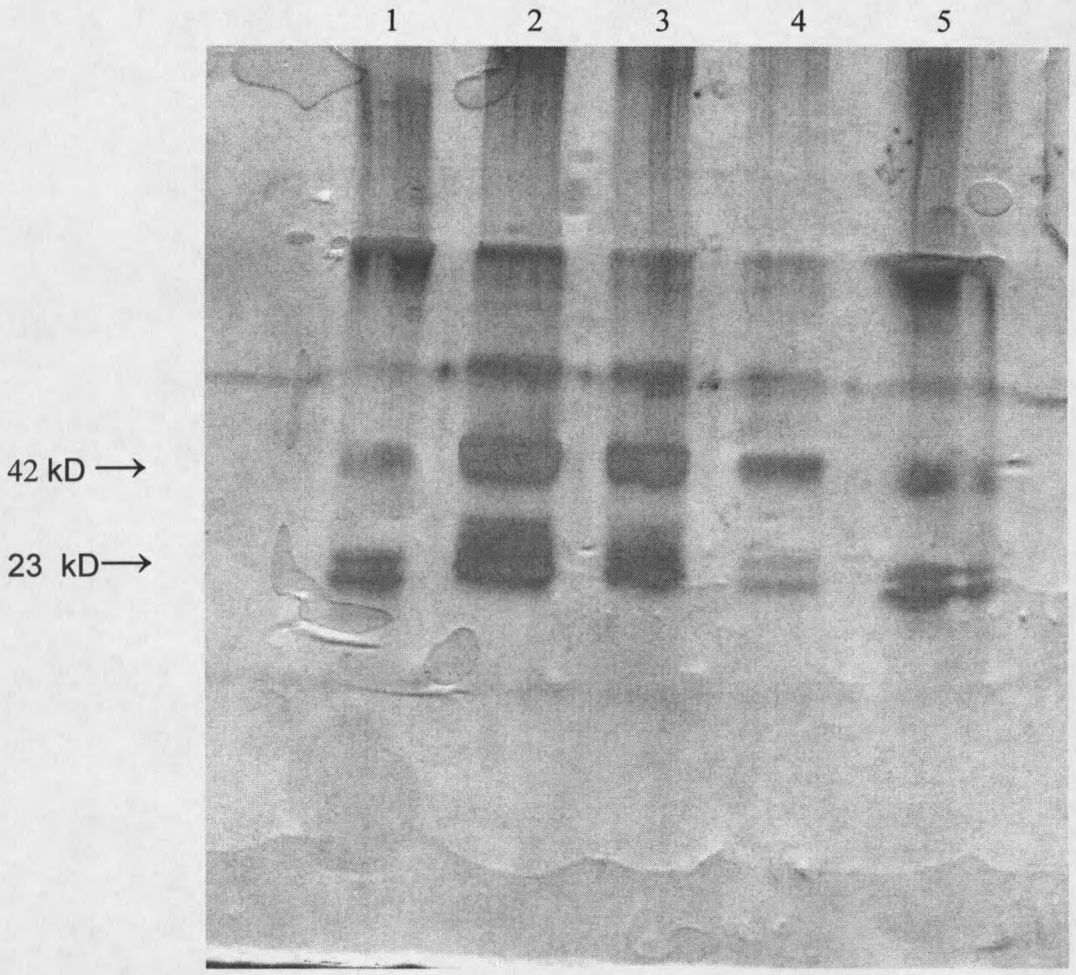


Fig 4.7. Silver stained gel of CPMV-19A.C conjugated using sulfo-SMCC. Proteins were separated on a 12.5% SDS-PAGE gel and stained with silver nitrate solution. Small and large subunits of CPMV coat protein are indicated by arrows. Lanes 1 and 5, unconjugated CPMV coat protein; lanes 2 and 3, peptide 19A.C-conjugated coat protein; lane 4, coat protein incubated with sulfo-SMCC only.

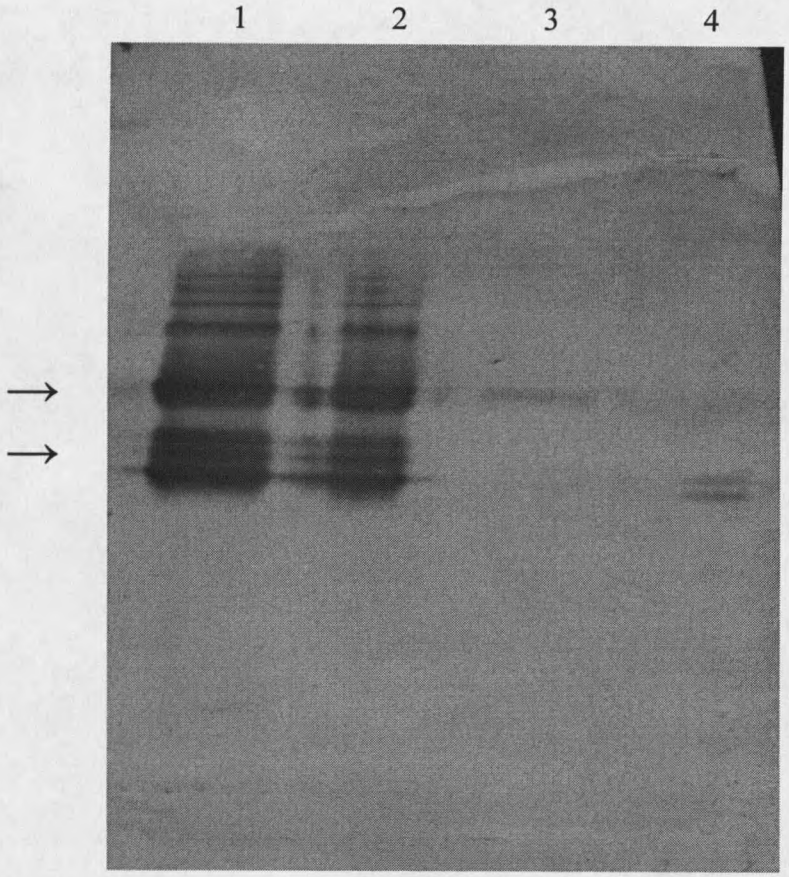


Fig 4.8. Western blot of CPMV-19A.C conjugated using sulfo-SMCC.
Proteins were separated on a 12.5% SDS-PAGE gel and blotted to a PVDF membrane. The mouse anti-KLH19A.C serum bound peptide19A.C attached to the small and large subunits of coat protein. The antigen-bound antibody was subsequently detected with alkaline phosphatase-labeled goat anti-mouse IgG. The presence of peptide is indicated by arrows. Lanes 1 and 2, CPMV-19A.C conjugate; lane 3, coat protein incubated with sulfo-SMCC only; lane 4, unconjugated coat protein.

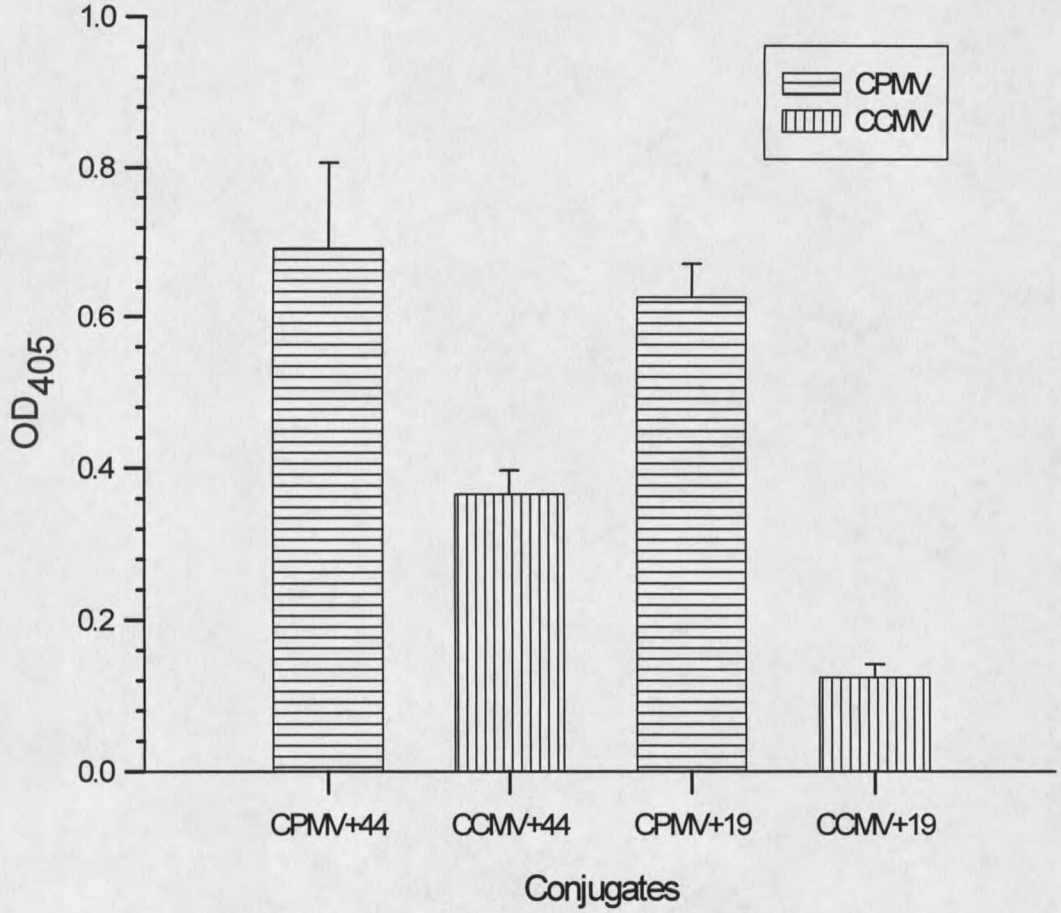


Fig 4.9. Comparison of the amount of peptides coupled to virus coat protein evaluated by ELISA. The amounts of peptide were measured on plates coated with 0.5 μg conjugates. Either mouse anti-KLH44F.C or anti-KLH19A.C serum at dilution 1:3,000 was added to wells coated with the corresponding peptide conjugate. The antigen-bound antibody was detected with alkaline phosphatase -labeled goat anti-mouse IgG. The OD values shown are the mean of triplicate samples minus the background reading obtained from the binding of antibody to unconjugated coat protein. Error bars indicate the standard deviation (SD) of the triplicate samples.

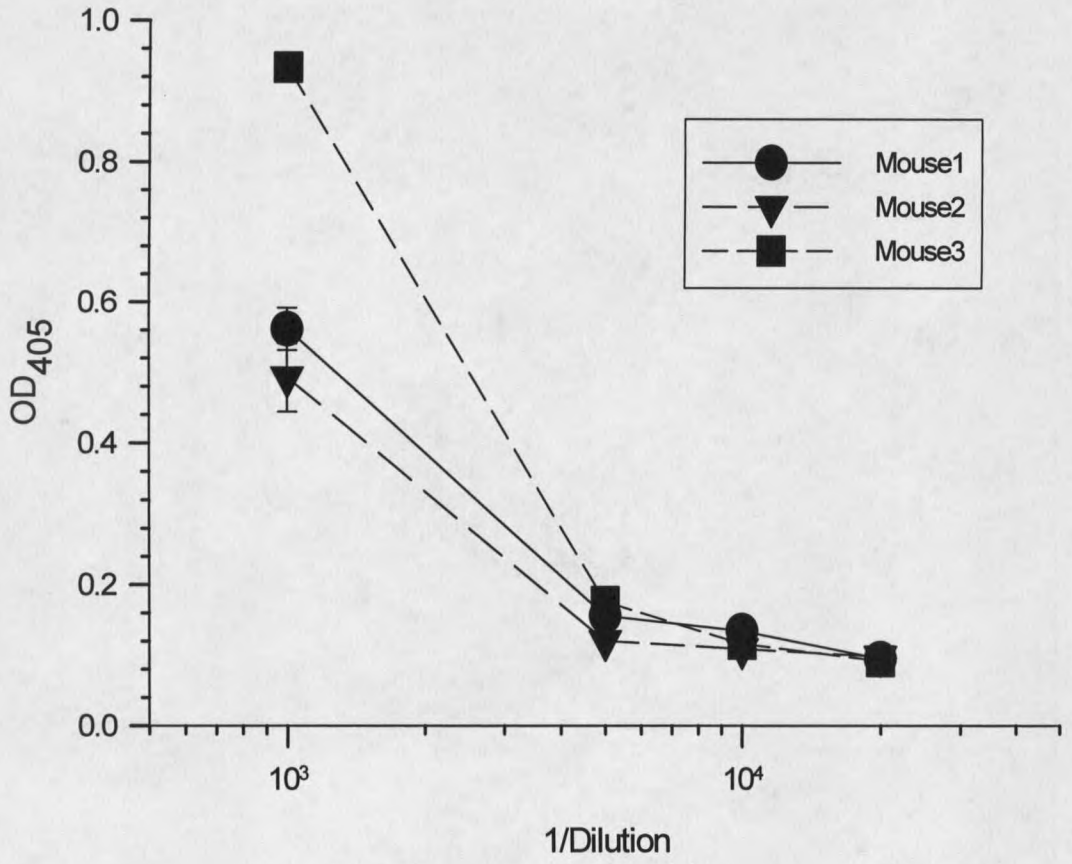


Fig 4.10. Anti-peptide activity of the first bleed sera from CCMV-44F.C immunized mice by ELISA. Mice were immunized with the conjugate in complete Freund's adjuvant (CFA) and boosted once in incomplete Freud's adjuvant (IFA). Serial dilutions of sera were added to wells coated with 0.1 μg OVA-44. The reactivity to peptide44F.C was detected using goat anti-mouse alkaline phosphatase conjugate. OD_{405} values that were greater than twice the background obtained from sera binding to unconjugated OVA coated wells at dilution 1:1,000 were considered positive (usually >0.16). All OD values shown are the mean of duplicate samples with SD shown as error bars.

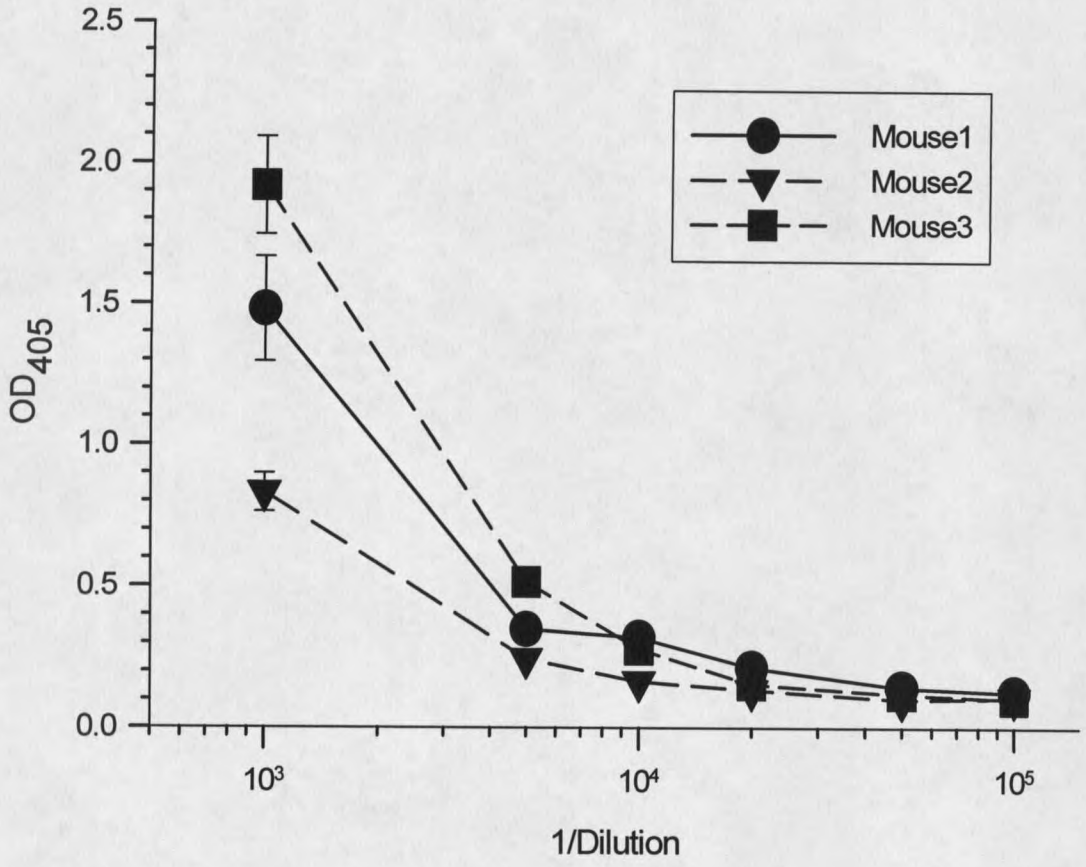


Fig 4.11. Anti-peptide activity of the second bleed sera from CCMV-44F.C immunized mice by ELISA. Mice were immunized with the conjugate in complete Freund's adjuvant (CFA) and boosted twice in IFA. Serial dilutions of sera were added to wells coated with 0.1 μg OVA-44. The reactivity to peptide44F.C was detected using goat anti-mouse alkaline phosphatase conjugate. OD_{405} values that were greater than twice the background obtained from sera binding to unconjugated OVA coated wells at dilution 1:1,000 were considered positive (usually >0.16). All OD values shown are the mean of duplicate samples with SD shown as error bars.

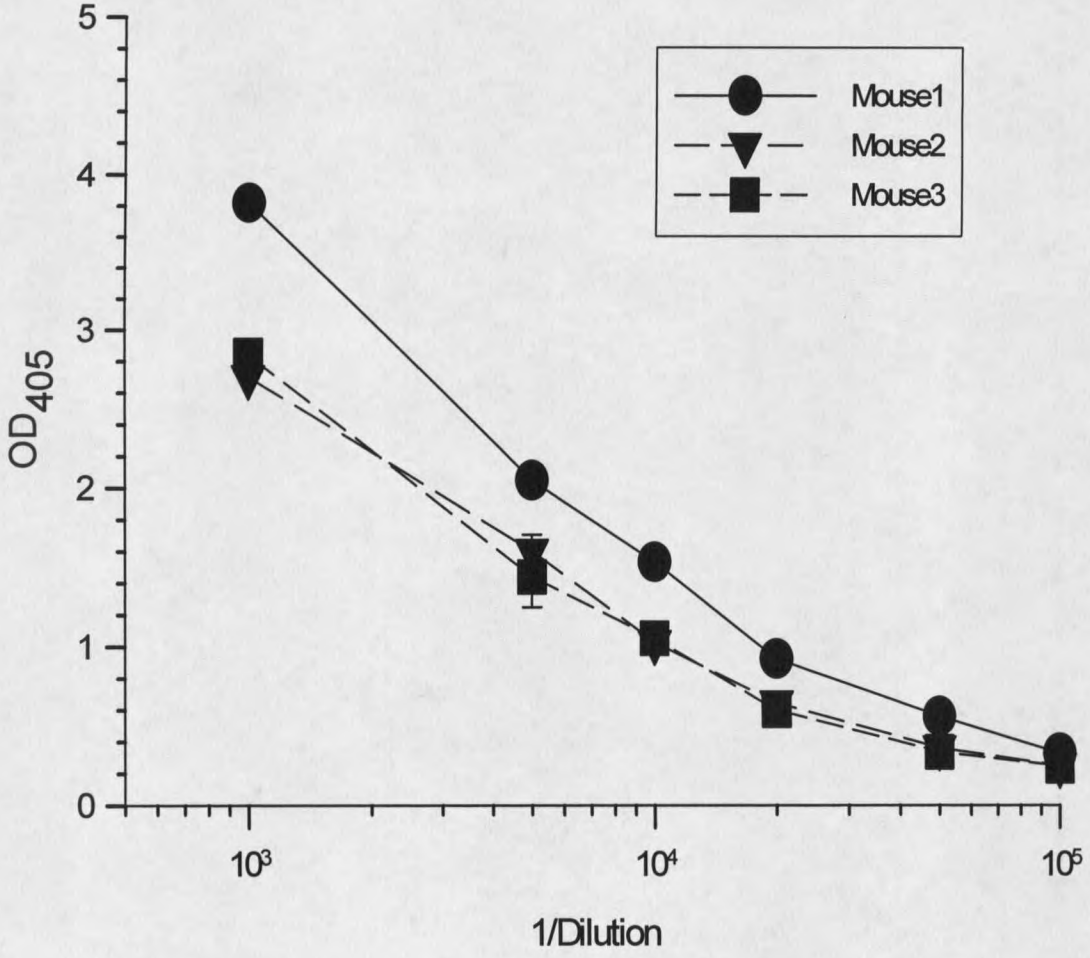


Fig 4.12. Anti-carrier activity of sera from CCMV-44F.C immunized mice. ELISA plates were coated with CCMV at 0.5 μg/well. Mouse sera were added to wells in serial dilutions and detected using goat anti-mouse alkaline phosphatase conjugate. The binding of pre-immune sera to the virus at dilution 1:1,000 usually gave OD value <0.10 and was used as a negative control. All OD values shown are the mean of duplicate samples with SD shown as error bars.

anti-peptide titer of 1:1,000 (Fig. 4.13), which was slightly increased after being boosted (Fig. 4.14). However, other mice had a high titer in the first bleed, which was further increased in the second bleed. Thus, the overall anti-peptide titer in these mice ranged from 1:10,000 to more than 1:100,000 (Fig. 4.14). Interestingly, sera from all 3 mice, including the one with low anti-peptide activity, showed very high antibody titers against the carrier (above 1:100,000) (Fig. 4.15). These results demonstrated that the peptide linked on the surface of CCMV coat protein was exposed to the immune system of the mice and elicited antibodies, although there were some variations between mice. Moreover, CCMV is a strong immunogen and induces high anti-carrier antibody titers.

Immunogenicity of Peptides in CPMV Conjugate-Immunized Mice

The immune response of mice immunized with CPMV-44 showed that sera from 3 mice had antibody titer against the peptide 44F.C in the range from 1:10,000 to above 1:20,000 in the first bleed (Fig. 4.16). Surprisingly, in the second bleed all mice had decreased titers ranging from 1:5,000-1:20,000 (Fig. 4.17). Mice that used to have high titers had markedly decreased titers. This pattern was also observed in mice immunized with CPMV-19. In the first bleed, sera had titers against peptide 19A.C from 1:1,000-1:20,000 (Fig. 4.18). When mice got the boost the titer dropped down in the range from 1:1,000-1:5,000. The titer of mouse 2 showed the biggest change, while that of the mouse 1 had a modest decrease. Mouse 3 had no anti-peptide 19A.C ELISA reactivity

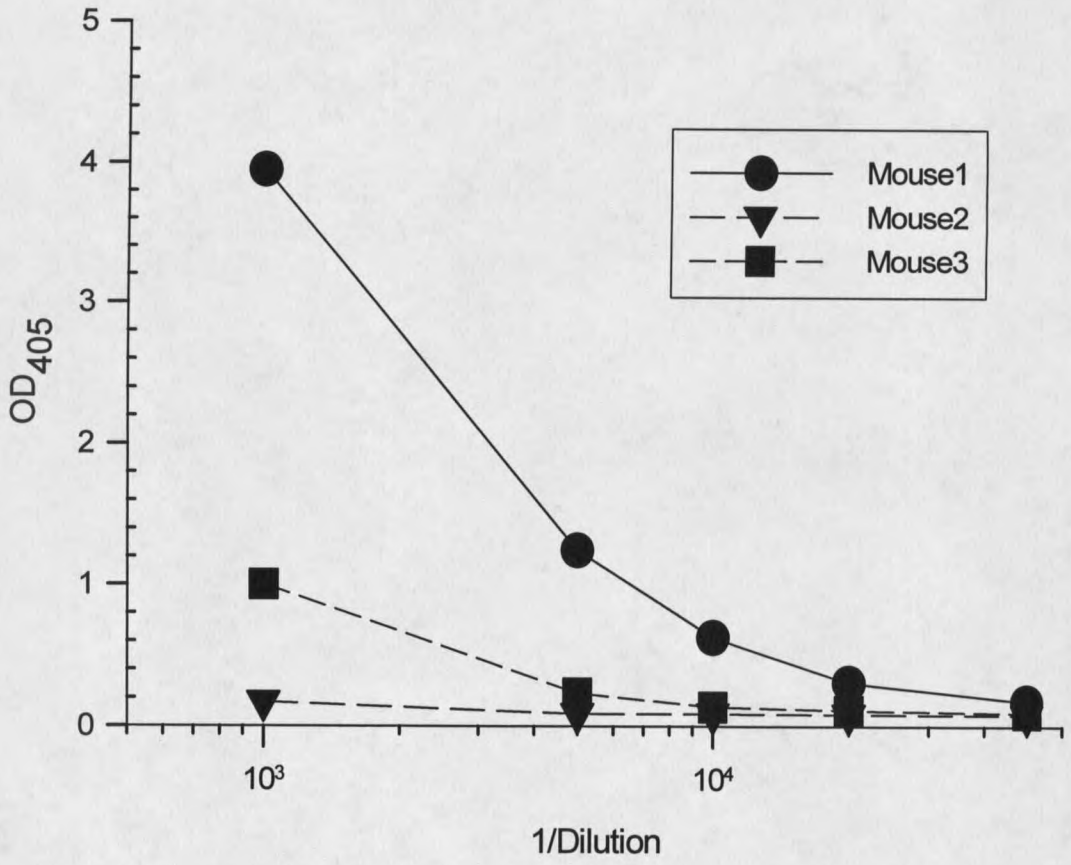


Fig 4.13. Anti-peptide activity of the first bleed sera from CCMV-19A.C immunized mice by ELISA. Mice were immunized with the conjugate in CFA and boosted once in IFA. Serial dilutions of sera were bound to wells coated with 0.1 μg OVA-19A.C. The reactivity to peptide19A.C was detected using goat anti-mouse alkaline phosphatase conjugate. OD_{405} values that were greater than twice the background obtained from sera binding to unconjugated OVA coated wells at dilution 1:1,000 were considered positive (usually >0.16). All OD values shown are the mean of duplicate samples with SD shown as error bars.

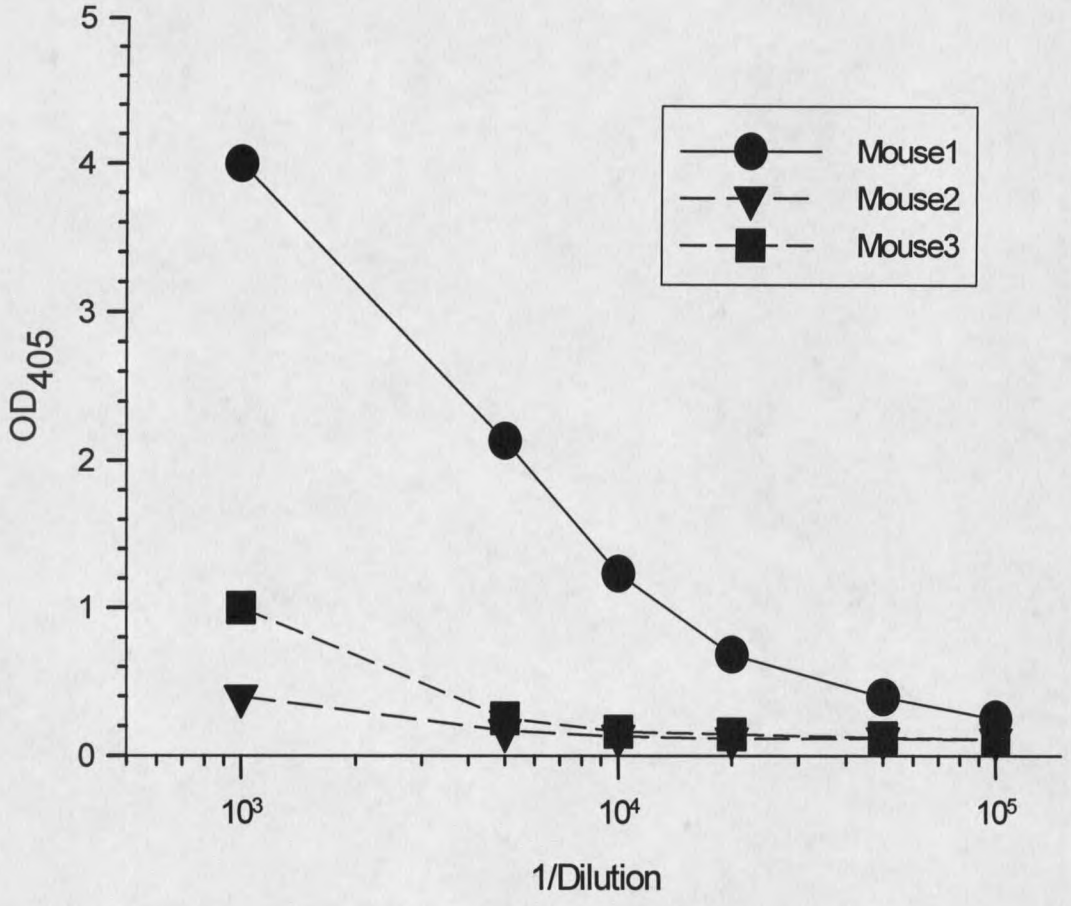


Fig 4.14. Anti-peptide activity of the second bleed sera from CCMV-19A.C immunized mice by ELISA. Mice were immunized with the conjugate in CFA and boosted twice with IFA. Serial dilutions of sera were bound to wells coated with 0.1 μg OVA-19A.C. The reactivity to peptide19A.C was detected using goat anti-mouse alkaline phosphatase conjugate. OD_{405} values that were greater than twice the background obtained from sera binding to unconjugated OVA coated wells at dilution 1:1,000 were considered positive (usually >0.16). All OD values shown are the mean of duplicate samples with SD shown as error bars.

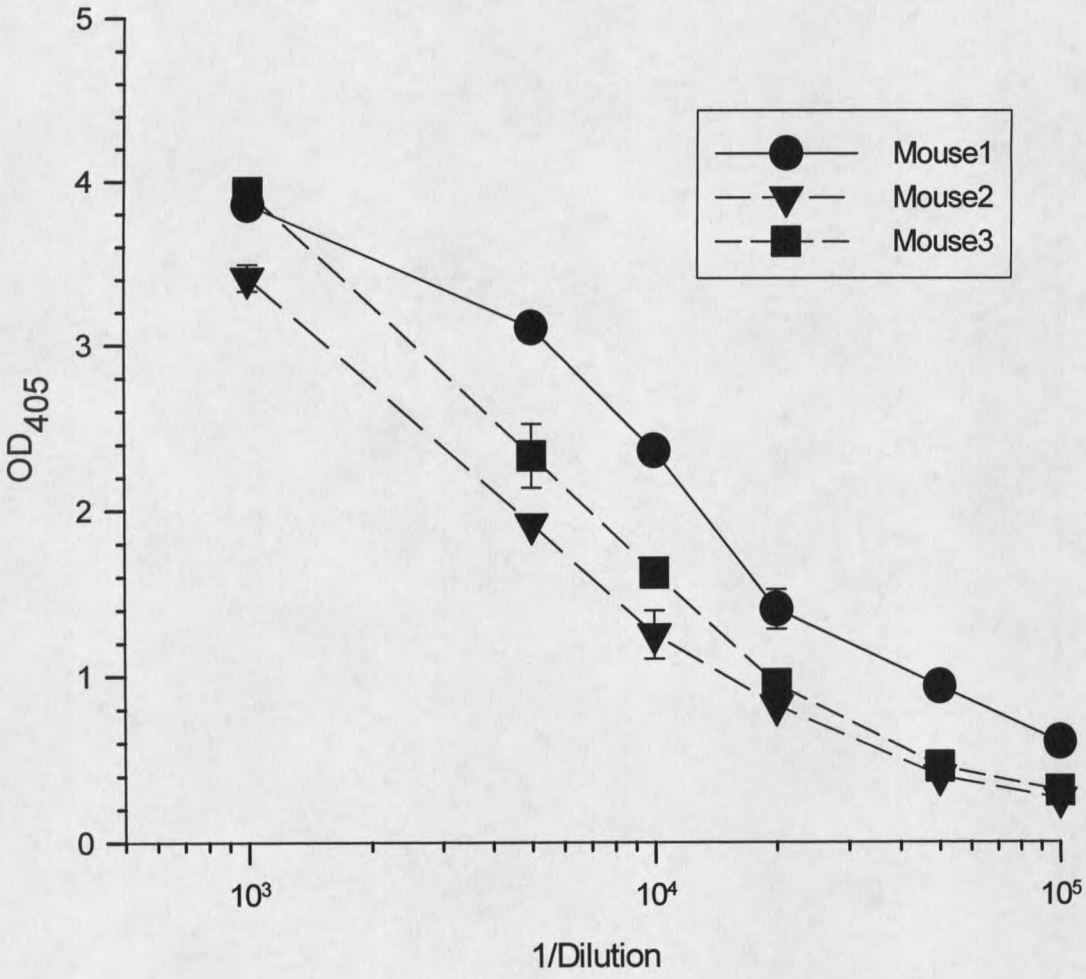


Fig 4.15. Anti-carrier activity of the second bleed sera from CCMV-19A.C immunized mice. ELISA plates were coated with CCMV at 0.5 μg/well. Mouse sera were added to wells in serial dilutions and detected by goat anti-mouse alkaline phosphatase conjugate. The binding of pre-immune sera to the virus at dilution 1:1,000 usually gave OD value <0.10 and was used as a negative control. All OD values shown are the mean of duplicate samples with SD shown as error bars.

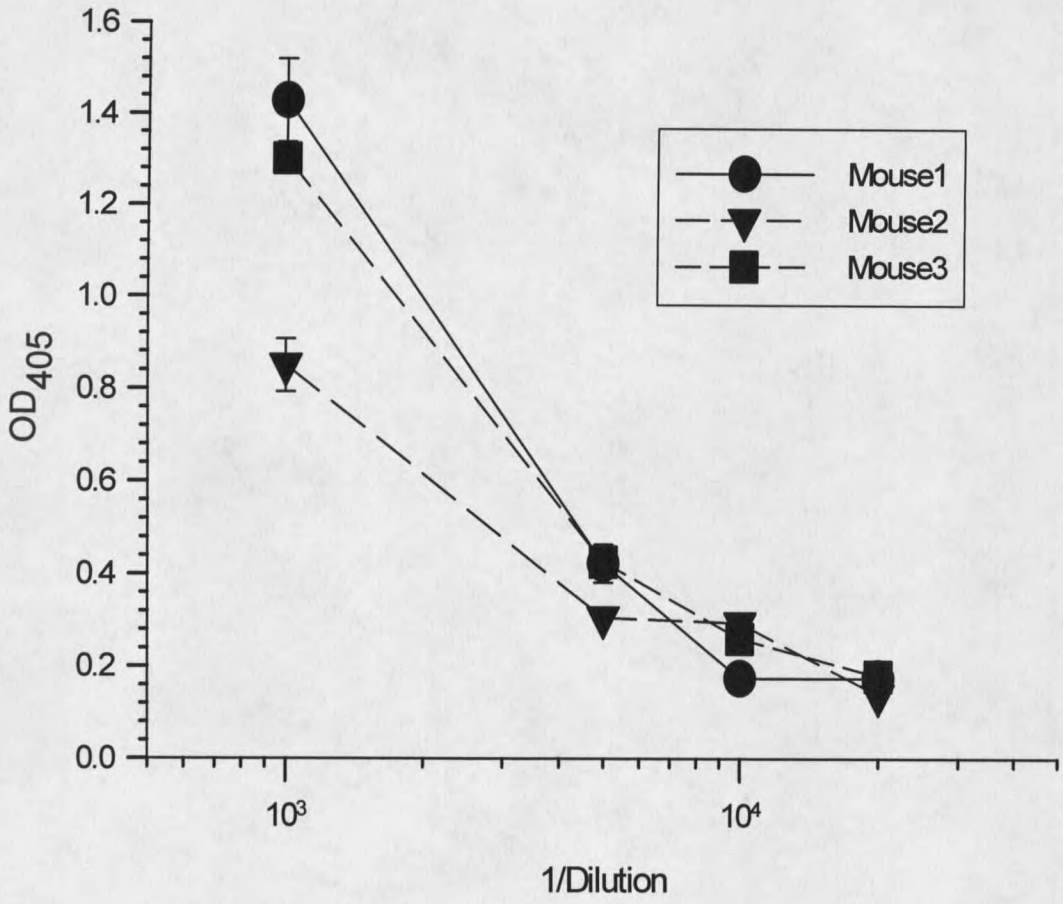


Fig 4.16. Anti-peptide activity of the first bleed sera from CPMV-44F.C immunized mice by ELISA. Mice were immunized with the conjugate in CFA and boosted once in IFA. Serial dilutions of sera were bound to wells coated with 0.1 μg OVA-44. The reactivity to peptide 44F.C was detected using goat anti-mouse alkaline phosphatase conjugate. OD_{405} values that were greater than twice the background obtained from sera binding to unconjugated OVA coated wells at dilution 1:1,000 were considered positive (usually >0.16). All OD values shown are the mean of triplicate samples with SD shown as error bars.

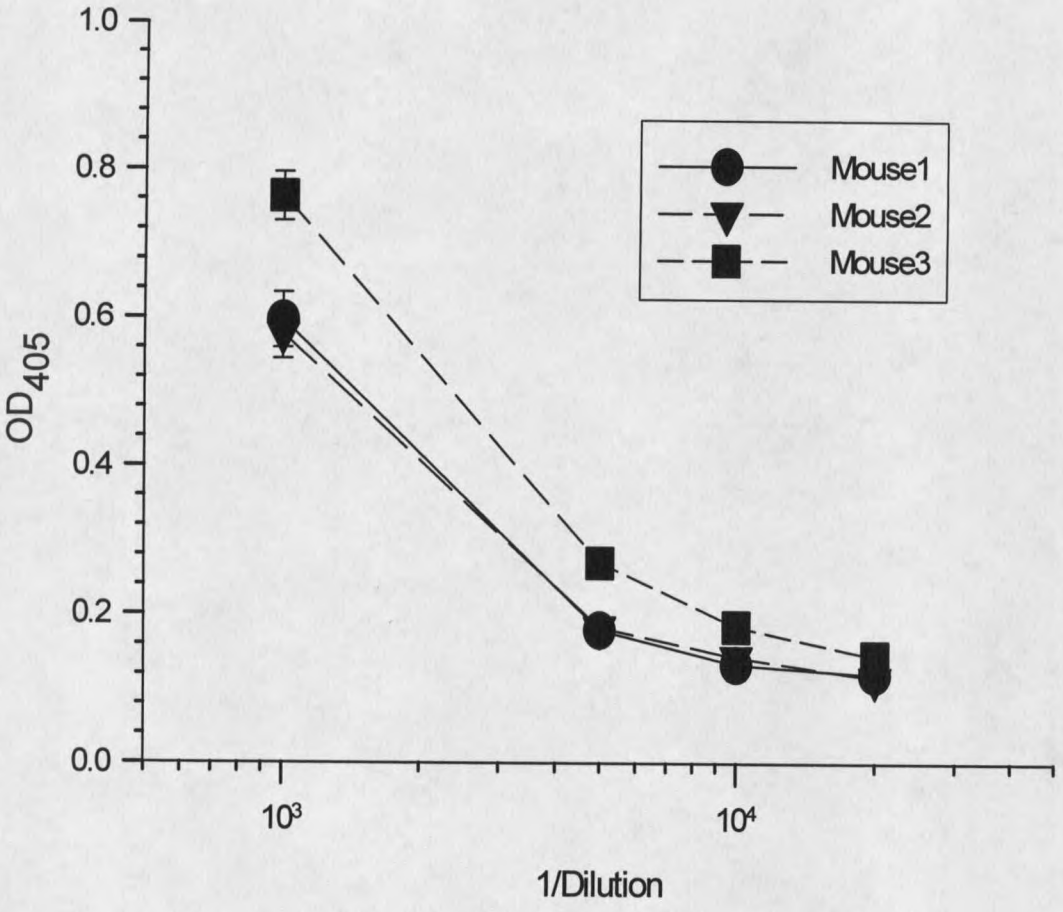


Fig 4.17. Anti-peptide activity of the second bleed sera from CPMV-44F.C immunized mice by ELISA. Mice were immunized with the conjugate CFA and boosted twice in IFA. Serial dilutions of sera were bound to wells coated with 0.1 μg OVA-44. The reactivity to peptide 44F.C was detected using goat anti-mouse alkaline phosphatase conjugate. OD_{405} values that were greater than twice the background obtained from sera binding to unconjugated OVA coated wells at dilution 1:1,000 were considered positive (usually >0.16). All OD values shown are the mean of duplicate samples with SD shown as error bars.

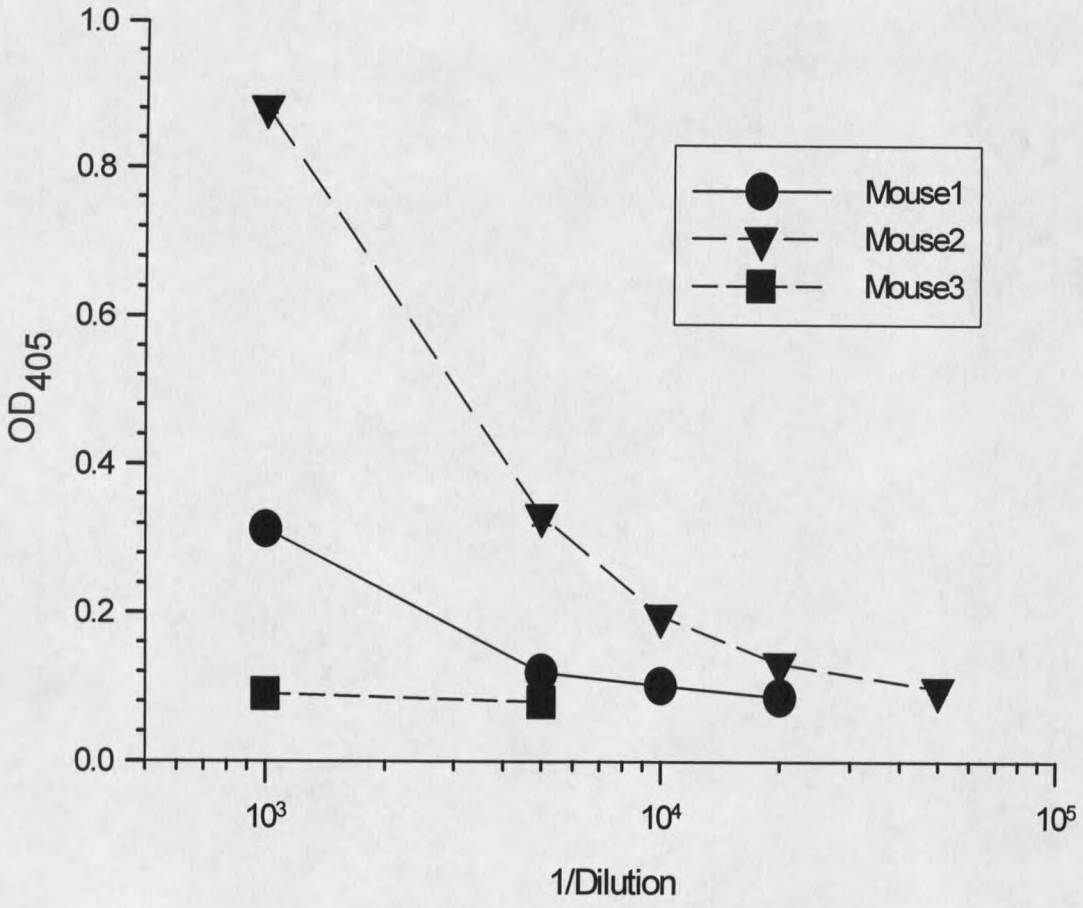


Fig 4.18. Anti-peptide activity of the first bleed sera from CPMV-19A.C immunized mice by ELISA. Mice were immunized with the conjugate in CFA and boosted once in IFA. Serial dilutions of sera were bound to wells coated with 0.1 μg OVA-19A.C. The reactivity to peptide 19A.C was detected using goat anti-mouse alkaline phosphatase conjugate. OD_{405} values that were greater than twice the background obtained from sera binding to unconjugated OVA coated wells at dilution 1:1,000 were considered positive (usually >0.16). All OD values shown are the mean of duplicate samples with SD shown as error bars.

(Fig. 4.18 and 4.19). The titer of anti-carrier antibodies was measured in mice inoculated with either CPMV-44 or CPMV-19 (Fig. 4.20 and 4.21, respectively). The sera from both conjugates showed high titers, which were more than 1:20,000 in all mice, indicating that CPMV also was a strong immunogen in inducing anti-carrier antibody titer. However, the anti-peptide antibody titers were lower than those obtained with CCMV conjugates after boosting.

Cysteine Mutants of CCMV

Sera from mice immunized with CCMV-peptide conjugates had high reactivity to the respective peptides. However, it was thought that the titer of antibodies against the peptide might be increased, if more peptide could be coupled to each CCMV virion. As shown in Fig. 1, peptide 44F.C had been linked to fewer than half of the CCMV coat protein subunits, while the degree of conjugation with peptide 19A.C was much less than that. To increase the yields of the conjugations, it was necessary to reduce viral aggregation and allow only one linker to attach to each subunit of the virus. This had been difficult, since each subunit has 3 or 4 lysine residues exposed on the surface of the CCMV virion. Since there was no cysteine residue on the surface of the virus, the reaction would be more controllable if a single cysteine could be introduced at a suitable location and then used to attach the peptide. Using site-directed mutagenesis, cysteine was substituted for residues S73, S130, or A152 in a background of the salt stable (K42R) CCMV coat protein. After electroporation

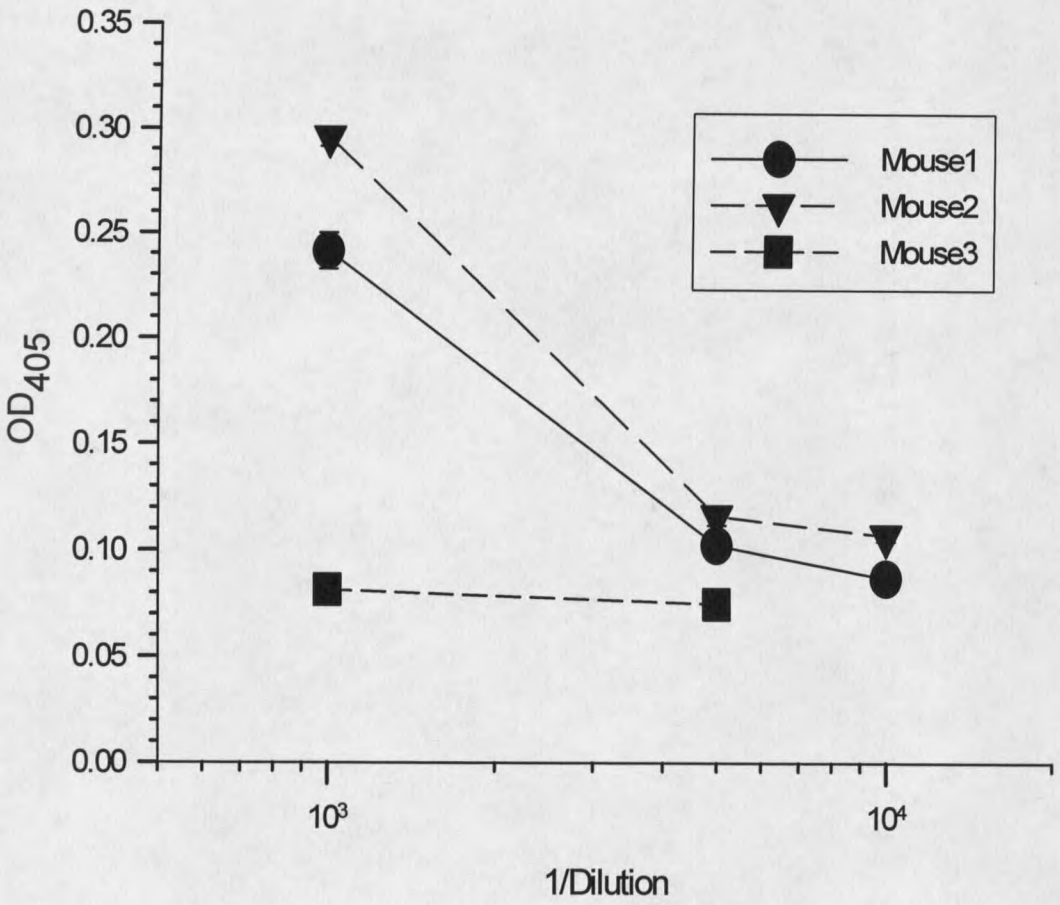


Fig 4.19. Anti-peptide activity of the second bleed sera from CPMV-19A.C immunized mice by ELISA. Mice were immunized with the conjugate in CFA and boosted twice in IFA. Serial dilutions of sera were bound to wells coated with 0.1 μg OVA-19A.C. The reactivity to peptide 19A.C was detected using goat anti-mouse alkaline phosphatase conjugate. OD_{405} values that were greater than twice the background obtained from sera binding to unconjugated OVA coated wells at dilution 1:1,000 were considered positive (usually >0.16). All OD values shown are the mean of triplicate samples with SD shown as error bars.

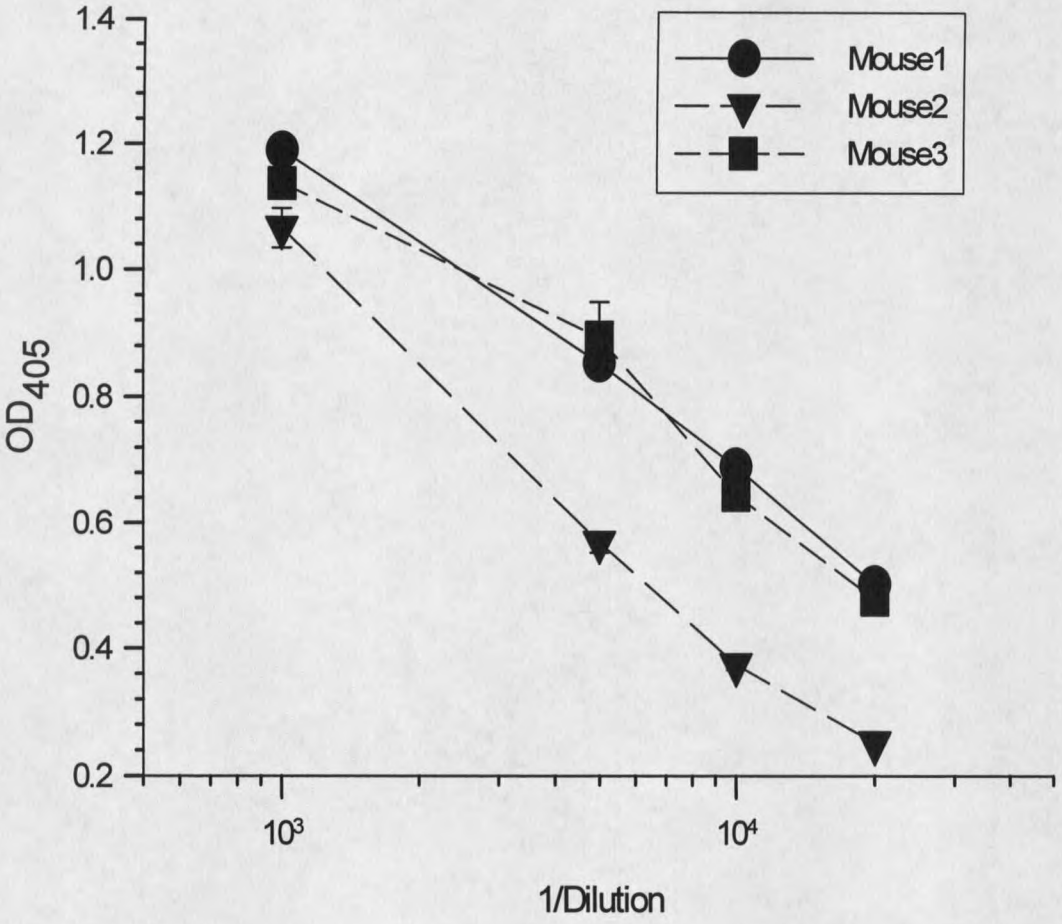


Fig 4.20. Anti-carrier activity of sera from CPMV-44F.C immunized mice. ELISA plates were with CPMV at 0.5 μg/well. Mouse sera from the second bleed were added to wells in serial dilutions and detected using goat anti-mouse alkaline phosphatase conjugate. The binding of pre-immune sera to the virus at dilution 1:1,000 usually gave OD value <0.10 and was used as a negative control. All OD values shown are the mean of duplicate samples with SD shown as error bars.

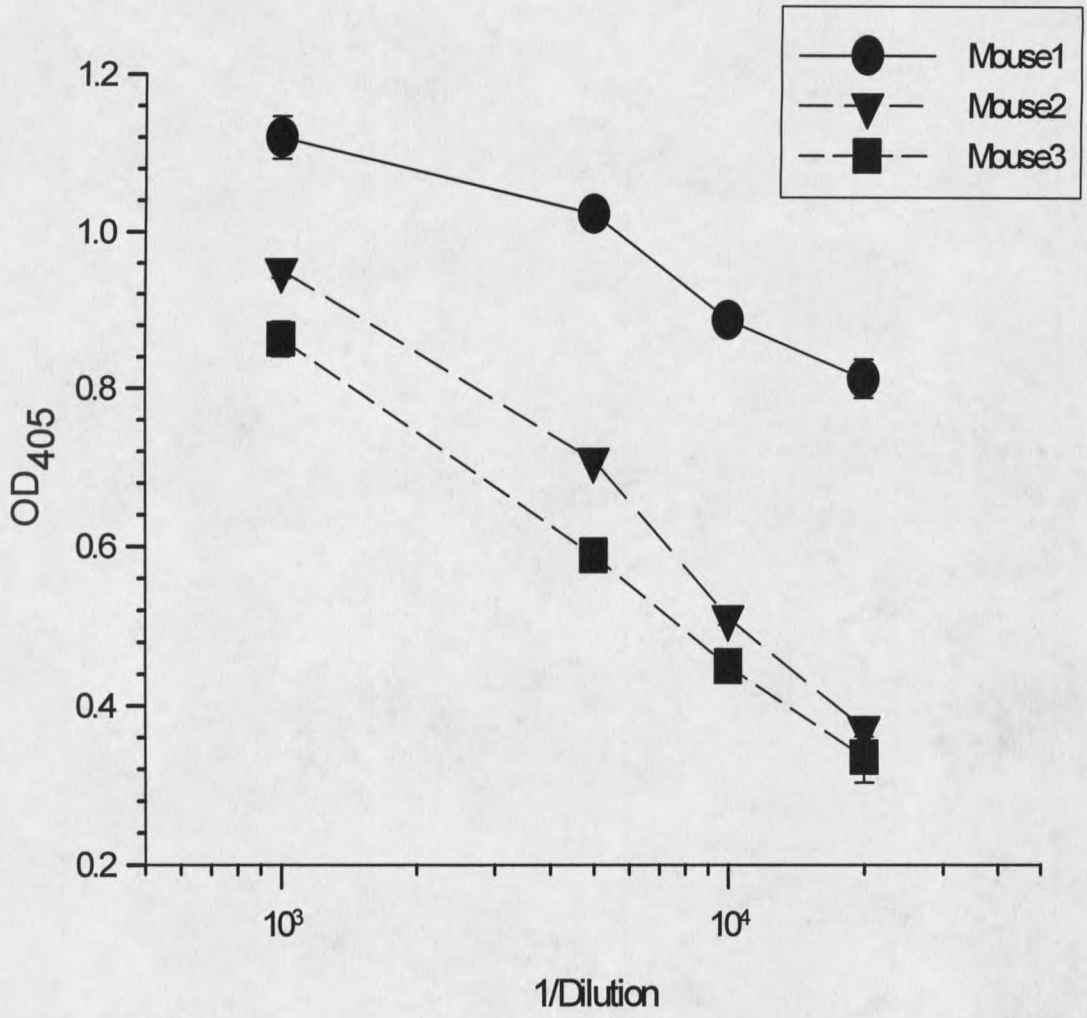


Fig 4.21. Anti-carrier activity of sera from CPMV-19A.C immunized mice. ELISA plates were coated with CPMV at 0.5 μg/well. Mouse sera from the second bleed were added to wells in serial dilutions and detected using goat anti-mouse alkaline phosphatase conjugate. The binding of pre-immune sera to the virus at dilution 1:1,000 usually gave OD value <0.10 and was used as a negative control. All OD values shown are the mean of duplicate samples with SD shown as error bars.

of each linearized plasmid containing a mutant coat protein gene into *Pichia pastoris*, the yeast colonies were screened by direct PCR for DNA integration (Fig. 4.22 A and B). The PCR products showed bands with the expected molecular weight (lane 4A, 1B, 3B for 73C, lane 5A, 5B, 7B for 130C and lane 8A, 8B for 152C) while water in the place of chromosomal DNA used as a negative control had no signal (lane 10 A and B). To confirm the single amino acid change, these transformants with positive PCR products were sequenced. All had the correct sequence (data not shown).

Expression Screening of CCMV Mutants

Yeast clones with the correct amino acid change were grown in 1-ml small-scale cultures for expression analysis by dot blot (Fig. 4.23). 8 out of 9 transformants had high expression at a similar level to the wild-type (K42R) control. 2 clones of each mutant were selected and grown in 1 liter-cultures for medium scale expression. After a period of derepression and MeOH induction, yeast cells were lysed and virus particles were isolated. All 3 mutants produced T=3 particles indistinguishable from wild type in terms of size and shape. The S130C virions are shown in Figure 4.24. This demonstrated that creating single amino acid changes at residue 73, 130 and 152 in the salt stable background had no effect on the stability of virions. Moreover, the yields of mutants produced were comparable to those of the wild type or the K42R (salt stable) parent strain.

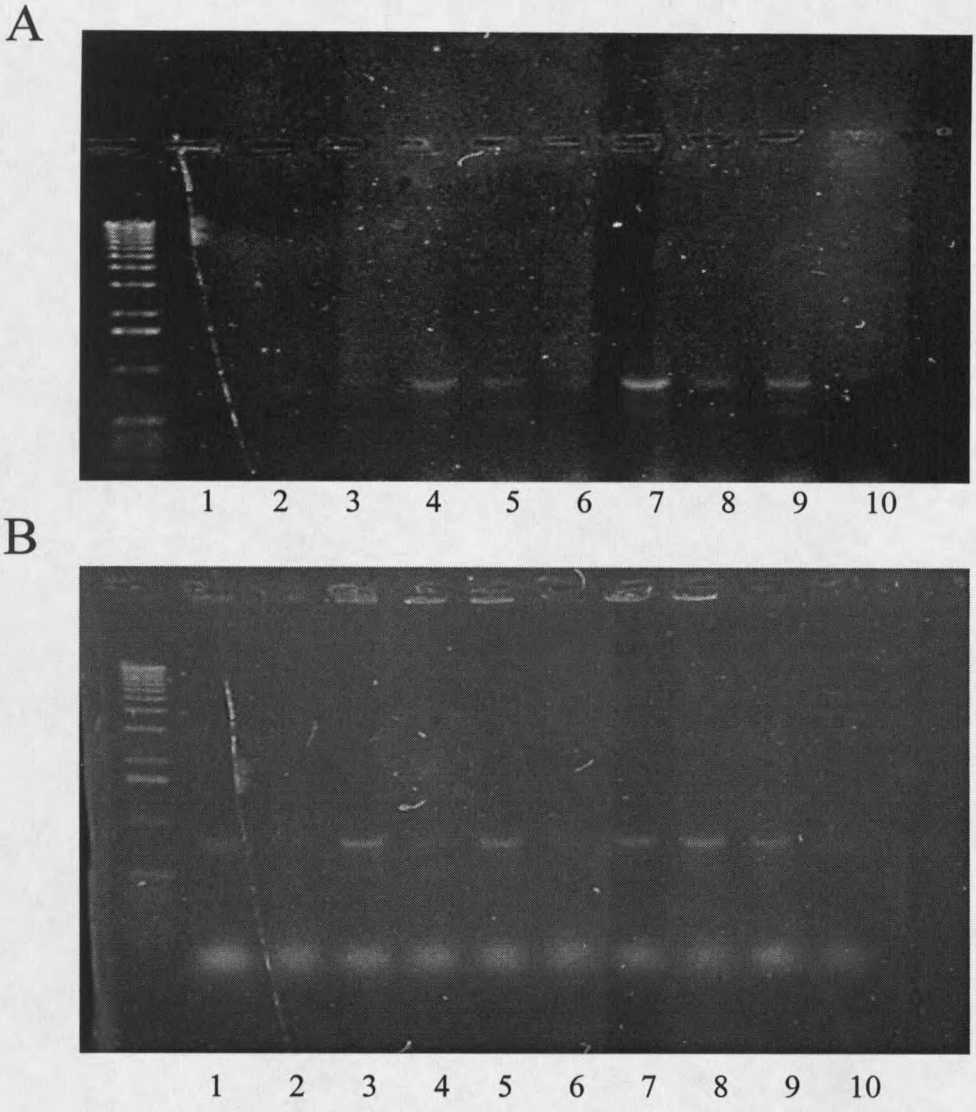


Fig 4.22. Direct PCR screening of *Pichia* clones. Single point mutant clones had products with the same molecular weight as wild-type chromosomal DNA (lane 9 A and B) used as a positive control. Positive clones selected were those in lanes 4,5,7,8 of gel A and lanes 1,3,5,7, and 8 of gel B. Water was used in place of template for a negative control run in lanes 10 A and B.

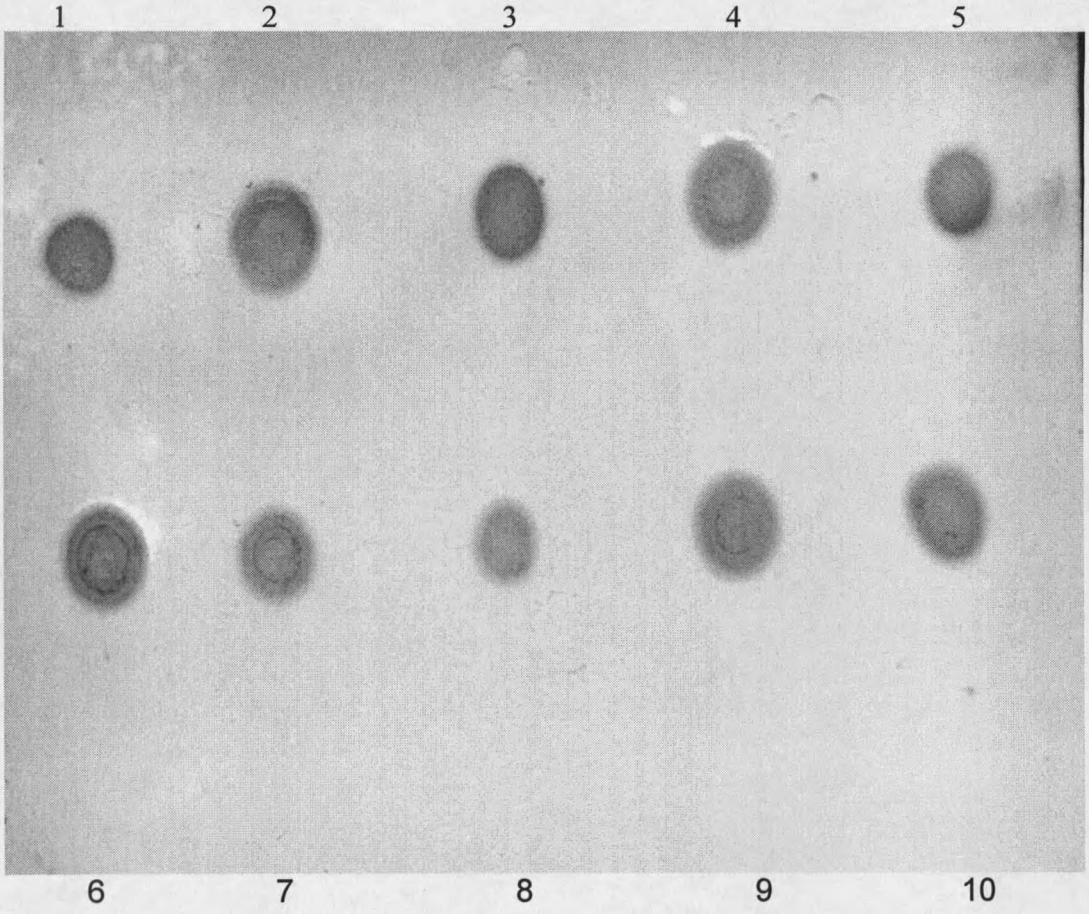


Fig 4.23. Expression screening by dot blot analysis. PCR-positive clones were grown in 1-ml cultures under methanol induction. Yeast cells resuspended in SDS buffer were broken with glass beads and proteins were harvested. 1 μl of proteins boiled in SDS buffer were spotted on a membrane and detected by using rabbit anti-CCMV polyclonal antibodies, followed by goat anti-rabbit AP conjugate. Numbers 1-3, S73C; numbers 4-5, A152C; numbers 6-9, S130C; number 10, wild type (K42R) used as a positive control.

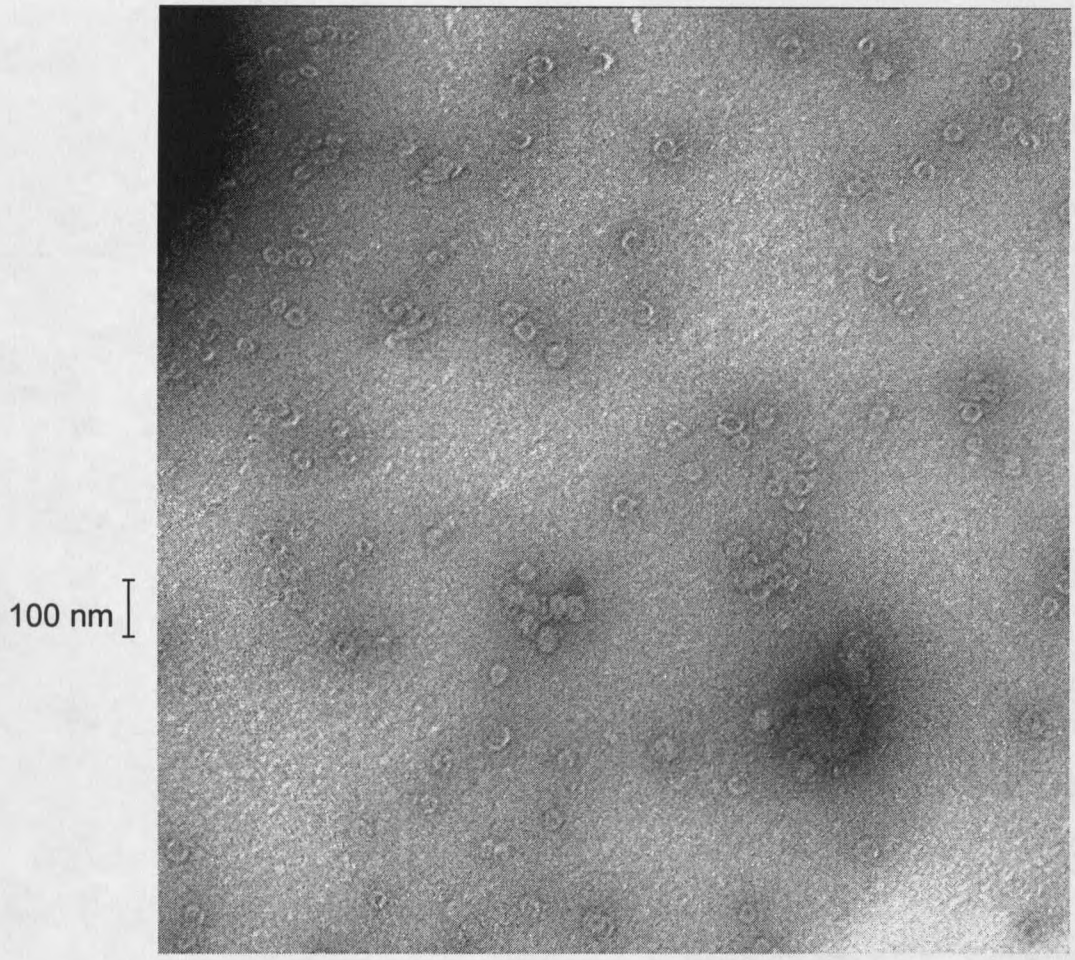


Fig 4.24. Electron micrograph of S130C. After purification, particles were absorbed to carbon-coated grids, stained with 1% uranyl acetate, and examined with a Leo LB electron microscope at magnification x50,000. Particles are ≈28nm in diameter.

Coupling the Peptide to Mutant CCMV Using a Homobifunctional Linker

Each mutant was coupled to peptide 44F.C using BMH, a homobifunctional linker, which linked the engineered cysteine sidechains on the virus to the cysteines at the C-terminal of the peptides. Peptide 44F.C was dissolved fresh and reacted with a 2-fold molar excess of BMH. A 5-fold molar excess of peptide-BMH conjugate over coat protein subunits was then reacted with TCEP-treated virus particles. SDS-PAGE and silver staining of the products showed that CCMV S130C produced the highest yield of conjugates (>50%), while the other mutants had much less coupling (data not shown). However, some coat protein dimer was also observed in S130C-44F.C. Using anti-KLH-44 antibodies, the amount of the peptide attached to the mutant CCMVs was assayed by ELISA. The amount of peptide was higher on S130C than on S73C or A152C (Fig. 4.25). To evaluate the amount of peptide on S130C quantitatively, the SDS-PAGE gel of mutant conjugates was stained with the fluorescent dye sypro ruby (Fig. 4.26) and the fluorescence intensity was subsequently read using a BioRad Molecular Imager™ FX (Fig. 4.27). It was clearly seen that S130C-44 had dramatically higher coupling (73% overall) compared to the other mutants. However, a lot of peptide was also linked to subunit dimers and some subunit monomers appeared to have two peptides attached (Fig. 4.26, lane 3).

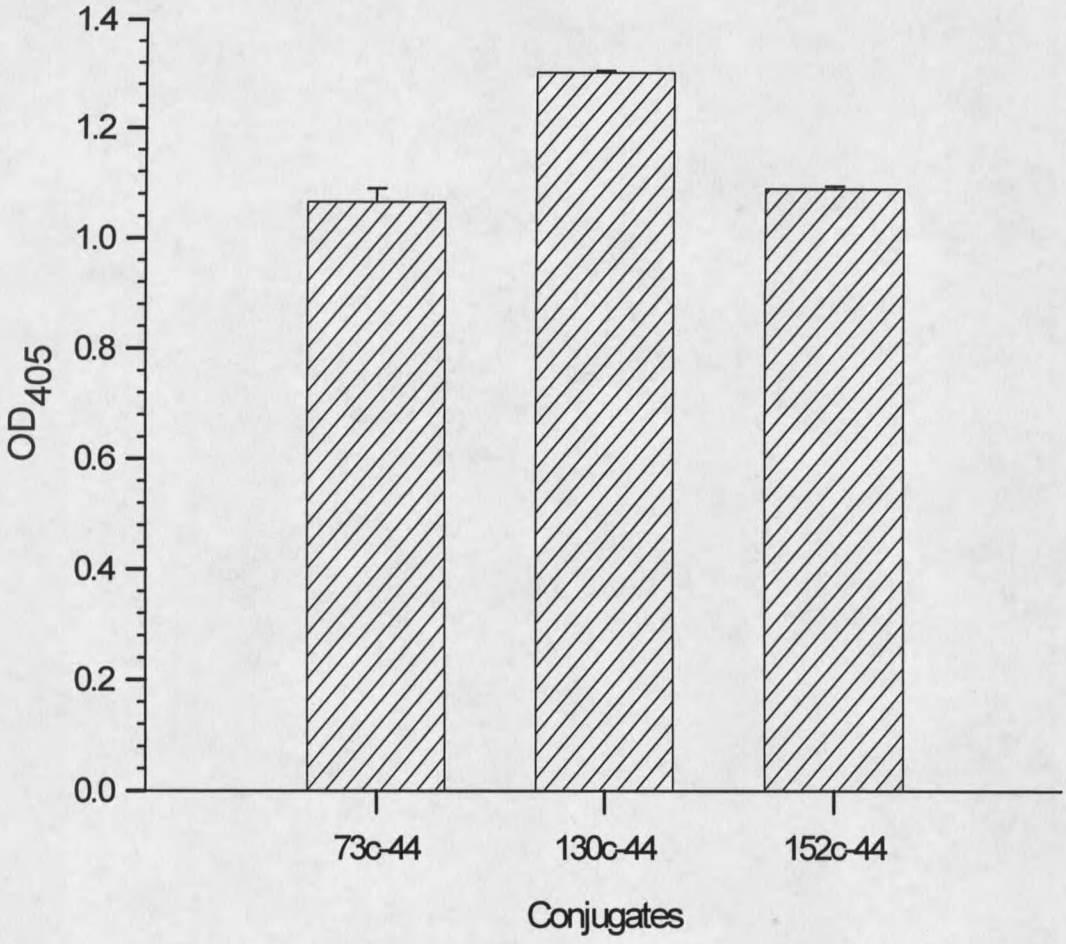


Fig 4.25. Comparison of the amount of peptides coupled to virus mutants evaluated by ELISA. Plates were coated with conjugates at 0.5 μg/well. Mouse anti-KLH-44F.C serum at dilution 1:3,000 was added to wells and detected by alkaline phosphatase -labeled goat anti-mouse IgG. The OD values shown are the mean of triplicate samples minus a background obtained from the binding of antibody to unconjugated coat protein. Error bars indicate the standard deviation of the triplicate samples.

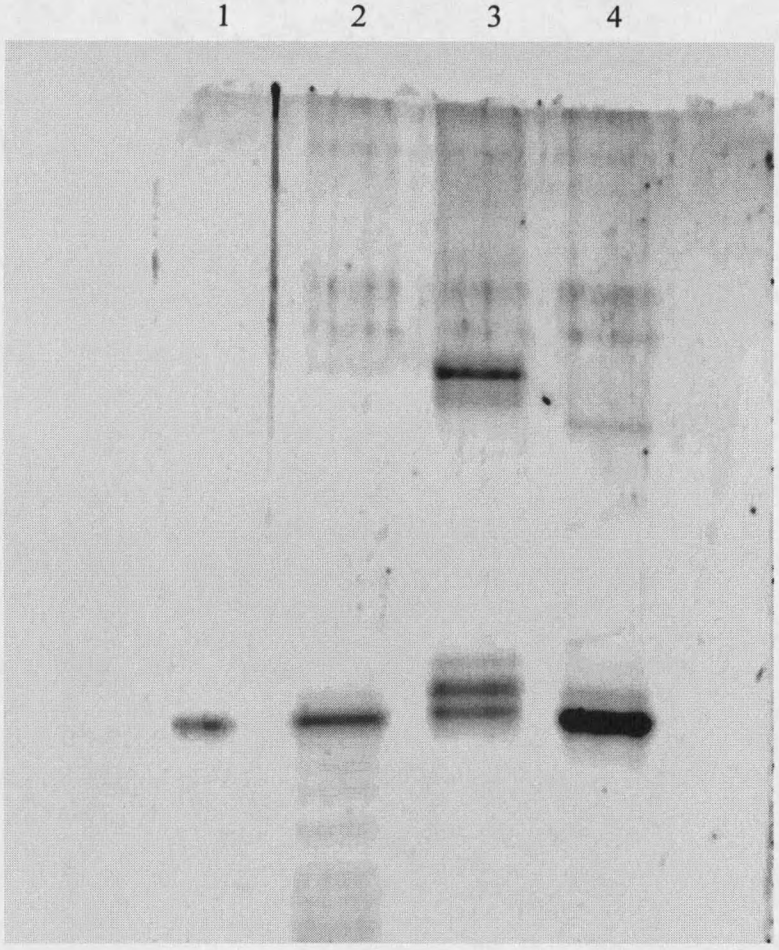


Fig 4.26. Sypro ruby staining of virus mutant conjugates. Proteins were separated electrophoretically on a 12.5% SDS-PAGE polyacrylamide gel and stained with Sypro ruby. Bands were visualized by fluorescence and image was scanned using a Molecular Imager ™ FX. Lane 1, unconjugated S130C; lane 2, S73C-44F.C; lane 3, S130C-44F.C; lane 4, A152C-44F.C.

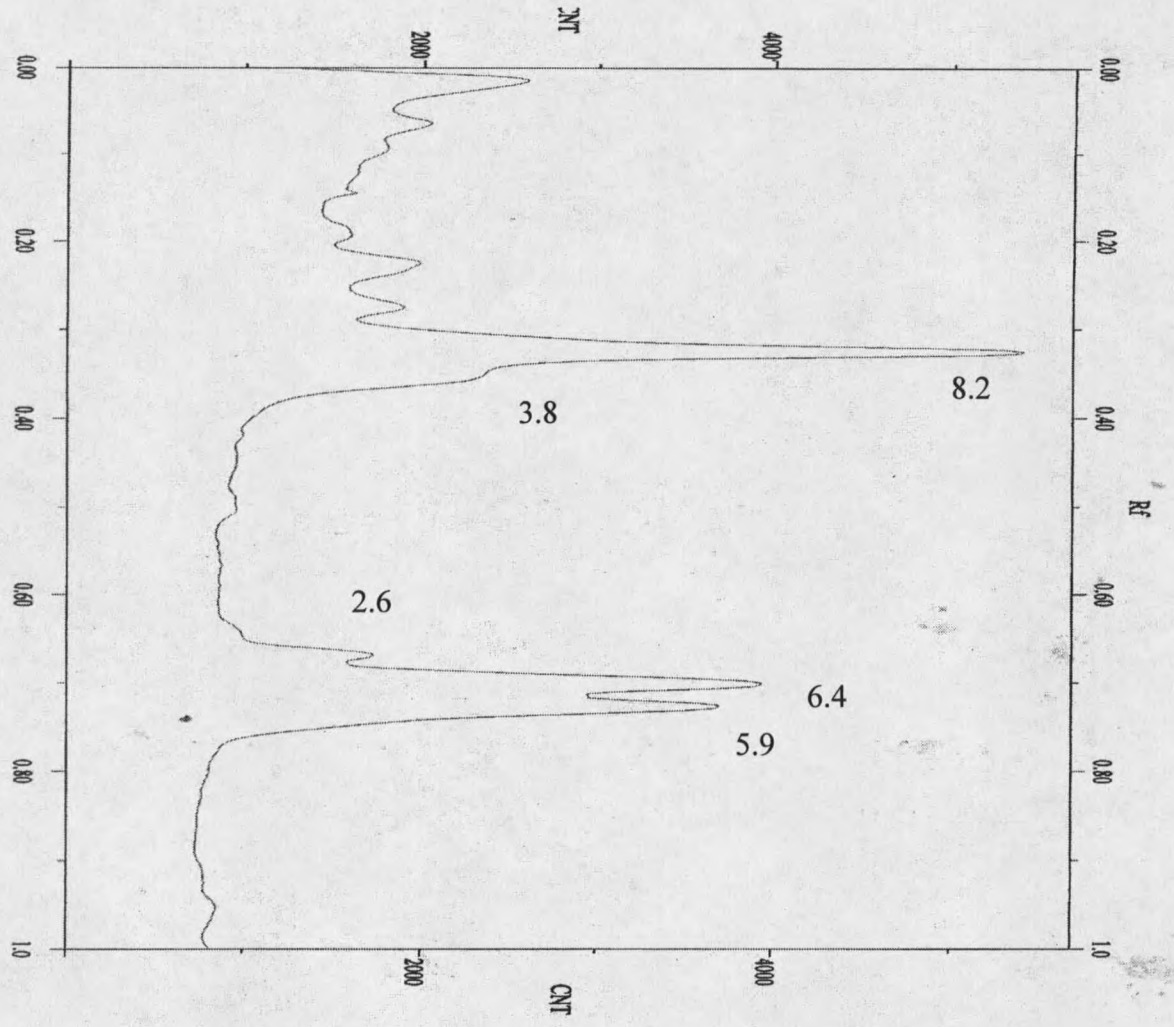


Fig 4.27. Fluorescence Intensity of sypro ruby gel staining of S130C-44F.C. Protein gel stained with sypro ruby was visualized by fluorescence and the image was scanned on a BioRad Molecular Imager ™ FX. Each peak represents the fluorescence intensity of an individual band in Fig 4.26, lane 3. Intensity of fluorescence denoted as peak CNT on the y-axis is plotted against relative front, the distance from the well to each band, on the x-axis. The number labeled at each peak represents relative quantity.

Comparison of Coupling to S130C between 44F.C and 19A.C

When peptides were attached to CCMV using SPDP or SMCC crosslinkers, CCMV-19 seemed to have a very low percentage of coupling compared to the conjugates with other peptides. To determine whether peptide 19A.C could efficiently link to the S130C virus, the S130C-19A.C conjugation products were run on SDS-PAGE and stained with sypro ruby and the fluorescence intensity quantitated. In this experiment, the amount of peptide 19A.C linked to S130C was comparable to the coupling of peptide 44F.C to S130C (Fig. 4.28, lane 4, 5 compared to lane 1, 2). Thus, there was no problem coupling peptide 19A.C to S130C in contrast to the results obtained with coupling to wild type virions using heterobifunctional linkers.

HPLC Purification of Peptide-Linker Conjugates

Although total percentage of peptide coupling was increased using the S130C mutant, much of the peptide was linked to subunit dimers rather than to the coat protein subunit. Since the dimerization caused by linker resulted in viral aggregation it was decided to remove the excess linker prior to coupling the peptide-linker conjugate to the virus. Reverse phase HPLC was run to purify the peptide-BMH mixture using a semi-preparative C-4 column and a gradient of 10-90% acetonitrile. The trace of the OD_{230} showed 4 peaks at retention times of 3, 16.5, 18 and 23 minutes (Fig. 4.29). The fractions were analyzed by MALDI-TOF mass spectroscopy. The fraction with a retention time of 18 minutes

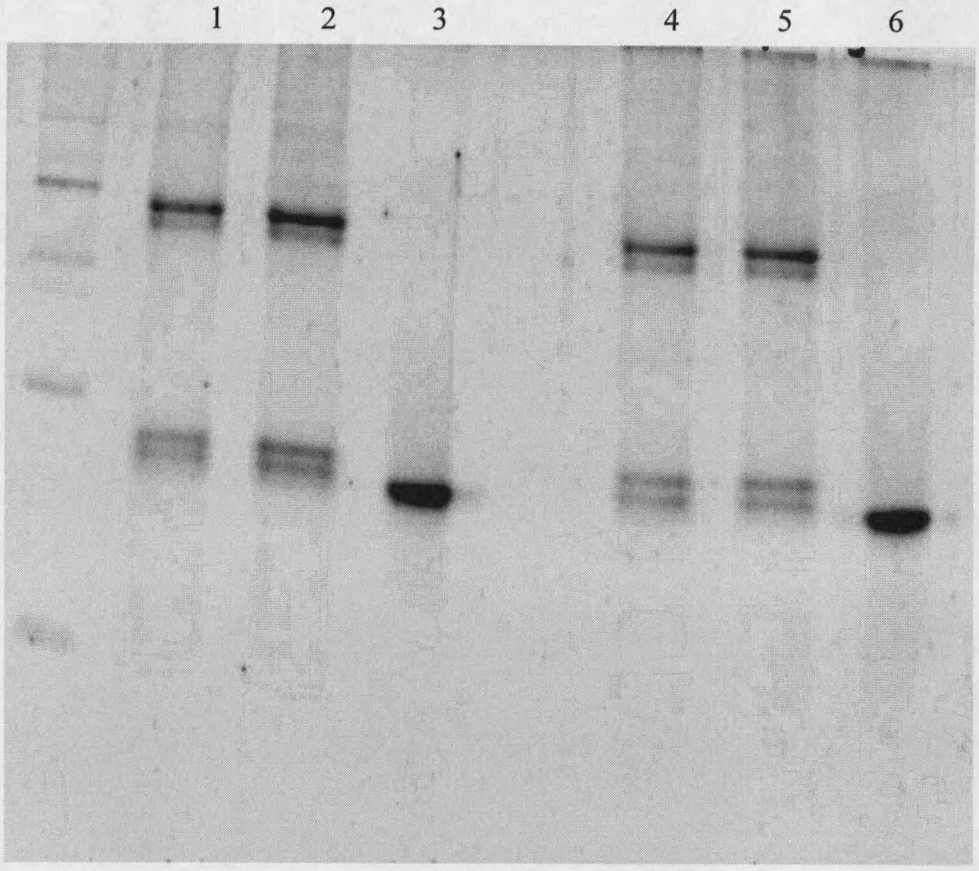


Fig 4.28. Sypro ruby staining of S130C-44F.C and S130C-19A.C conjugates. Proteins were separated on a 12.5% SDS-PAGE gel and stained with Sypro ruby. Gel was visualized by fluorescence and image was scanned using the Molecular Imager ™ FX. Lanes 1 and 2, S130C-44F.C conjugate; lane 3, S130C unconjugated; lanes 4 and 5, S130C-19A.C conjugate; lane 6, unconjugated S130C.

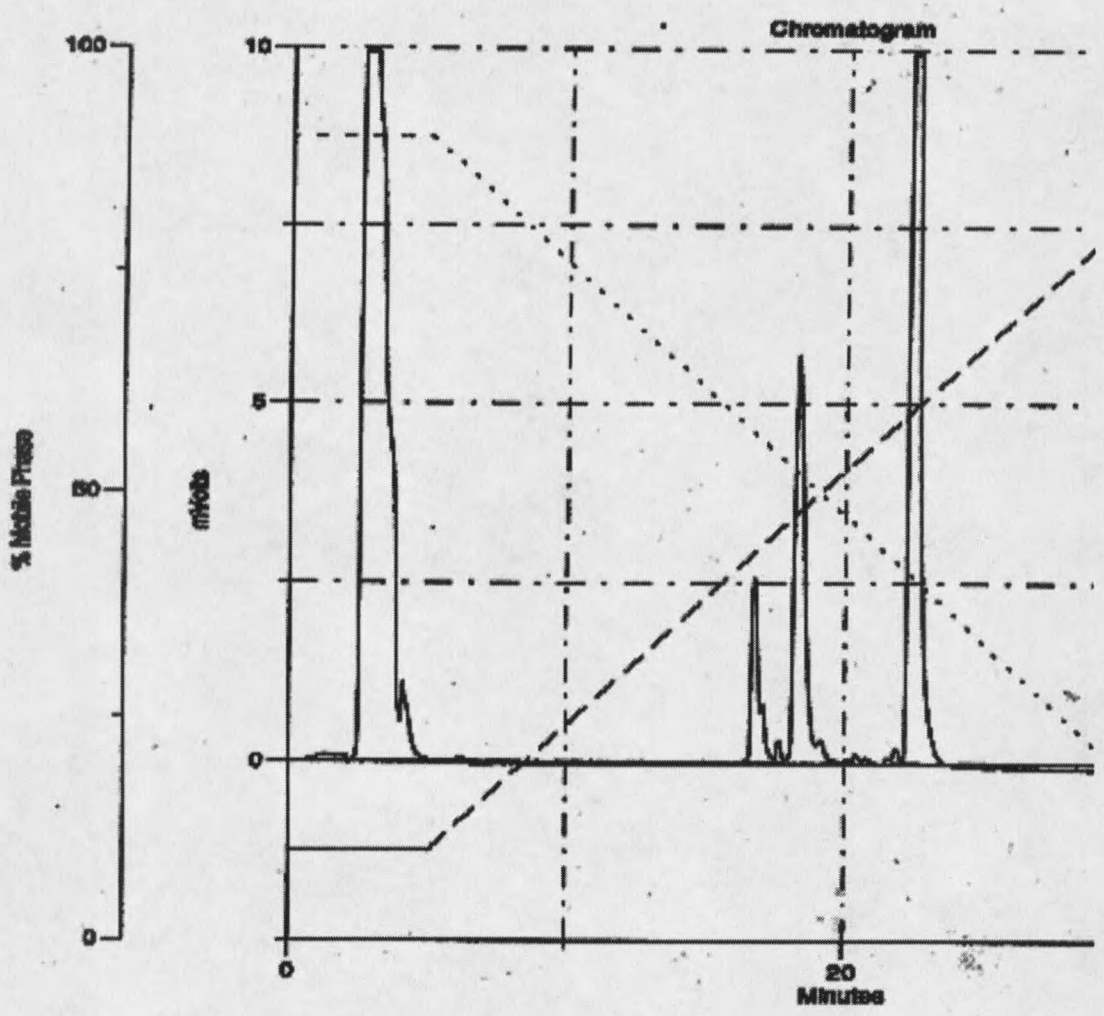


Fig 4.29. Reverse-phase HPLC chromatography. Chromatography was carried out on a semi-preparative C4 column, as described in Material and Methods. Fractions were collected and analyzed by MALDI-TOF mass spectroscopy. The y-axis represents absorbance at 230 nm (3AU=10 mV full scale)

contains most of the peptide-linker conjugate and showed a dominant peak with the expected molecular weight of the conjugate at 1321.6 (Fig. 4.30). This fraction was coupled to CCMV S130C and the product was analyzed by SDS-PAGE and sypro ruby staining, as shown in Figure 4.31. Most of the peptide was found to be linked to the coat protein subunit at 1 peptide per subunit (seen as the strongest band) with small amounts of unconjugated subunit and subunit with two peptides attached. With the additional HPLC purification step the production of dimers or multimers caused by excess linker was prevented.

Immunization of Mice with CCMV S130C-Peptide Conjugates

To evaluate whether having more peptide conjugated to the CCMV particles would induce the production of more anti-peptide antibodies than in the previous experiments, mice were immunized with S130C-44 or S130C-19 conjugates and their sera were tested by ELISA to measure the titer of antibodies against the peptide to which they were raised. After the first boost, sera from S130C-44 immunized mice had titers ranging from 1:1,000 to 1:10,000 (Fig. 4.32). There was variation in the group, with one mouse having a strikingly high titer. All 3 mice had higher titers after a second boost and the range of titers was from 1:5,000 to 1:10,000 (Fig. 4.33), where titers was lower than that seen previously with SPDP-conjugated CCMV-44, which had been 1:10,000-1:50,000 (Fig. 4.11). This indicated that having more peptide attached to the virus would not induce a higher antibody titer. Similar results were obtained from mice

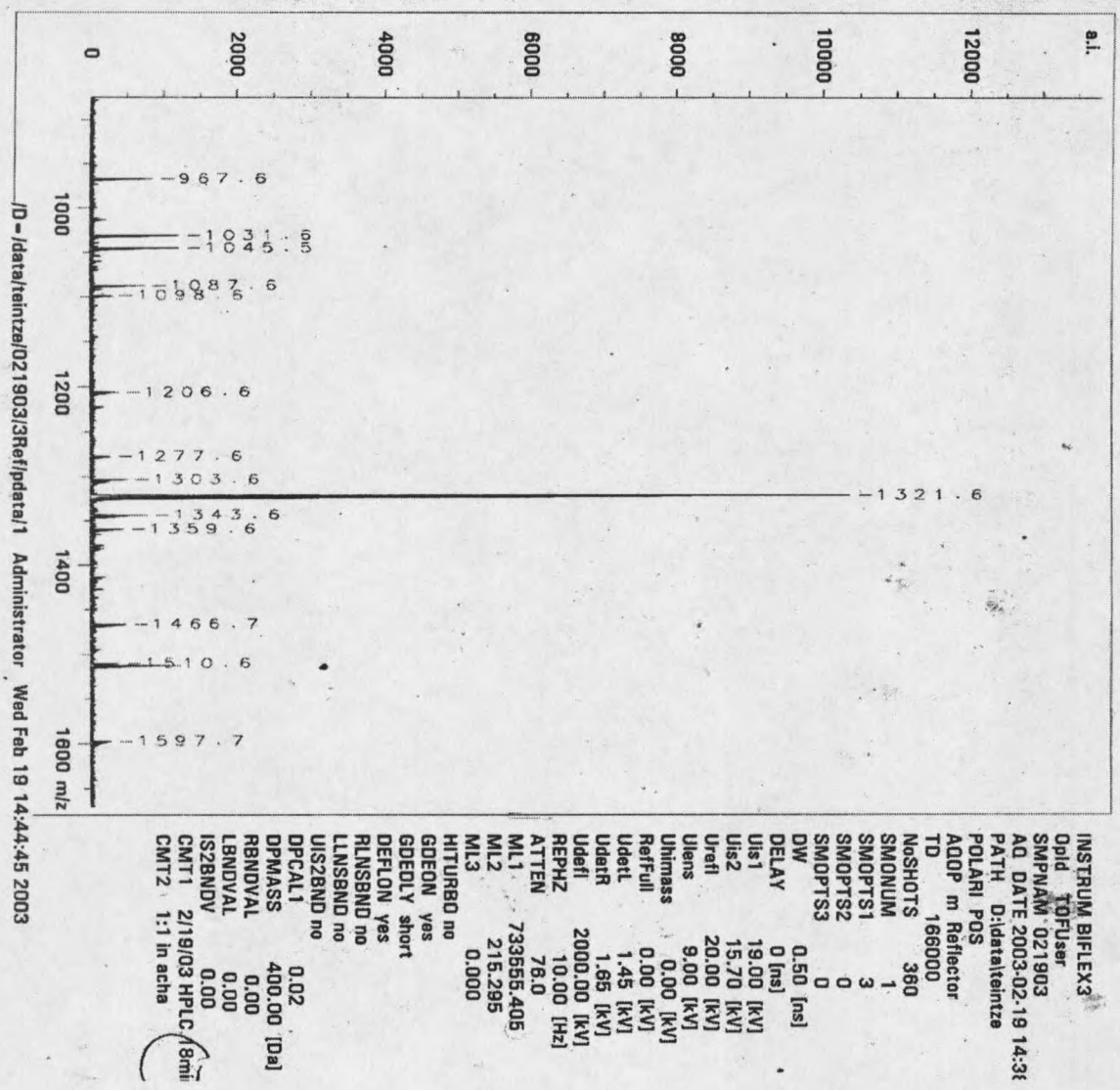


Fig 4.30. MALDI-TOF mass spectroscopy of the HPLC-purified fraction eluted at a retention time of 18 minutes. The spectrum shows the singly charged peptide ion of *m/z* 1321.6, corresponding to the BMH-peptide conjugate. Experiment was performed by R. Wilkinson.

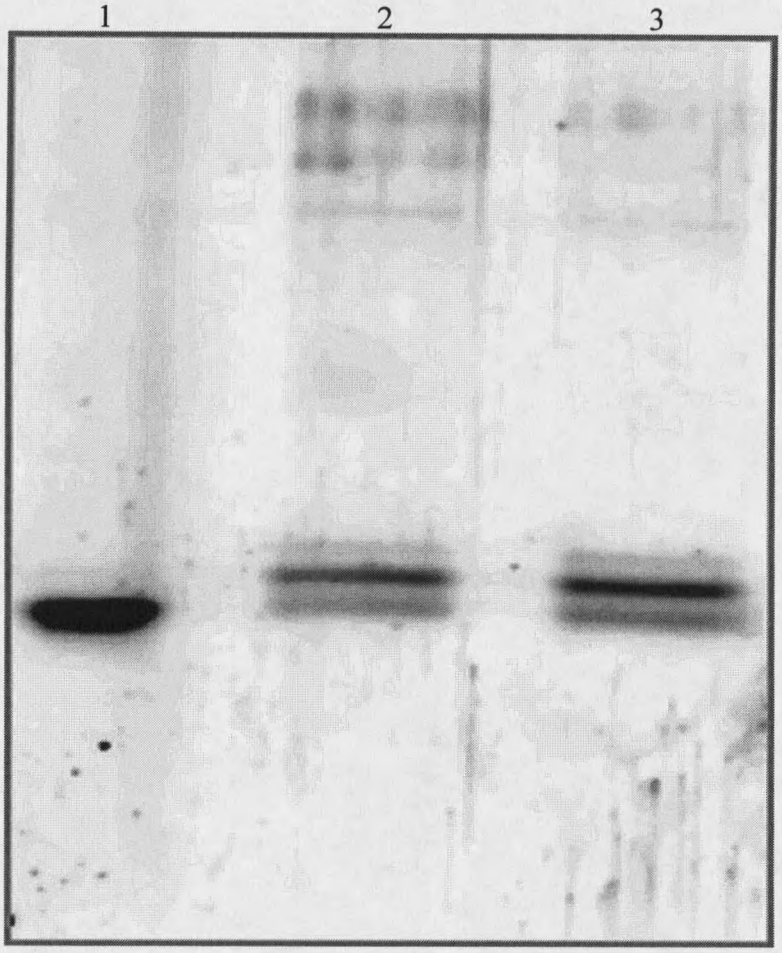


Fig 4.31. Sypro ruby staining of S130C-44F.C conjugate after HPLC purification of excess BMH. Proteins were separated on a 12.5% SDS-PAGE gel and stained with Sypro ruby. Gel was visualized by fluorescence and image was scanned using the Molecular Imager ™ FX. Lane 1, unconjugated S130C; lanes 2 and 3, S130C-44F.C conjugate.

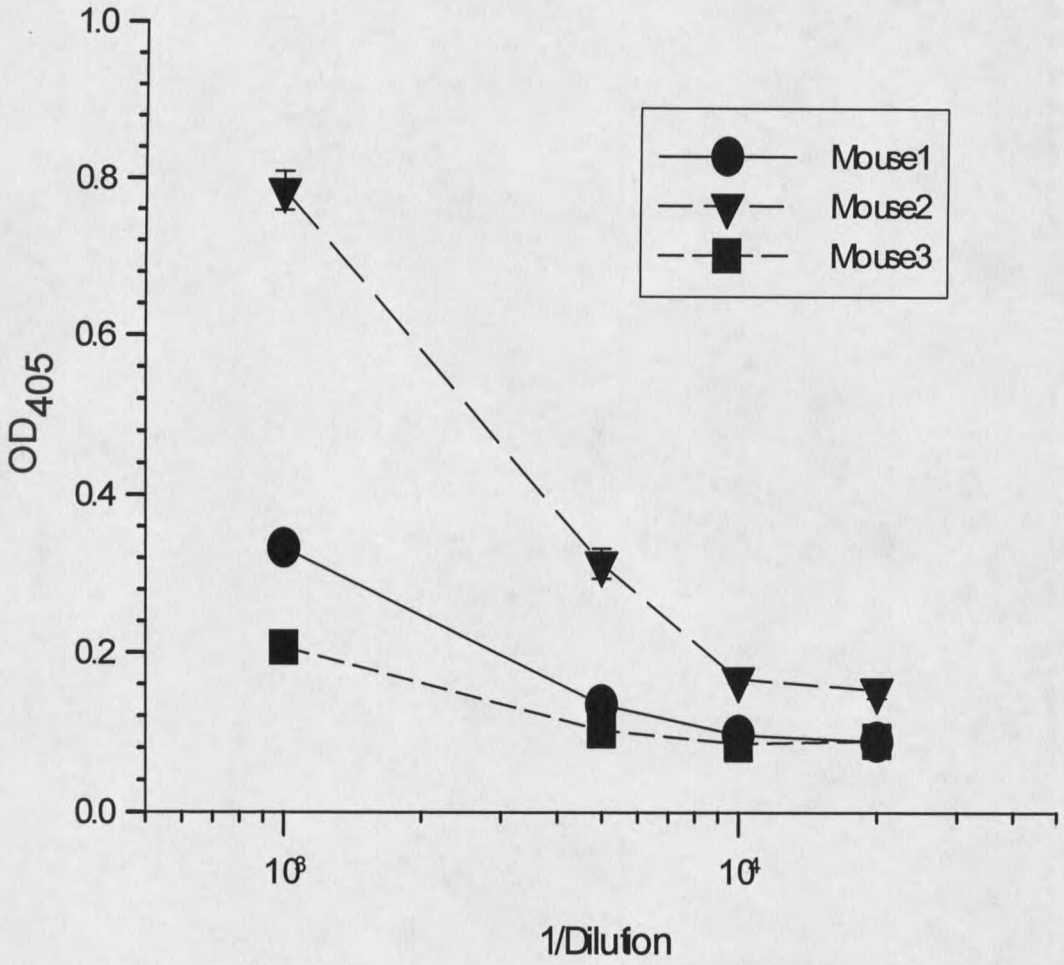


Fig 4.32. Anti-peptide activity of the first bleed sera from S130C-44F.C immunized mice by ELISA. Mice were immunized with the conjugate in CFA and boosted once in IFA. Serial dilutions of sera were bound to wells coated with 0.1 μg OVA-44F.C. The reactivity to peptide 44F.C was detected using goat anti-mouse alkaline phosphatase conjugate. OD_{405} values that were greater than twice the background obtained from sera binding to unconjugated OVA coated wells at dilution 1:1,000 were considered positive (usually >0.16). All OD values shown are the mean of triplicate samples with SD

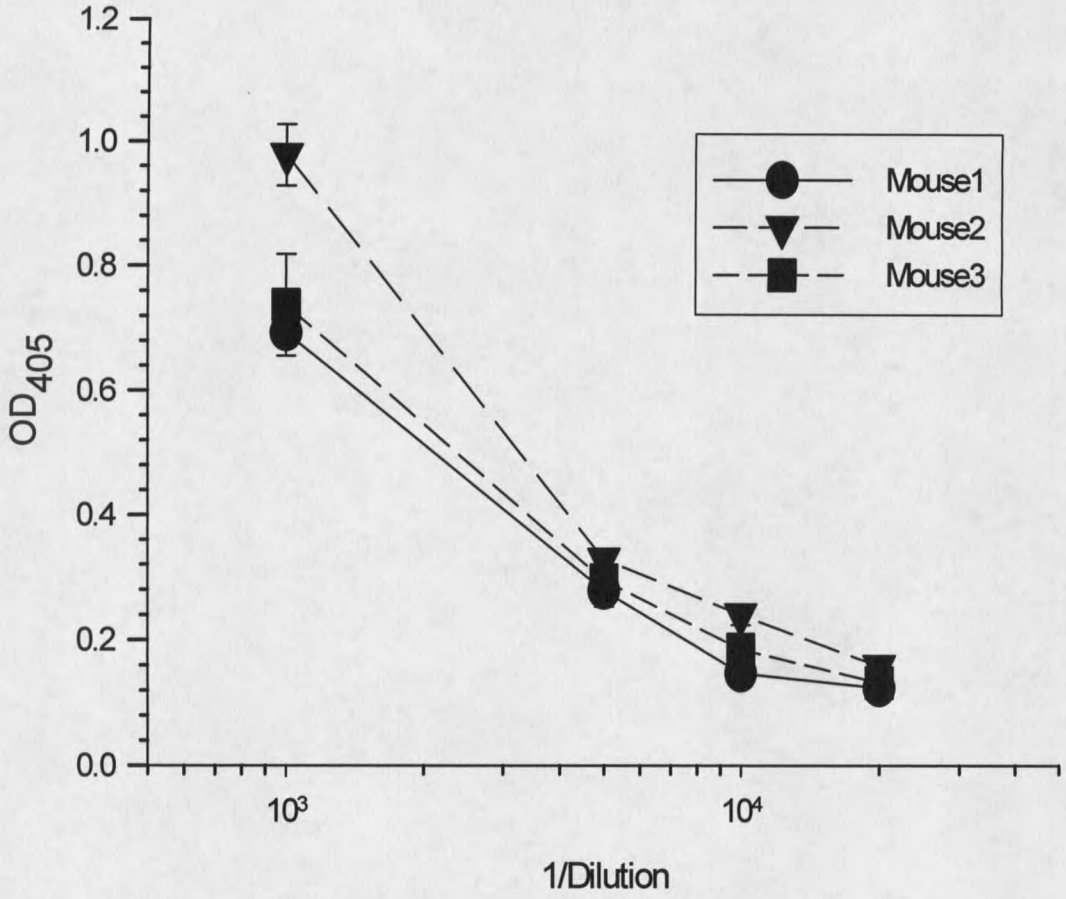


Fig 4.33. Anti-peptide activity of the second bleed sera from S130C-44F.C immunized mice by ELISA. Mice were immunized with the conjugate in CFA and boosted twice in IFA. Serial dilutions of sera were bound to wells coated with 0.1 μg OVA-44F.C. The reactivity to peptide 44F.C was detected using goat anti-mouse alkaline phosphatase conjugate. OD_{405} values that were greater than twice the background obtained from sera binding to unconjugated OVA coated wells at dilution 1:1,000 were considered positive (usually >0.16). All OD values shown are the mean of duplicate samples with SD shown as error bars.

immunized with S130C-19 conjugates. The sera collected after the first boost were lower than 1:1,000 but increased to 1:1,000-1:20,000 after the second boost (Fig. 4.34 and 4.35, respectively). However, the titer was still much lower compared to that of the mice immunized with the SPDP-conjugated CCMV-19 which had ranged from 1:10,000 to 1:100,000 (Fig. 4.14). This result supported the conclusion that more peptide per virion would not induce higher anti-peptide activity. The anti-carrier titers were also measured to determine whether the S130C virus mutant still was immunogenic. The results showed that S130C-44 and S130C-19 could induce strong immune responses against the virus carrier at titers above 1:20,000 (Fig. 4.36 and 4.37, respectively), comparable to the anti-carrier titers observed with the SPDP conjugates (Fig. 4.12 and 4.15).

Immunization with KLH-44 and KLH-19

Keyhole limpet hemocyanin (KLH) is a widely used carrier, which is well known to induce strong immune responses to attached peptides. maleimide-activated mcKLH (Pierce Chemical Co.) was conjugated to peptide 44F.C or 19A.C and the conjugate was used to immunize mice. Sera from these mice were assayed for anti-peptide and anti-carrier activity. After the first boost, the anti-peptide titers of the sera from KLH-44 immunized mice ranged from 1:5,000 to more than 1:20,000 (Fig. 4.38). The titer increased after the second boost for two of the mice, but that from mouse 2 dropped, so the average titer was about

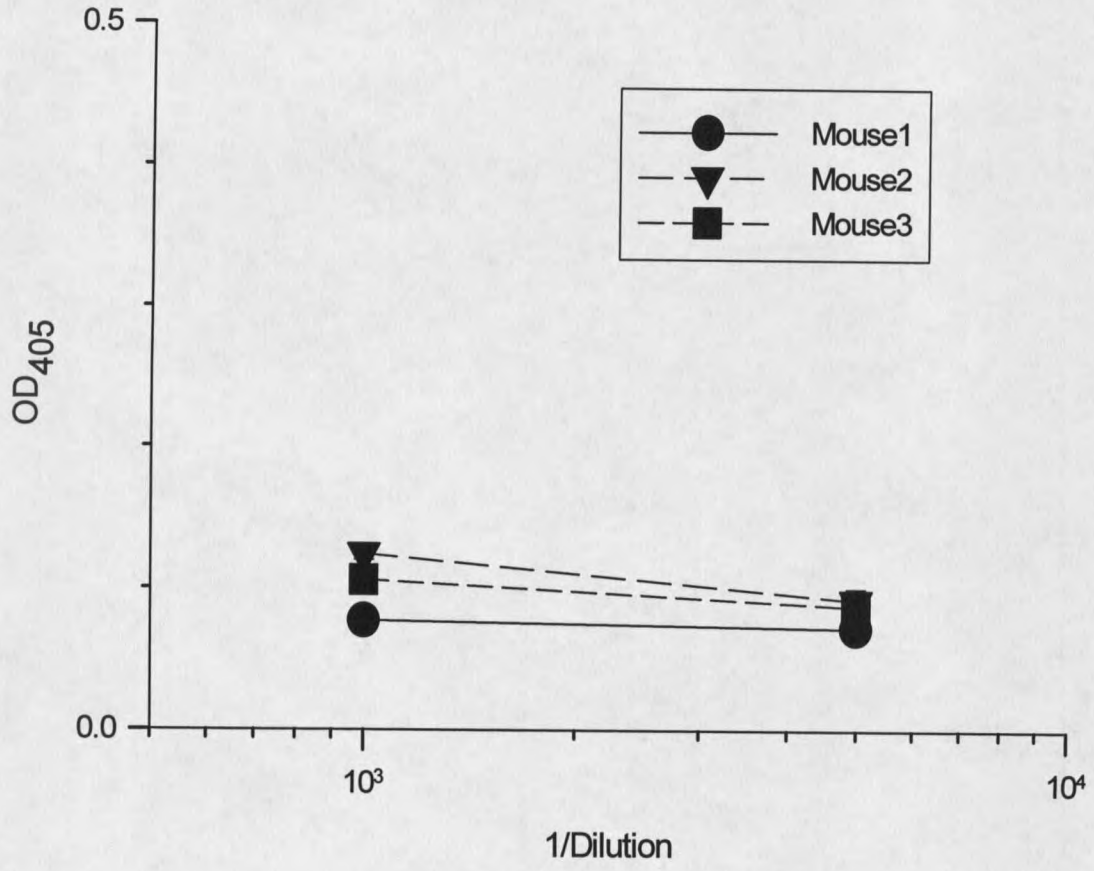


Fig 4.34. Anti-peptide activity of the first bleed sera from S130C-19A.C immunized mice by ELISA. Mice were immunized with the conjugate in CFA and boosted once in IFA. Serial dilutions of sera were bound to wells coated with 0.1 μg OVA-19A.C. The reactivity to peptide 19A.C was detected using goat anti-mouse alkaline phosphatase conjugate. OD_{405} values that were greater than twice the background obtained from sera binding to unconjugated OVA coated wells at dilution 1:1,000 were considered positive (usually >0.16). All OD values shown are the mean of triplicate samples with SD shown as error bars.

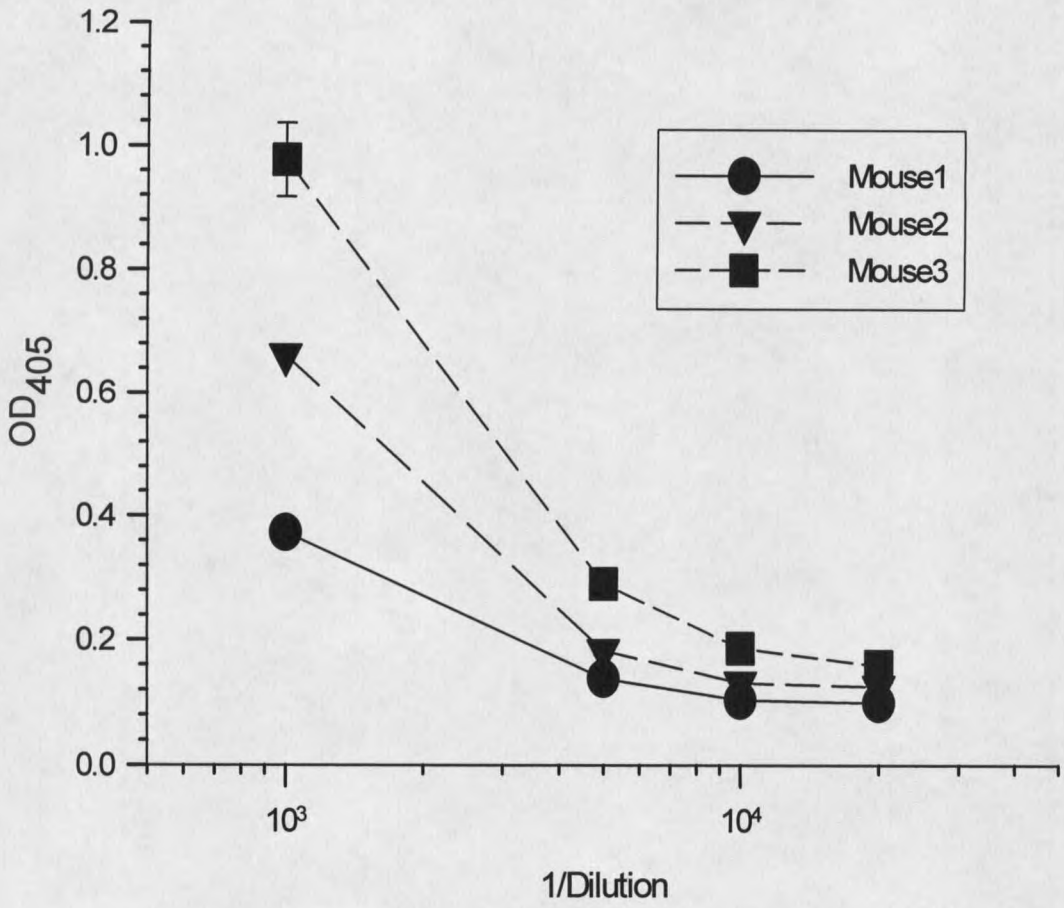


Fig 4.35. Anti-peptide activity of the second bleed sera from S130C-19A.C immunized mice by ELISA. Mice were immunized with the conjugate in CFA and boosted twice in IFA. Serial dilutions of sera were bound to wells coated with 0.1 μg OVA-19A.C. The reactivity to peptide 19A.C was detected using goat anti-mouse alkaline phosphatase conjugate. OD405 values that were greater than twice the background obtained from sera binding to unconjugated OVA coated wells at dilution 1:1,000 were considered positive (usually >0.16). All OD values shown are the mean of duplicate samples with SD shown as error bars.

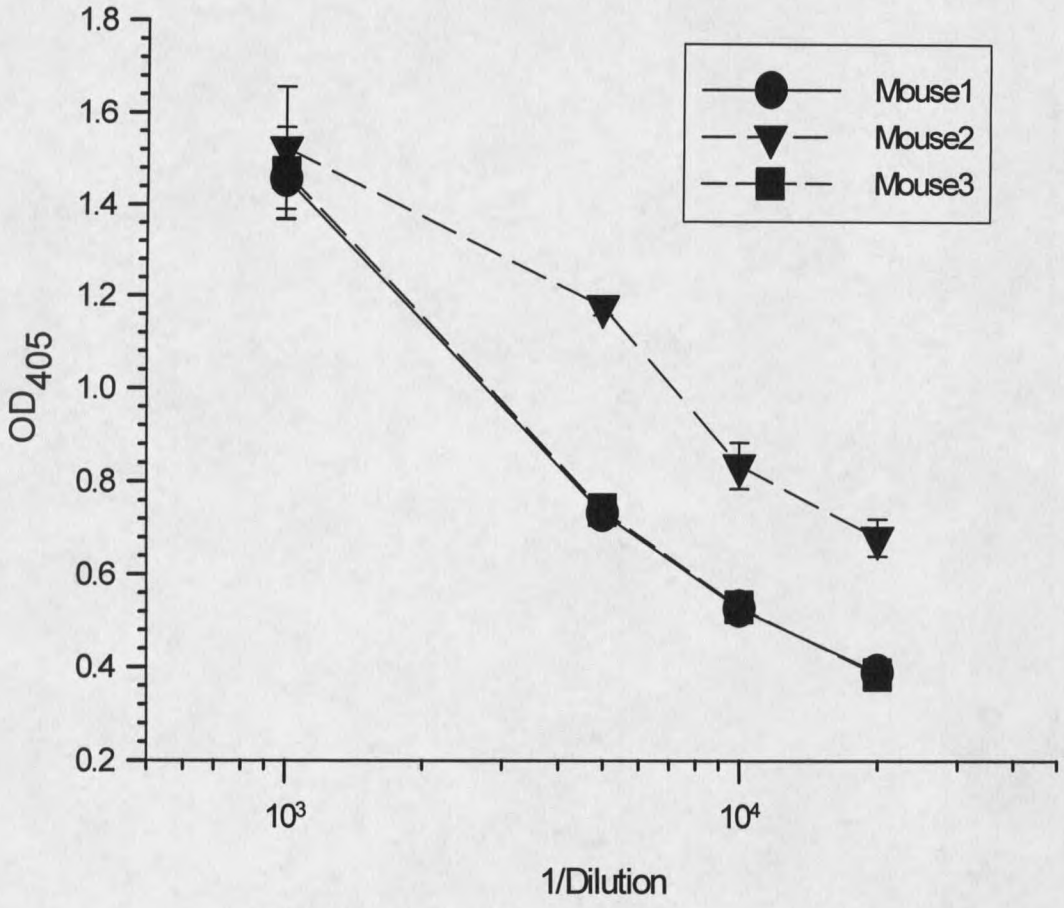


Fig 4.36. Anti-carrier activity of sera from S130C-44F.C immunized mice. ELISA plates were coated CCMV S130C at 0.5 μg/well. Mouse sera from the second bleed were added to wells in serial dilutions and detected using goat anti-mouse alkaline phosphatase conjugate. The binding of pre-immune sera to the virus at dilution 1:1,000 usually gave OD value <0.10 and was used as a negative control. All OD values shown are the mean of triplicate samples with SD shown as error bars.

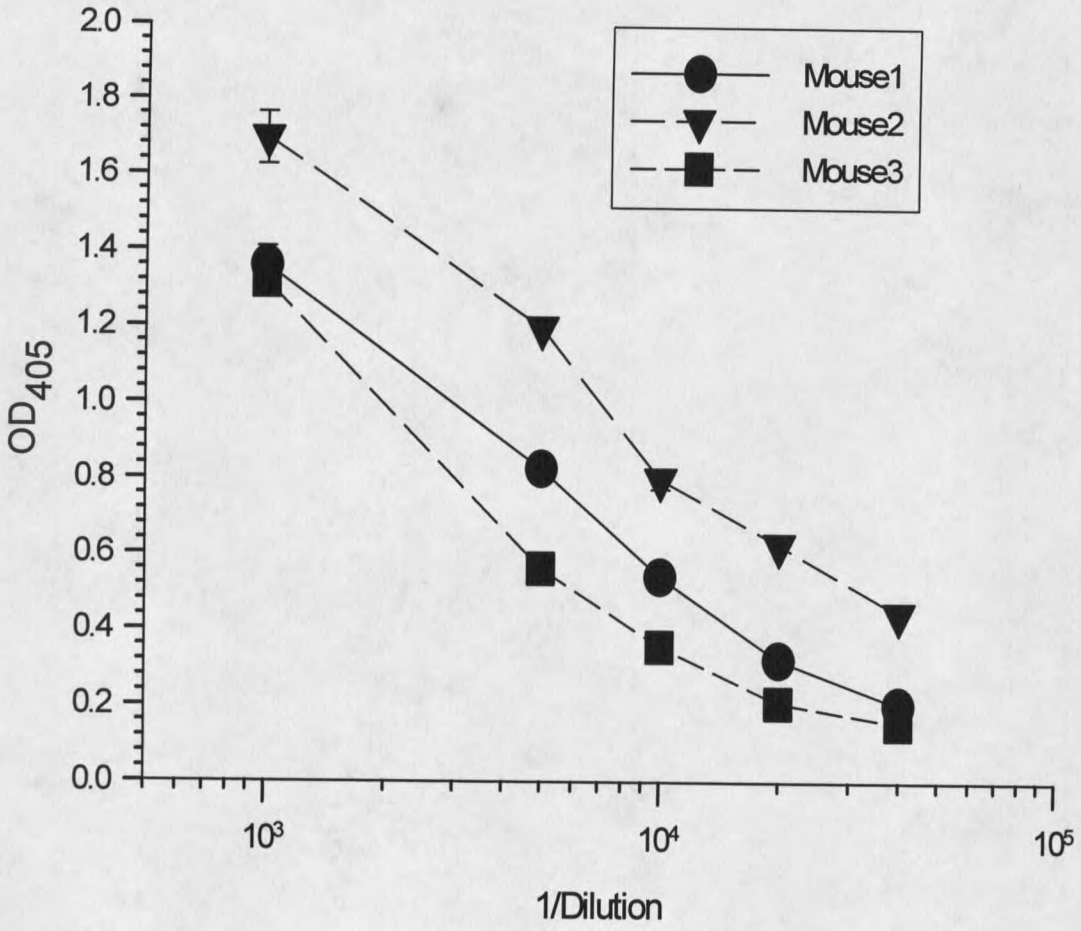


Fig 4.37. Anti-carrier activity of sera from S130C-19A.C immunized mice. ELISA plates were coated with CCMV S130C at 0.5 μg/well. Mouse sera from the second bleed were added to wells in serial dilutions and detected using goat anti-mouse alkaline phosphatase conjugate. The binding of pre-immune sera to the virus at dilution 1:1,000 usually gave OD value <0.10 and was used as a negative control. All OD values shown are the mean of duplicate samples with SD shown as error bars.

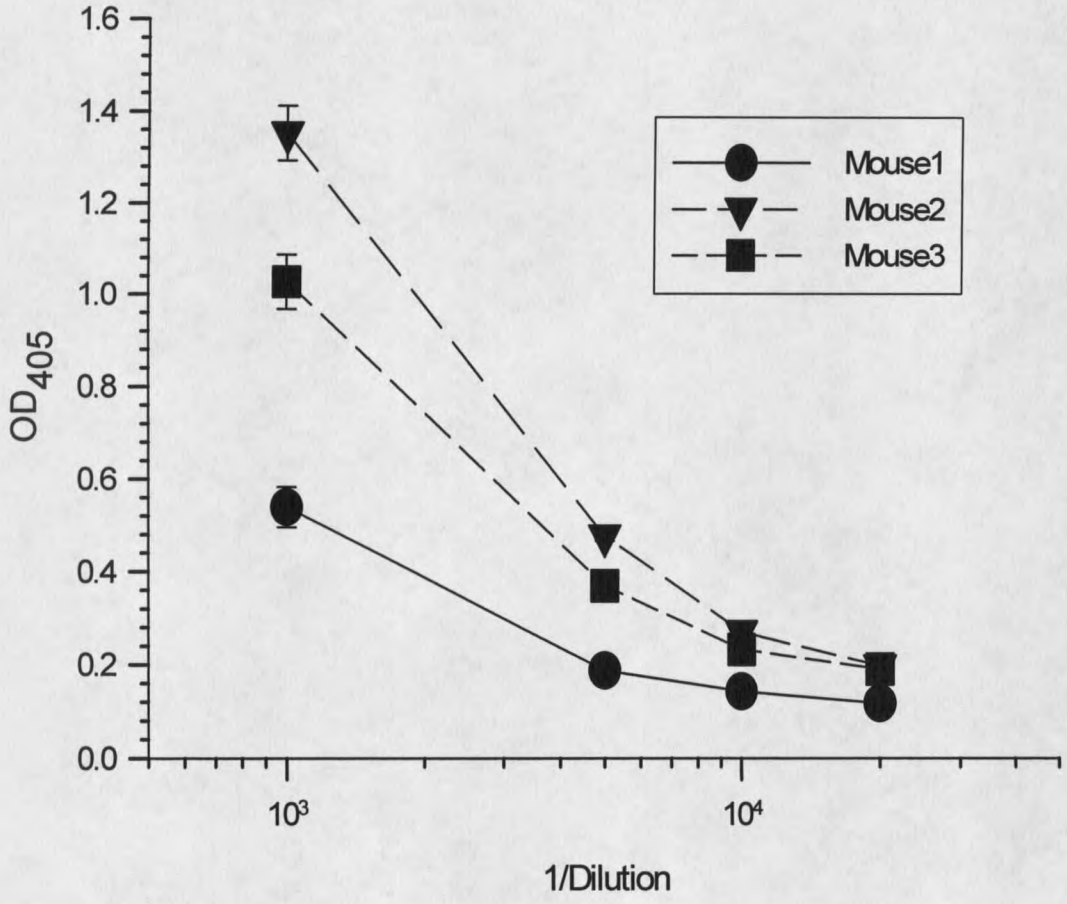


Fig 4.38. Anti-peptide activity of the first bleed sera from KLH-44F.C immunized mice by ELISA. Mice were immunized with the conjugate in CFA and boosted once in IFA. Serial dilutions of sera were bound to wells coated with 0.1 μg OVA-44F.C. The reactivity to peptide 44F.C was detected using goat anti-mouse alkaline phosphatase conjugate. OD_{405} values that were greater than twice the background obtained from sera binding to unconjugated OVA coated wells at dilution 1:1,000 were considered positive (usually >0.16). All OD values shown are the mean of triplicate samples with SD shown as error bars.

the same (fig. 4.39). For anti-carrier activity, the titers of sera against KLH were higher than 1:40,000 (fig. 4.40).

The sera from the first bleed of KLH-19 immunized mice had anti-peptide titers ranging from 1:5,000 to more than 1:20,000, which increased slightly in the second bleed (Fig. 4.41 and 4.42, respectively). Comparing sera from all the conjugate-immunized mice, CCMV appeared to be the best carrier, inducing the strongest anti-peptide antibody titers for both peptide 44 F.C and 19 A.C in the presence of Freund's adjuvant. Compared between both peptides, 19 A.C was more effective in inducing an anti-peptide immune response than 44 F.C even though there was less of it coupled to the CCMV coat proteins.

Isotyping of Sera from Mice Immunized with CCMV, CPMV and KLH Conjugates

The antibody isotypes in the sera from mice immunized with carrier-peptide conjugates formulated with complete Freund's adjuvant (CFA) were determined. The sera from CCMV-44F.C and KLH-44 F.C immunized mice had both IgG2a and IgG1 high levels, indicating both Th1 and Th2 responses (Fig. 4.43 and 4.44, respectively). However, IgG2b was also high in the sera from KLH-44 immunized mice. Interestingly, the sera from mice-immunized with CPMV-44 in CFA had IgG1 antibody dominant over IgG2a in all mice. The level of IgG2a was comparable with that of IgG2b and higher than IgG3 (Fig. 4.45). This suggests that the CPMV-44 induced a Th2 oriented response.

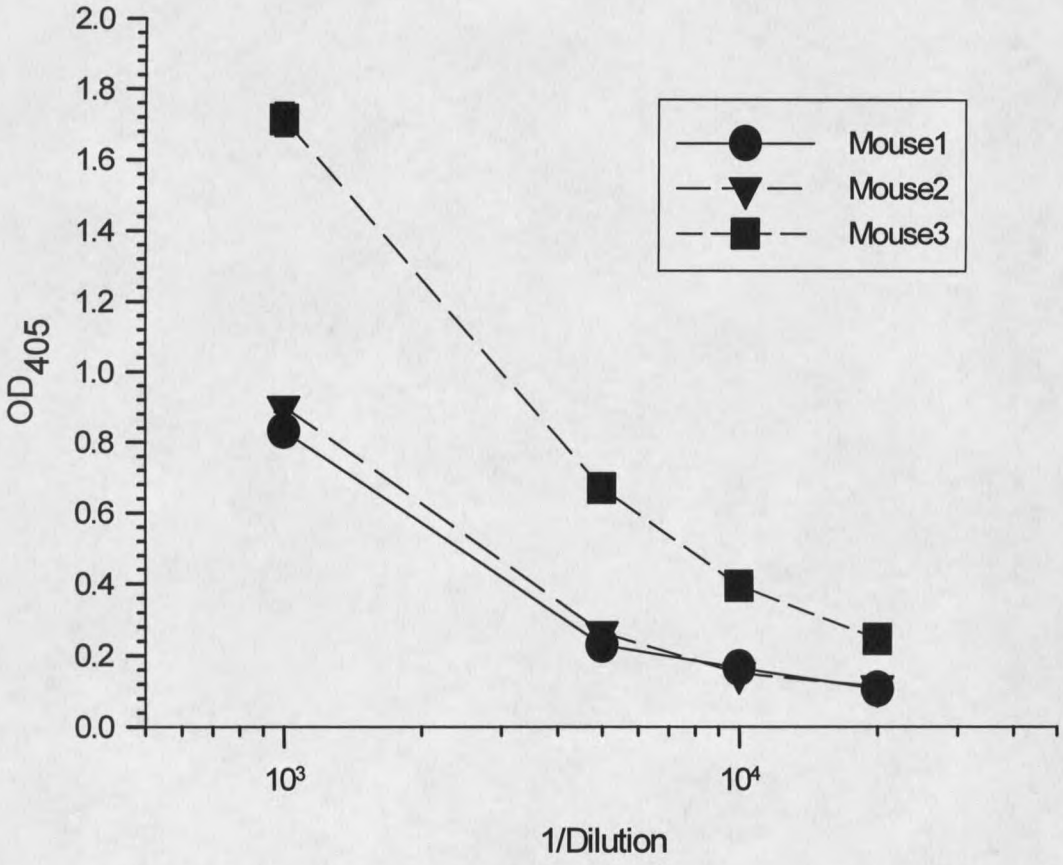


Fig 4.39. Anti-peptide activity of the second bleed sera from KLH-44F.C immunized mice by ELISA. Mice were immunized with the conjugate in CFA and boosted twice in IFA. Serial dilutions of sera were bound to wells coated with 0.1 μg OVA-44F.C. The reactivity to peptide 44F.C was detected using goat anti-mouse alkaline phosphatase conjugate. OD_{405} values that were greater than twice the background obtained from sera binding to unconjugated OVA coated wells at dilution 1:1,000 were considered positive (usually >0.16). All OD values shown are the mean of triplicate samples with SD shown as error bars.

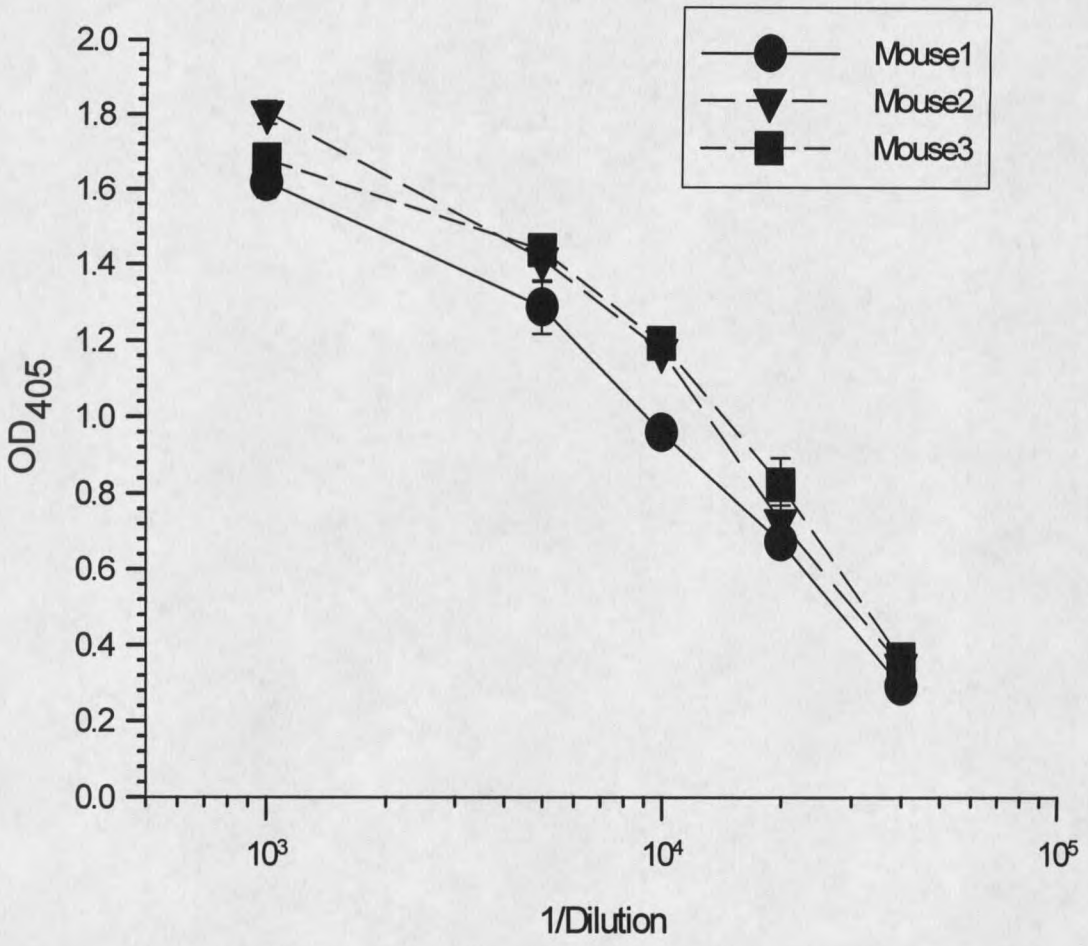


Fig 4.40. Anti-carrier activity of sera from KLH-44F.C immunized mice. ELISA plates were coated with KLH at 0.1 μg/well. Mouse sera from the second bleed were added to wells in serial dilutions and detected by goat anti-mouse alkaline phosphatase conjugate. The binding of pre-immune sera to unconjugated KLH at dilution 1:1,000 usually gave OD value <0.10 and used as a negative control. All OD values shown are the mean of duplicate samples with SD shown as error bars.

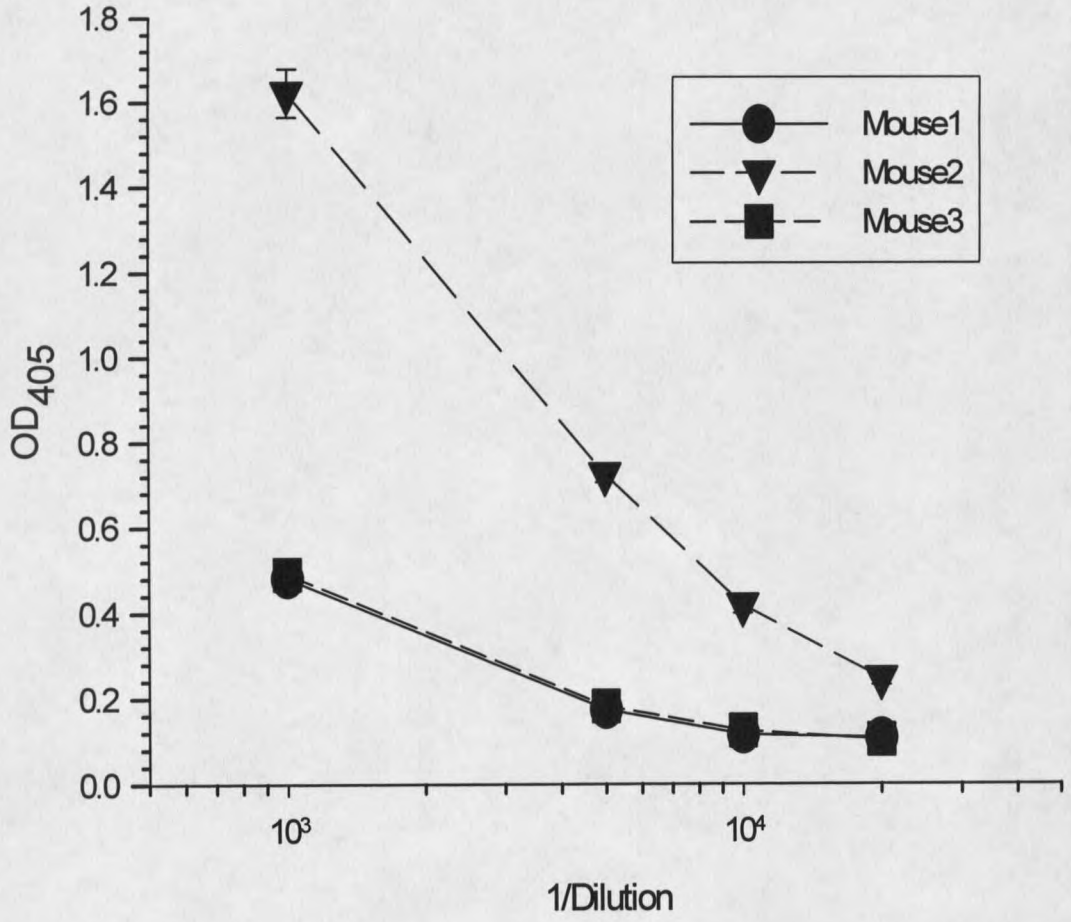


Fig 4.41. Anti-peptide activity of the first bleed sera from KLH-19A.C immunized mice by ELISA. Mice were immunized with the conjugate in CFA and boosted once in IFA. Serial dilutions of sera were bound to wells coated with 0.1 μg OVA-19A.C. The reactivity to peptide 19A.C was detected by goat anti-mouse alkaline phosphatase conjugate. OD_{405} values that were greater than twice the background obtained from sera binding to unconjugated OVA coated wells at dilution 1:1,000 were considered positive (usually >0.16). All OD values shown are the mean of triplicate samples with SD shown as error bars.

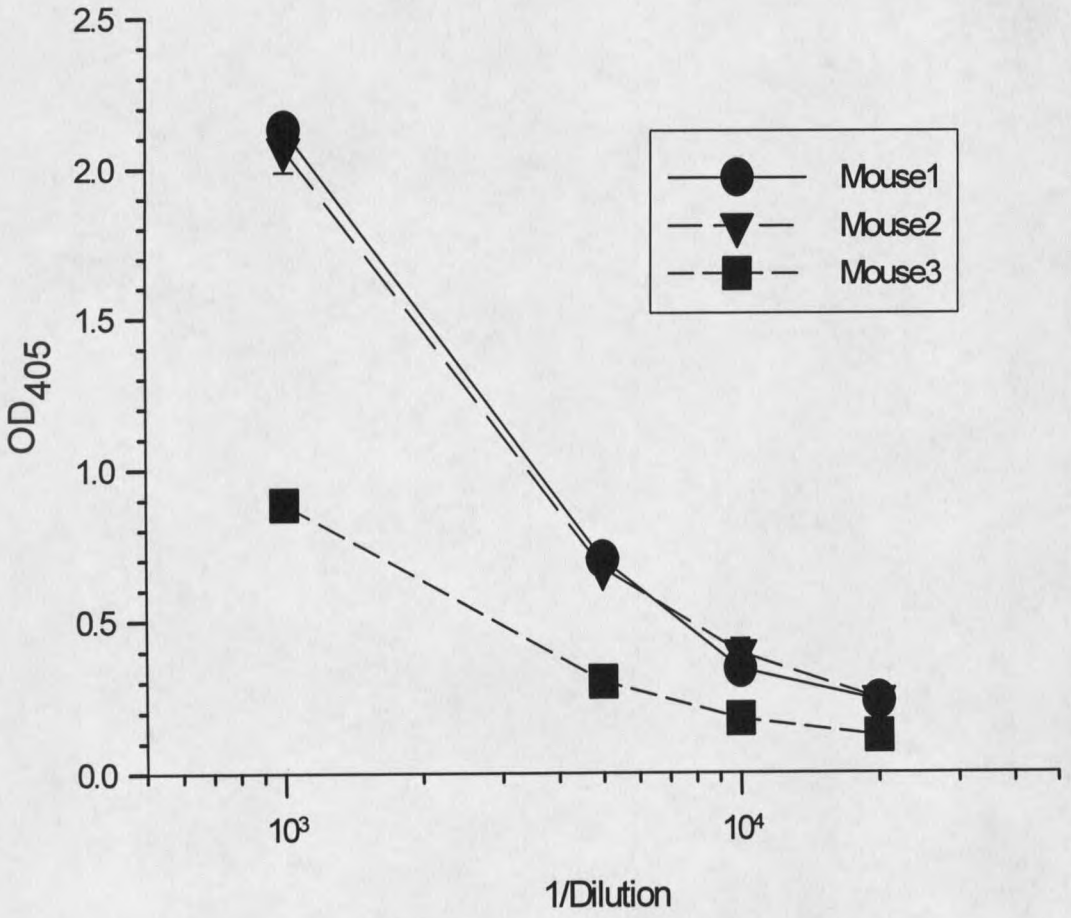


Fig 4.42. Anti-peptide activity of the second bleed sera from KLH-19A.C immunized mice by ELISA. Mice were immunized with the conjugate in CFA and boosted twice in IFA. Serial dilutions of sera were bound to wells coated with 0.1 μg OVA-19A.C. The reactivity to peptide 19A.C was detected by goat anti-mouse alkaline phosphatase conjugate. OD_{405} values that were greater than twice the background obtained from sera binding to unconjugated OVA coated wells at dilution 1:1,000 were considered positive (usually >0.16). All OD values shown are the mean of triplicate samples with SD shown as error bars.

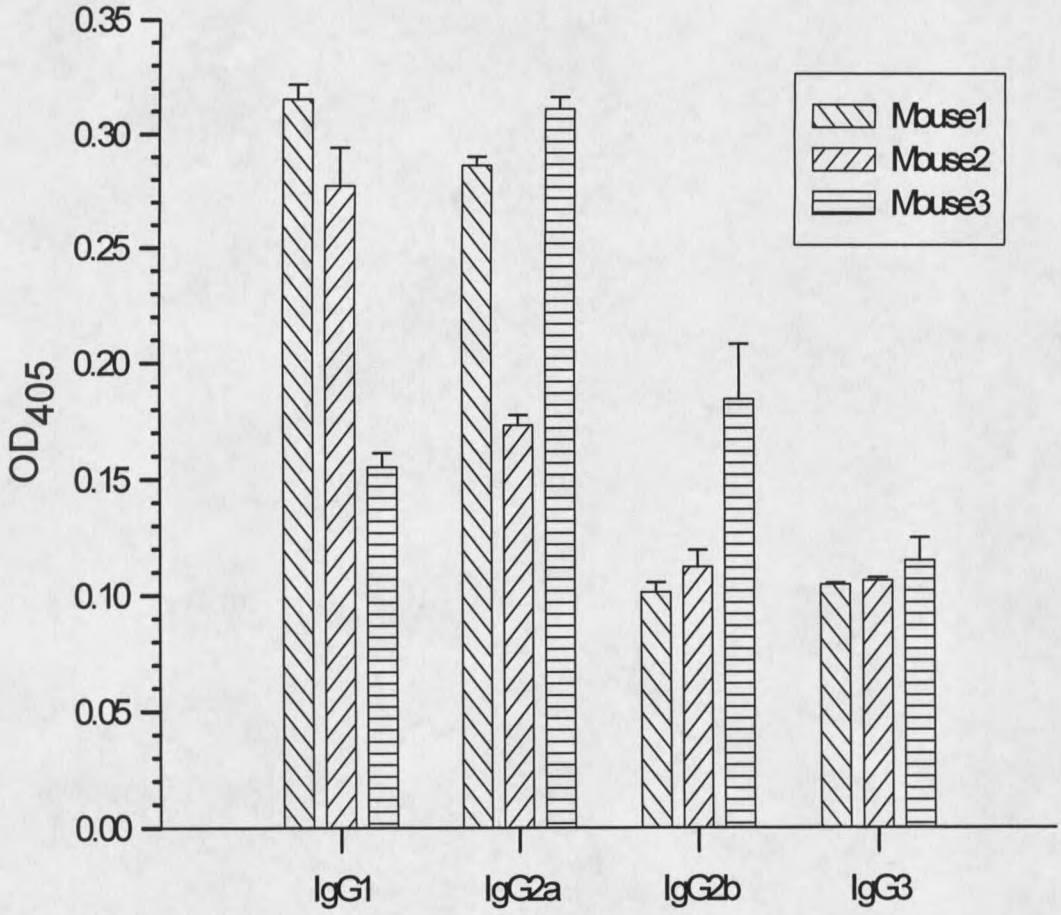


Fig 4.43. Isotype determination of IgG in mice immunized with CCMV-44F.C conjugate in the presence of CFA. Sera at dilution 1:200 were bound to wells coated with 0.1μg of OVA-44F.C conjugate. ELISA was performed as described in Materials and Methods. Shown are the levels of IgG1, IgG2a, IgG2b or IgG3 specific for peptide 44F.C. Histograms represent the mean OD_{405} value of triplicate samples with SD shown as error bars.

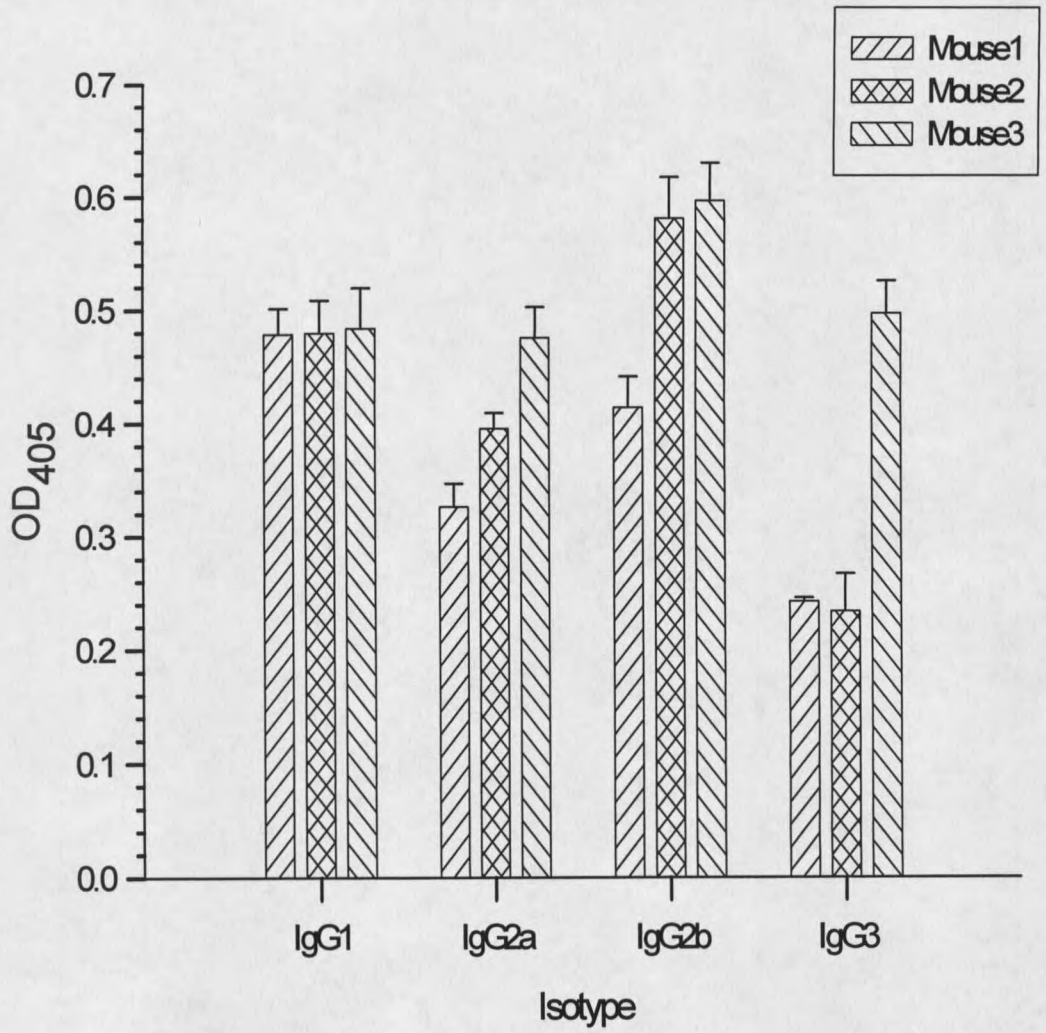


Fig 4.44. Isotype determination of IgG in mice immunized with KLH-44F.C conjugate in the presence of CFA. Sera at dilution 1:200 were bound to wells coated with 0.1μg of OVA-44F.C conjugate. ELISA was performed as described in Materials and Methods. Shown are the levels of IgG1, IgG2a, IgG2b or IgG3 specific for peptide 44F.C. Histograms represent the mean OD_{405} value of triplicate samples with SD shown as error bars.

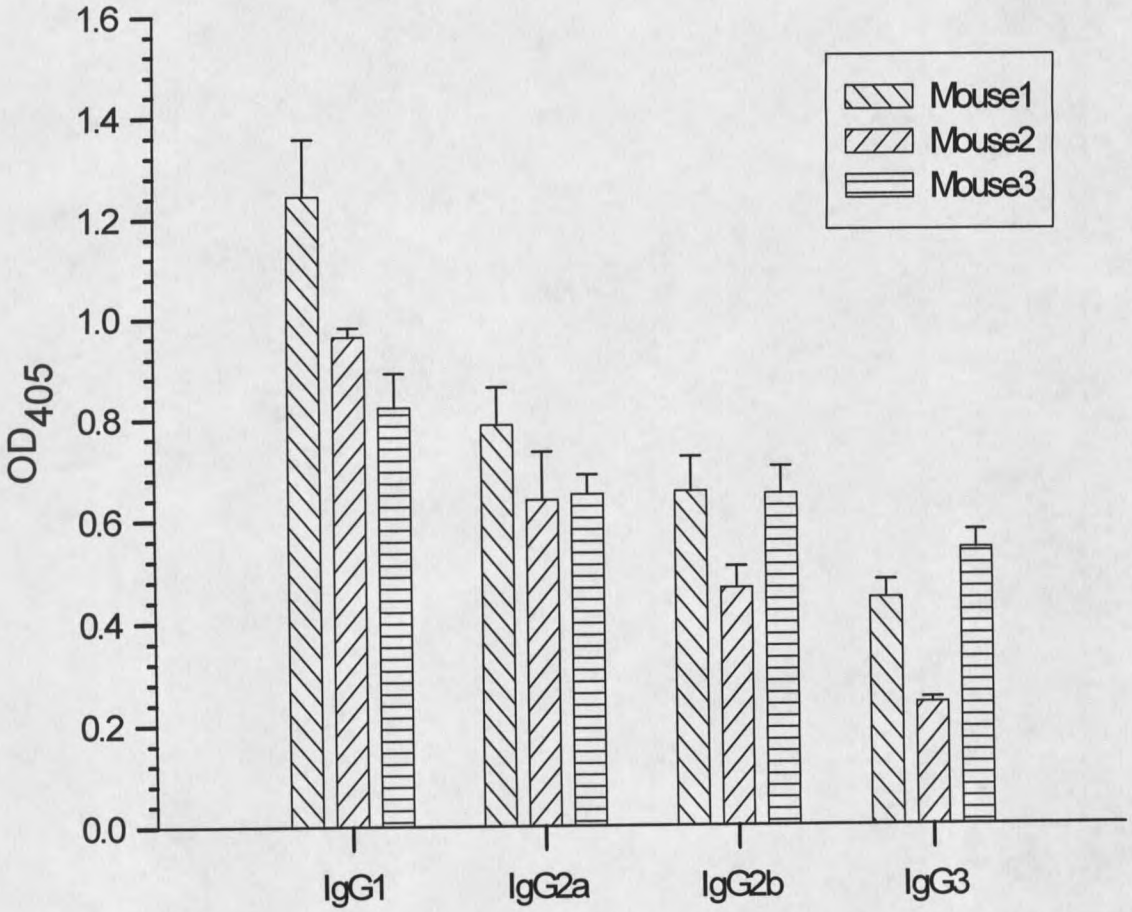


Fig 4.45. Isotype determination of IgG in mice immunized with CPMV-44F.C conjugate in the presence of CFA. Sera at dilution 1:200 were bound to wells coated with 0.1μg of OVA-44F.C conjugate. ELISA was performed as described in Materials and Methods. Shown are the levels of IgG1, IgG2a, IgG2b or IgG3 specific for peptide 44F.C. Histograms represent the mean OD_{405} value of triplicate samples with SD shown as error bars.

Immunization of Mice Using Conjugates without an Adjuvant

Immunization of mice with carrier-peptide conjugates in CFA induced strong immune responses with both Th1 and Th2 orientations. To determine whether the conjugates themselves were strong immunogens, the conjugates were administered without an adjuvant and the sera were assayed for anti-peptide and anti-carrier activities. The sera from mice immunized intraperitoneally (i.p.) with KLH-44 and boosted once or twice i.p. had titers against peptide 44F.C just slightly above background. However, after a third subcutaneous (s.c.) boost, anti-peptide activity was detected at titers of 1:1,000-1:5,000 (Fig. 4.46). In contrast, the anti-carrier titers were high (above 1:20,000) and comparable to the levels found using CFA (Fig. 4.47). No anti-peptide activities were detected in sera from CCMV S130C-44F.C conjugate immunized mice injected either i.p. or s.c., even after 3 boosts (Fig. 4.48). The anti-carrier titers were also significantly lower (1:1,000), compared to those obtained using CFA (Fig. 4.49).

Isotyping of Sera from Mice Immunized without an Adjuvant

When mice were immunized with KLH-peptide conjugates without an adjuvant, the sera obtained had comparable titers of all IgG subtypes: IgG1, IgG2a, IgG2b, and IgG3 (Fig. 4.50). In contrast, sera of the third bleed from mice immunized 3 times i.p. and once s.c. using S130C-44F.C without CFA had the

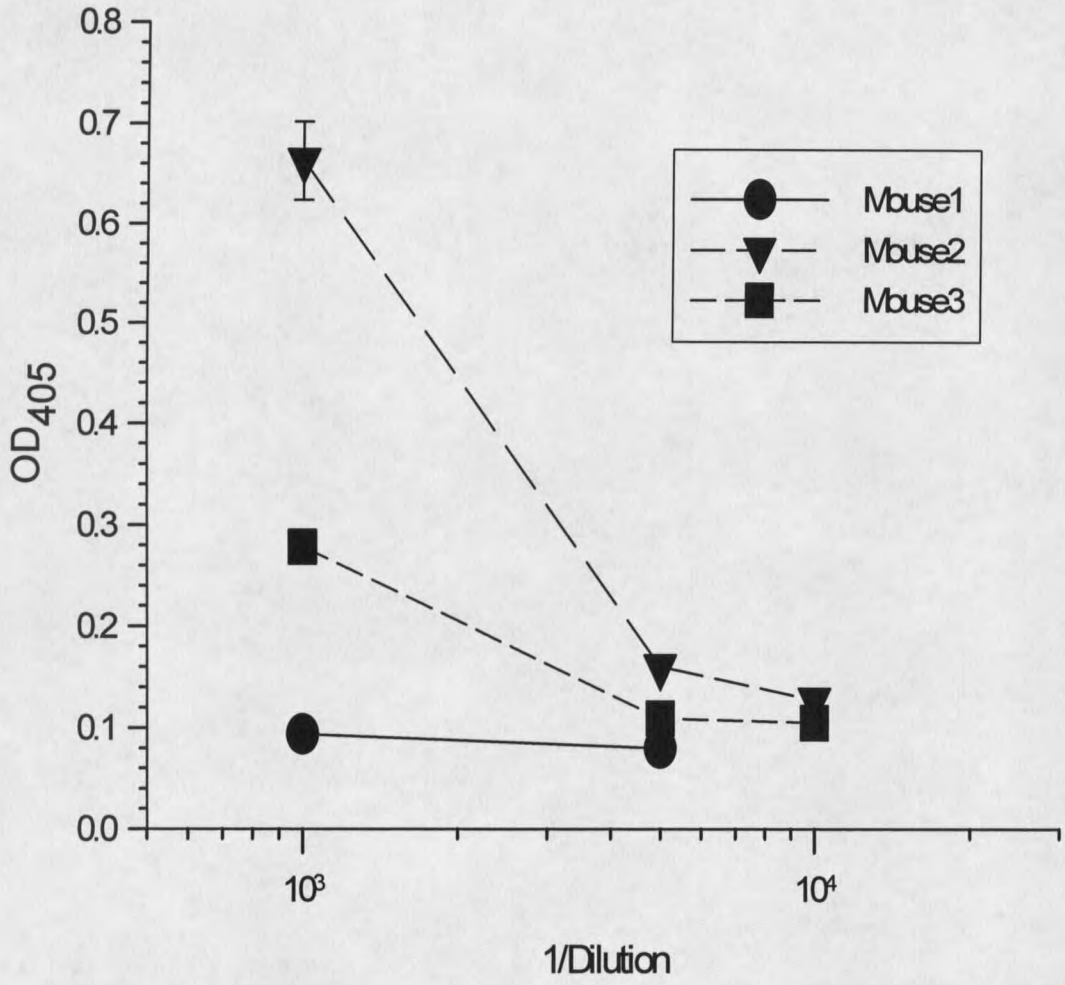


Fig 4.46. Anti-peptide activity of the third bleed sera from KLH-44F.C immunized mice without CFA. Serial dilutions of sera were bound to wells coated with 0.1 μg OVA-44F.C. The reactivity to peptide 44F.C was detected by goat anti-mouse alkaline phosphatase conjugate. OD_{405} values that were greater than twice the background obtained from sera binding to unconjugated OVA coated wells at dilution 1:1,000 were considered positive (usually >0.16). All OD values shown are the mean of triplicate samples with SD shown as error bars.

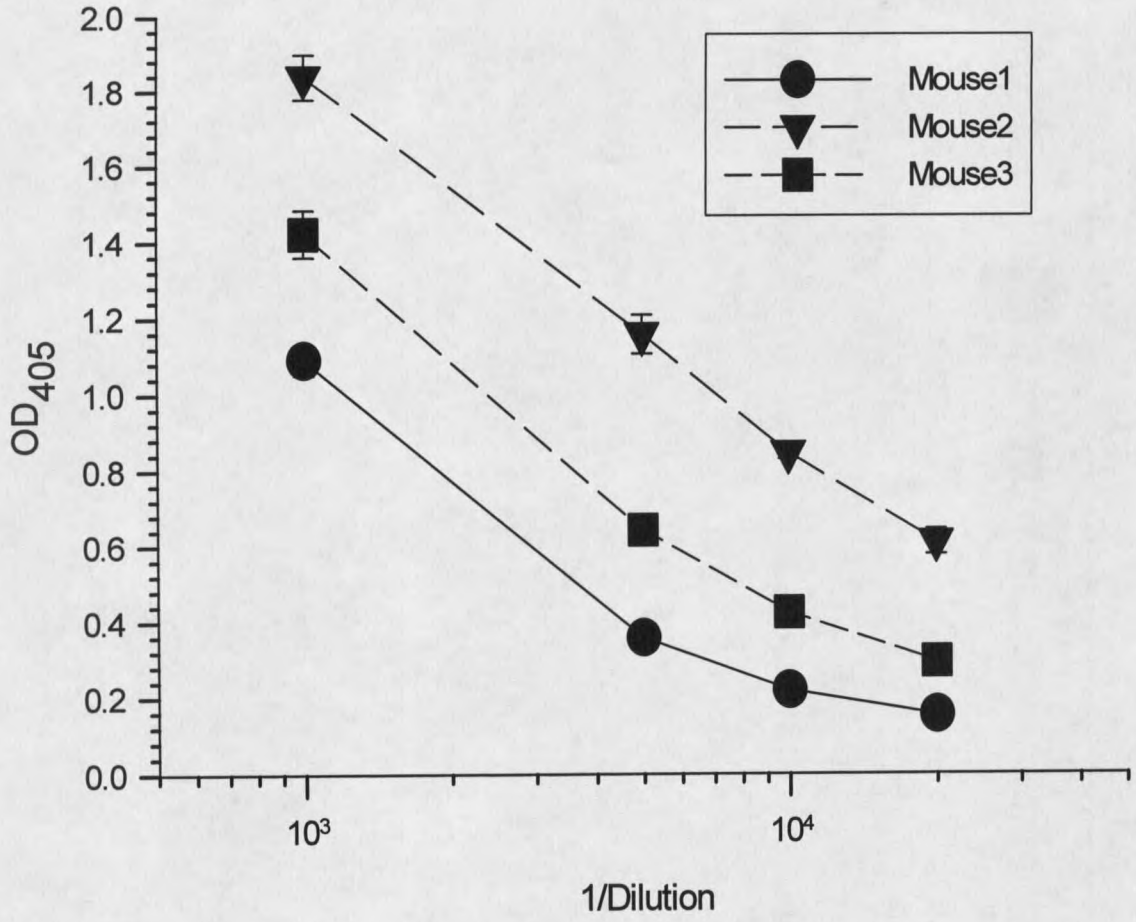


Fig 4.47. Anti-carrier activity of the third bleed sera from KLH-44F.C immunized mice without CFA. ELISA plates were coated with KLH at 0.1 μg/well. Mouse sera were added to wells in serial dilutions and detected using goat anti-mouse alkaline phosphatase conjugate. The binding of pre-immune sera to unconjugated KLH at dilution 1:1,000 usually gave OD value <0.10 and was used as a negative control. All OD values shown are the mean of triplicate samples with SD shown as error bars.

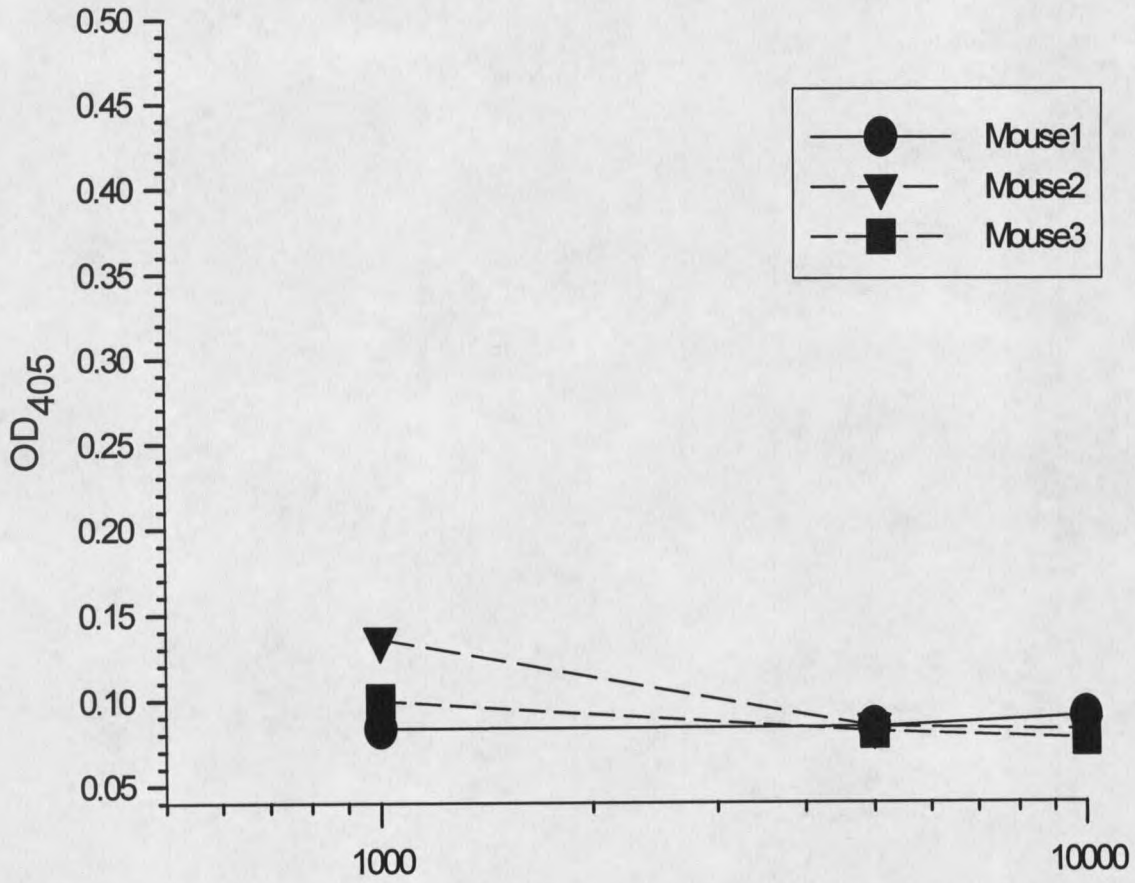


Fig 4.48. Anti-peptide activity of the third bleed sera from S130C-44F.C immunized mice without CFA. Serial dilutions of sera were bound to wells coated with 0.1 μg OVA-44F.C. The reactivity to peptide 44F.C was detected by goat anti-mouse alkaline phosphatase conjugate. OD_{405} values that were greater than twice the background obtained from sera binding to unconjugated OVA coated wells at dilution 1:1,000 were considered positive (usually >0.16). All OD values shown are the mean of triplicate samples with SD shown as error bars.

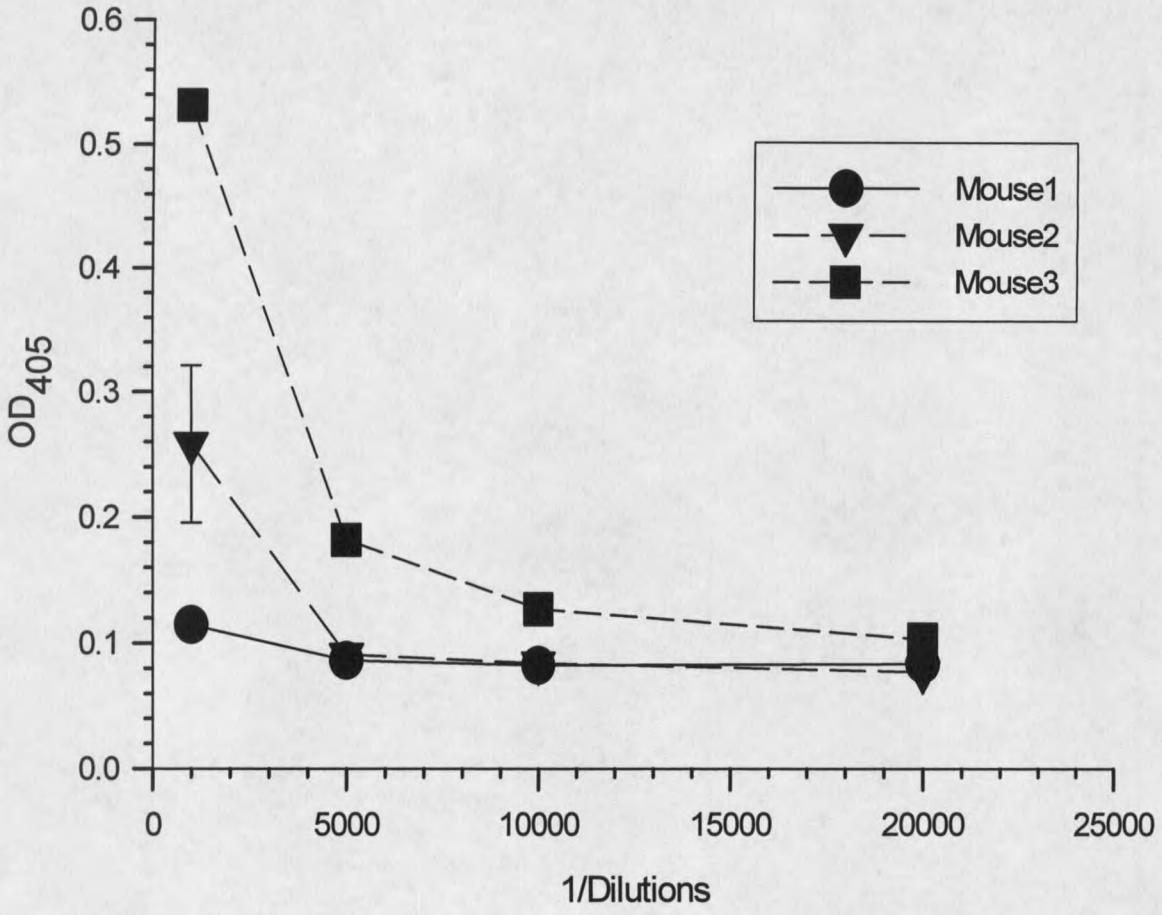


Fig 4.49 Anti-carrier activity of the third bleed sera from S130C-44F.C immunized mice without CFA. ELISA plates were coated with CCMV S130C at 0.5 μg/wells. Mouse sera were added to wells in serial dilutions and detected using goat anti-mouse alkaline phosphatase conjugate. The binding of pre-immune sera to unconjugated CCMV S130C at dilution 1:1,000 usually gave OD value <0.10 and was used as a negative control. All OD values shown are the mean of triplicate samples with SD shown as error bars.

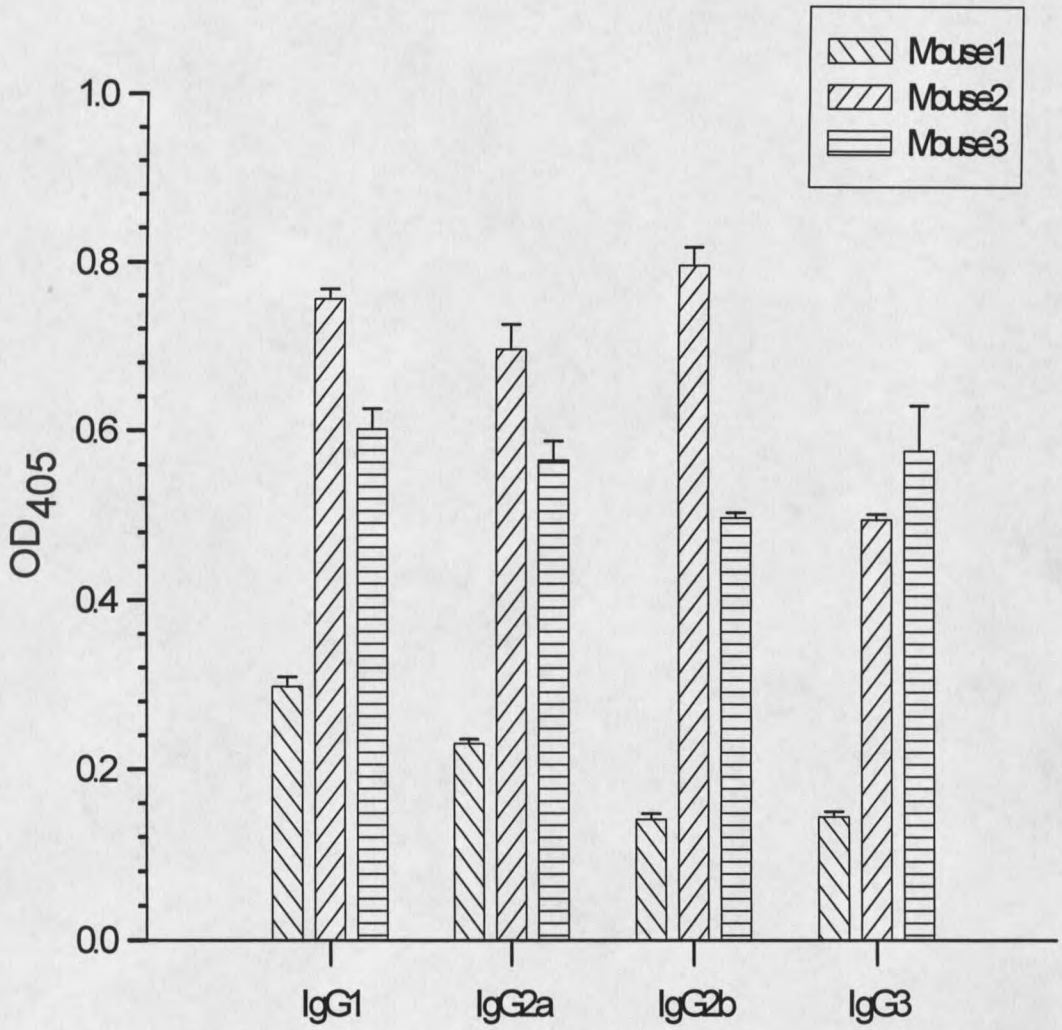


Fig 4.50. Isotype determination of IgG in mice immunized with KLH-44F.C conjugate without CFA. Sera at dilution 1:200 were bound to wells coated with 0.1 µg OVA-44F.C conjugate. ELISA was performed as described in Materials and Methods. Shown are the levels of IgG1, IgG2a, IgG2b or IgG3 specific for peptide 44F.C. Histograms represent the mean OD_{405} value of triplicate samples with SD shown as error bars.

IgG1 subtype dominant over all other subtypes (Fig. 4.51). Thus, it appeared that the S130C-44 conjugate induced a Th2 orientated response in these mice.

Anti-Gp120 Antibodies

Sera from mice immunized with carrier-peptide conjugates had anti-peptide activity against the respective peptide used, peptide 44F.C or 19A.C. These results demonstrated that CD4 binding site mimetic sequences displayed on the surface of virus carriers or KLH are immunogenic in mice. Those sera were also analyzed for anti-gp120 and anti-gp160 antibodies. Sera from only 1 out of 3 CPMV-44F.C-immunized mice had significant anti-gp160IIIB activity compared to the pre-immune serum at the same dilution (Fig. 4.52). Both anti-gp160IIIB and also anti-gp120Bal activity was observed in the same mouse (Fig. 4.53). The sera from mice immunized with CPMV-19A.C showed anti-gp160IIIB activity in 2 out of 3 mice (Fig. 4.54) and had anti-gp120Bal activity in all mice, compared to pre-immune sera at the same dilution (Fig. 4.55). These results were similar to those obtained with KLH-44F.C where 2 out of 3 mice had significantly higher anti-gp160IIIB and anti-gp120Bal activity than pre-immune serum at dilutions, 1:300 and 1:1,000 (Fig. 4.56 and 4.57, respectively). Sera from all KLH-19 immunized mice had significantly higher anti-gp160IIIB and anti-gp120Bal activity than pre-immune controls (Fig. 4.58 and 4.59, respectively). Similar results were obtained with sera from S130C-44F.C and -19A.C immunized mice, where all mice in the group had strikingly higher anti-gp120Bal

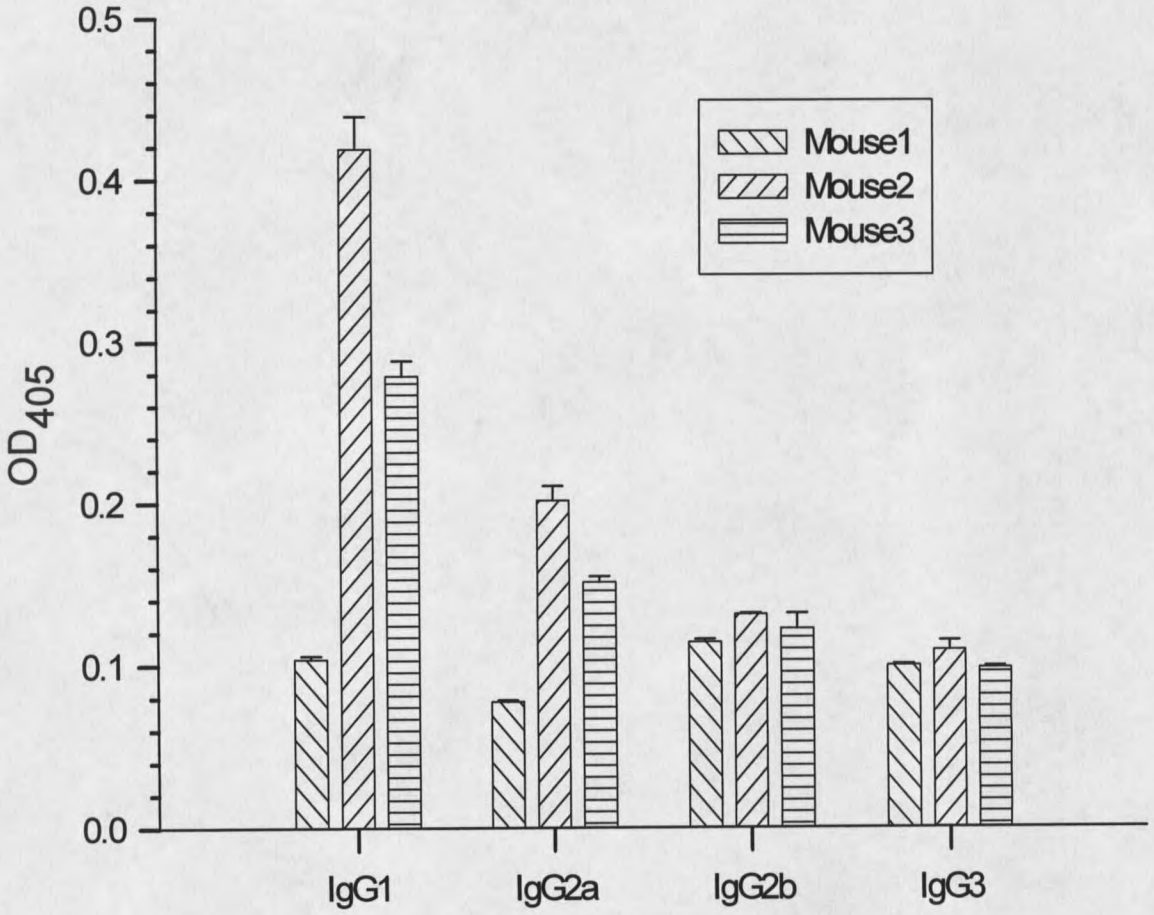


Fig 4.51. Isotype determination of IgG in mice immunized with 130C-44F.C conjugate without CFA. Sera at dilution 1:200 were bound to wells coated with 0.1μg of OVA-44F.C conjugate. ELISA was performed as described in Materials and Methods. Shown are the levels of IgG1, IgG2a, IgG2b or IgG3 specific for peptide 44F.C. Histograms represent the mean OD_{405} value of triplicate samples with SD shown as error bars.

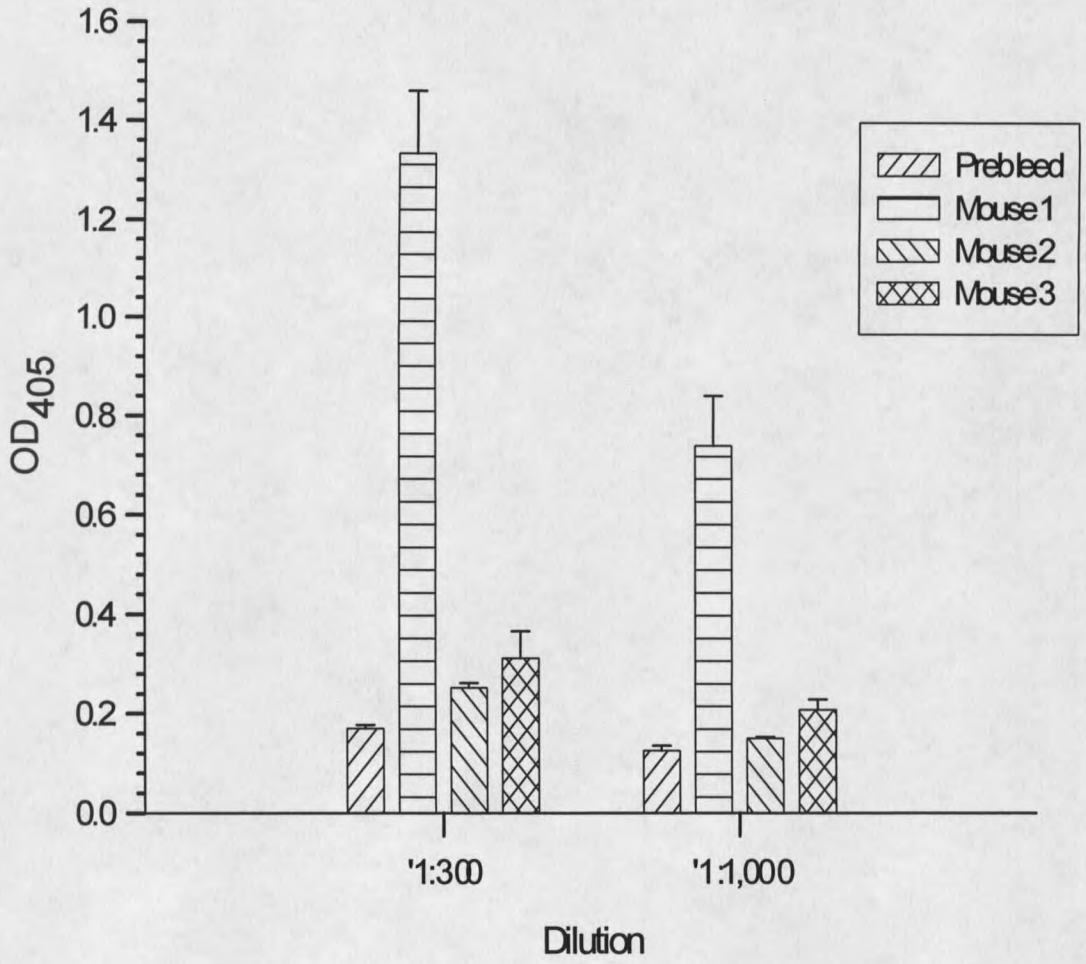


Fig 4.52. Detection of anti-gp160IIIB antibodies in sera from CPMV-44F.C immunized mice. Dilutions of sera were bound to wells coated with 0.1 μg rgp160IIIB as indicated and detected using goat anti-mouse AP conjugate. The binding of pre-immune sera at the same dilutions was used as a negative control. Histograms represent the mean OD_{405} value of triplicate samples with SD shown as error bars. Experiment was performed by Pincus group.

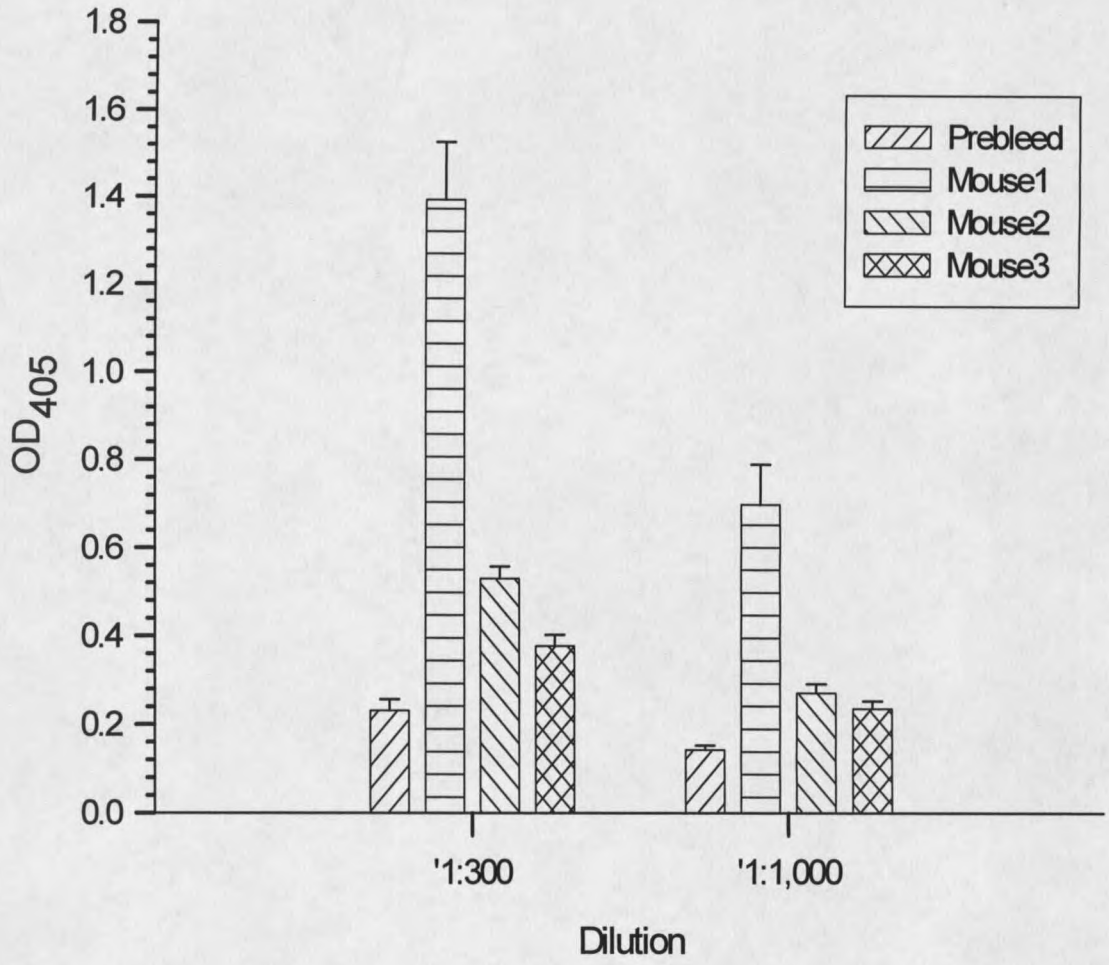


Fig 5.53. Detection of anti-gp120 antibodies in sera from CPMV-44F.C immunized mice. Sera at the dilutions indicated were added to wells coated with 0.1 μg HIV-1 gp120BaL and detected using goat anti-mouse AP conjugate. The binding of pre-immune sera at the same dilutions was used as a negative control. Histograms represent the mean OD_{405} value of triplicate samples with SD shown as error bars. Experiment was performed by Pincus group.

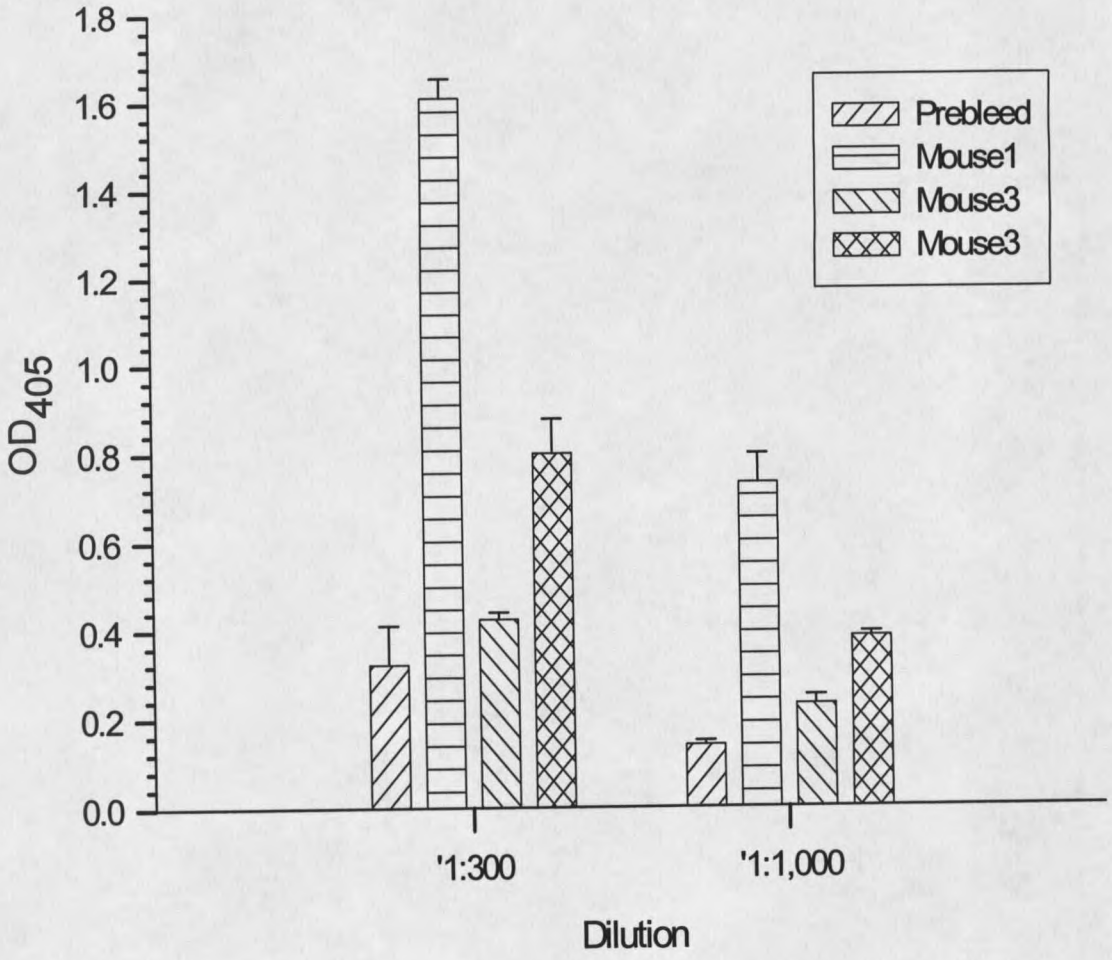


Fig 4.54. Detection of anti-gp160IIIB antibodies in sera from CPMV-19A.C immunized mice. Sera at dilutions indicated were bound to wells coated with 0.1 μg rgp160IIIB and detected using goat anti-mouse AP conjugate. The binding of pre-immune sera at the same dilutions was used as a negative control. Histograms represent the mean OD_{405} value of triplicate samples with SD shown as error bars. Experiment was performed by Pincus group.

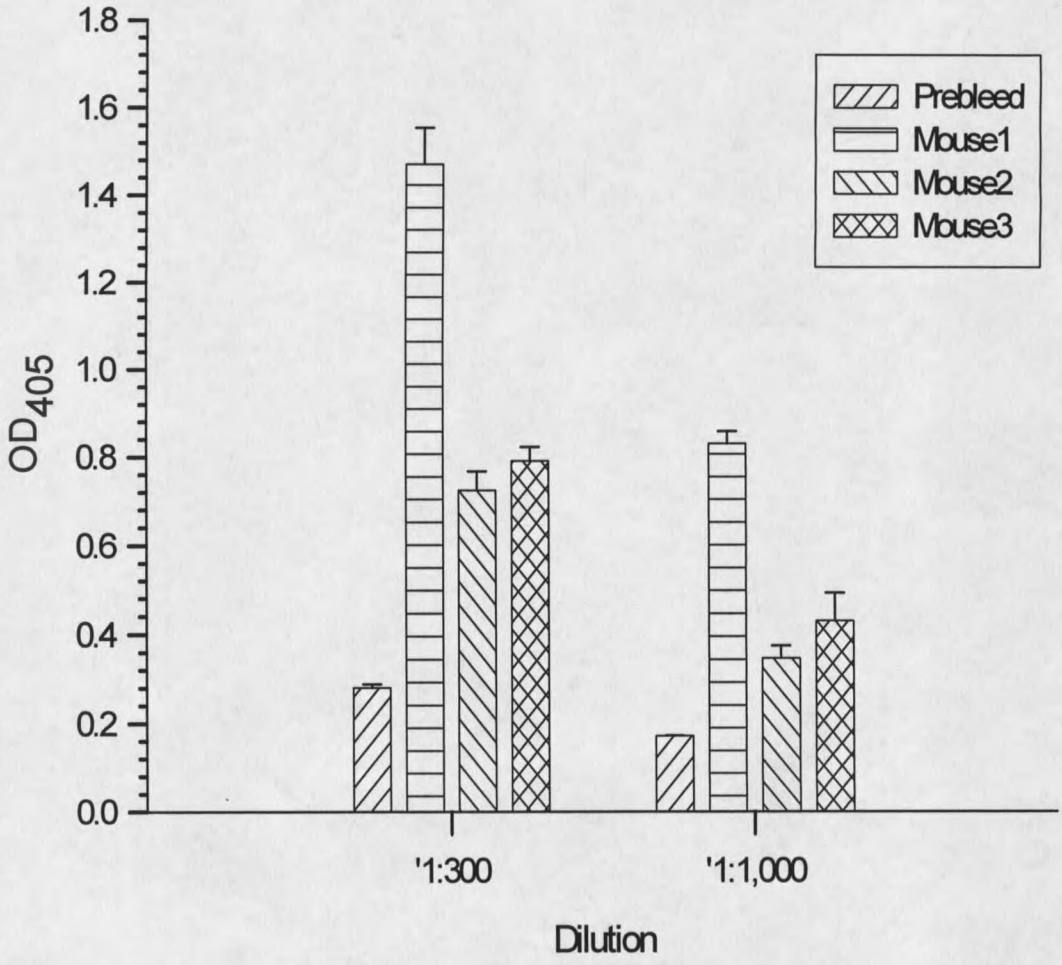


Fig 4.55. Detection of anti-gp120 antibodies in sera from CPMV-19.C immunized mice. Sera at the dilutions indicated were bound to wells coated with 0.1 μg HIV-1 gp120BaL and detected using goat anti-mouse AP conjugate. The binding of pre-immune sera at the same dilutions was used as a negative control. Histograms represent the mean OD_{405} value of triplicate samples with SD shown as error bars. Experiment was performed by Pincus group.

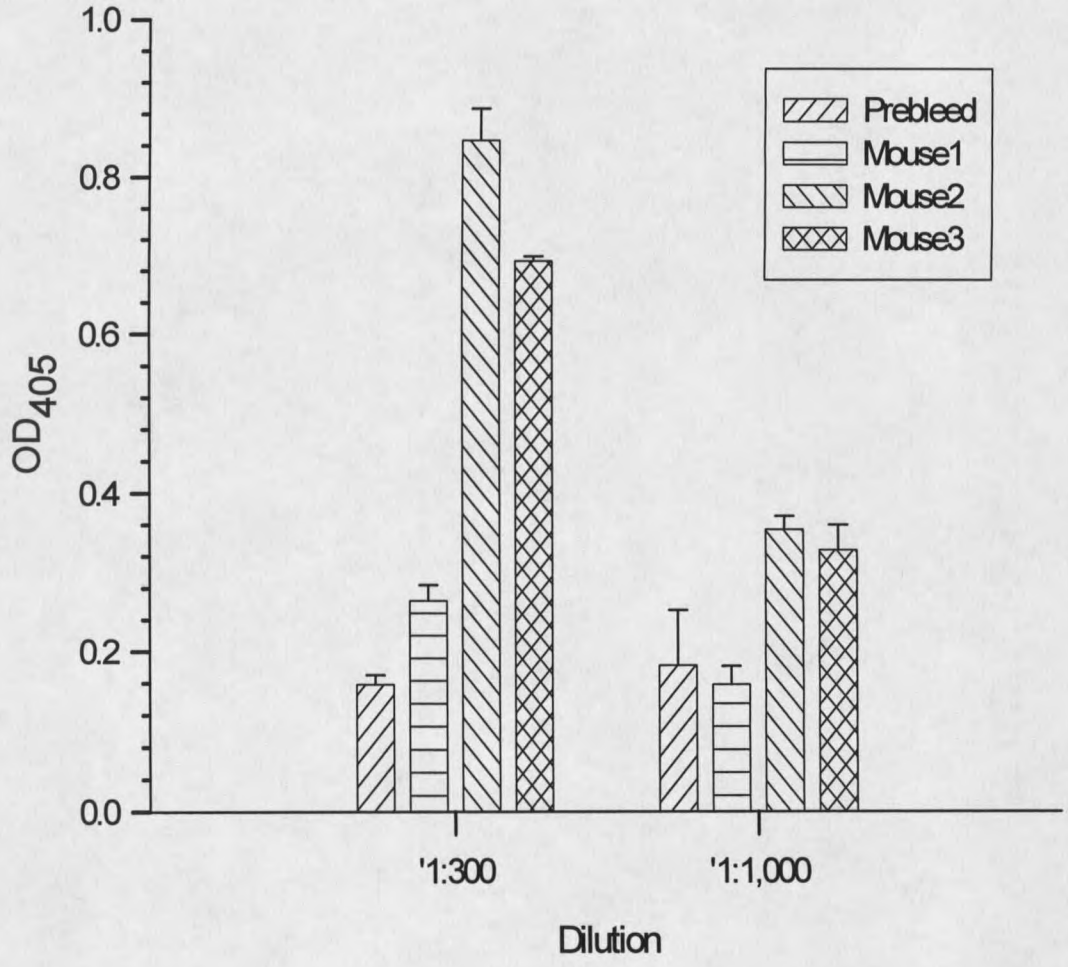


Fig 4.56. Detection of anti-gp160IIIB antibodies in sera from KLH-44F.C immunized mice. Sera at the dilutions indicated were bound to wells coated with 0.1 μg rgp160IIIB and detected using goat anti-mouse AP conjugate. The binding of pre-immune sera at the same dilutions was used as a negative control. Histograms represent the mean OD_{405} value of triplicate samples with SD shown as error bars. Experiment was performed by Pincus group.

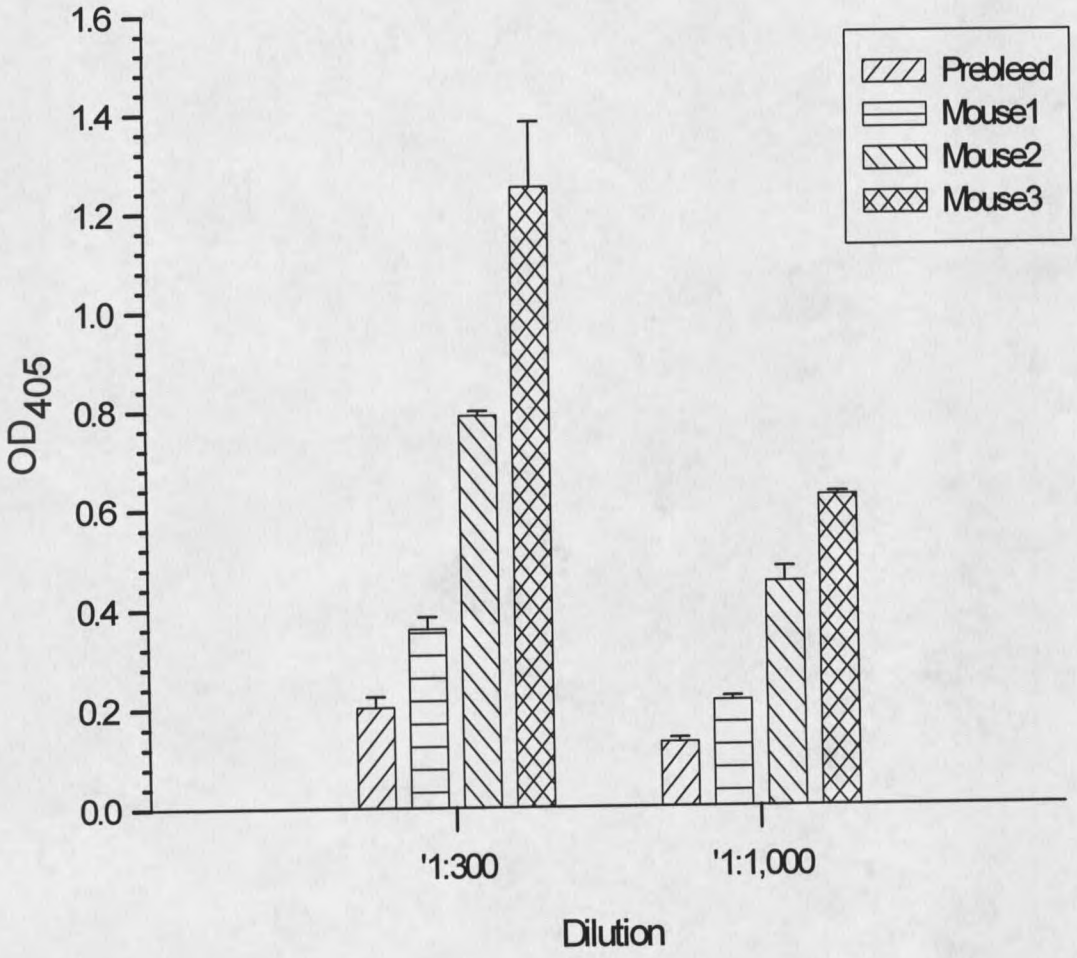


Fig 4.57. Detection of anti-gp120 antibodies in sera from KLH-44F.C immunized mice. Sera at the dilutions indicated were bound to wells coated with 0.1 μg HIV-1 gp120 and detected using goat anti-mouse AP conjugate. The binding of pre-immune sera at the same dilutions was used as a negative control. Histograms represent the mean OD_{405} value of triplicate samples with SD shown as error bars. Experiment was performed by Pincus group.

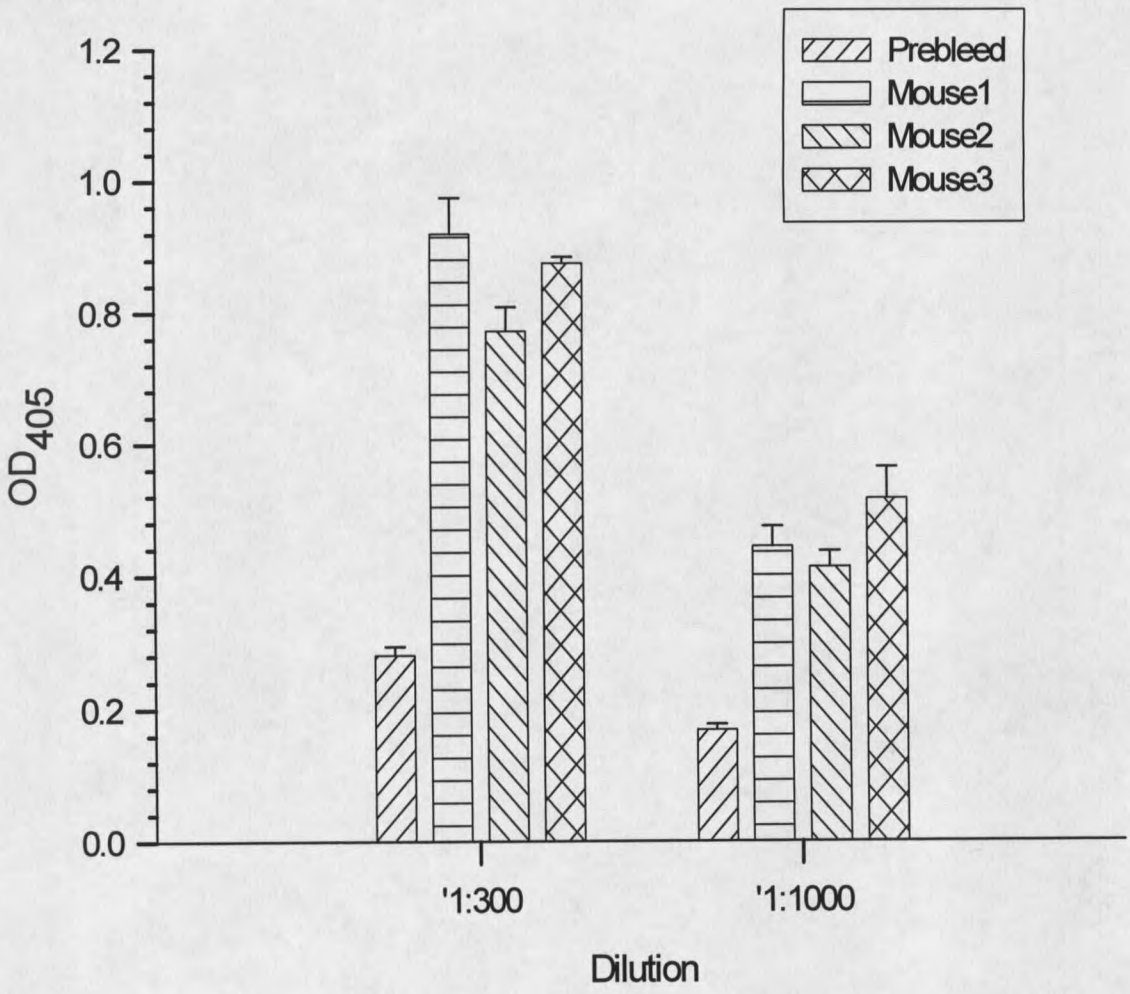


Fig 4.58. Detection of anti-gp160IIIB antibodies in sera from KLH-19A.C immunized mice. Sera at the dilutions indicated were bound to wells coated with 0.1 μg rgp160IIIB and detected using goat anti-mouse AP conjugate. The binding of pre-immune sera at the same dilutions was used as a negative control. Histograms represent the mean OD_{405} value of triplicate samples with SD shown as error bars. Experiment was performed by Pincus group.

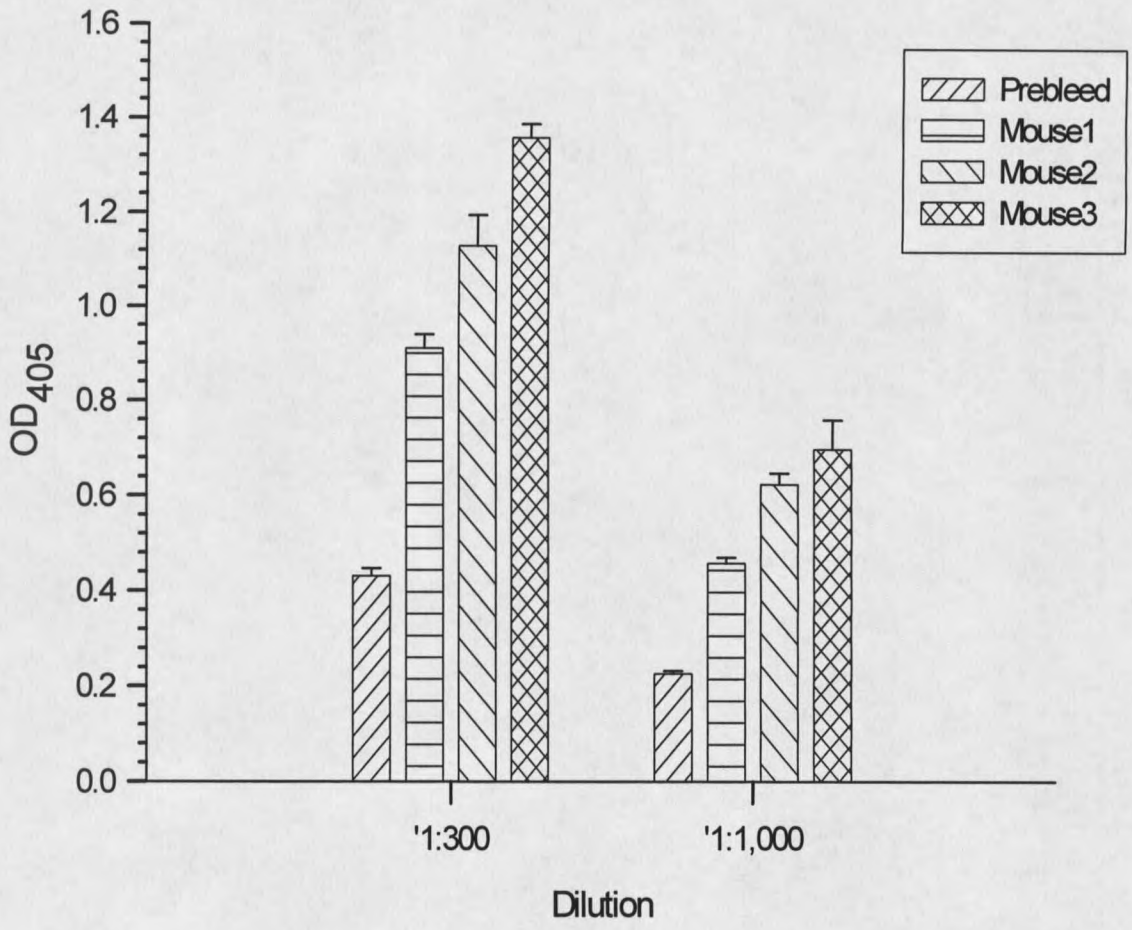


Fig 4.59. Detection of anti-gp120 antibodies in sera from KLH-19A.C immunized mice. Sera at the dilutions indicated were bound to wells coated with 0.1 μg HIV-1 gp120BaL and detected using goat anti-mouse AP conjugate. The binding of pre-immune sera at the same dilutions was used as a negative control. Histograms represent the mean OD_{405} value of triplicate samples with SD shown as error bars. Experiment was performed by Pincus group.

activity than pre-immune sera (Fig. 4.60 and 4.61, respectively). These results indicated that the peptides used not only induced anti-peptide antibodies but also induced anti-gp120 and anti-gp160 activities in mice, at least when compared to pre-immune sera. To verify that that anti-HIV activities observed were specific to the peptide attached to carriers, the anti-gp120 activities of CCMV- and CPMV-peptide conjugates were compared to those of sera from mice immunized with conjugates of the same viruses with an irrelevant peptide, S9, or with CCMV alone. As shown in Figure 4.62, CPMV-S9 and CCMV-S9 sera cross-reacted with to gp120Bal while sera from mice immunized with CCMV alone did not. For both CPMV-19 and CPMV-44 immunized mice, only 1 out of 3 had significantly higher anti-gp120 titer than those immunized with the irrelevant peptide. One of the CCMV-19 immunized mice and 2 out of 3 CCMV-44 immunized mice had a markedly higher anti-gp120 titer than those mice immunized with irrelevant peptide (Fig. 4.62). These sera were also used in FACS experiments looking for binding to HIV-infected cells expressing gp120 on their surface, as well as in HIV neutralization assays (both performed by Pincus lab). The results did not show any significant binding by the immune sera to HIV-infected cells nor any neutralization activity (data not shown).

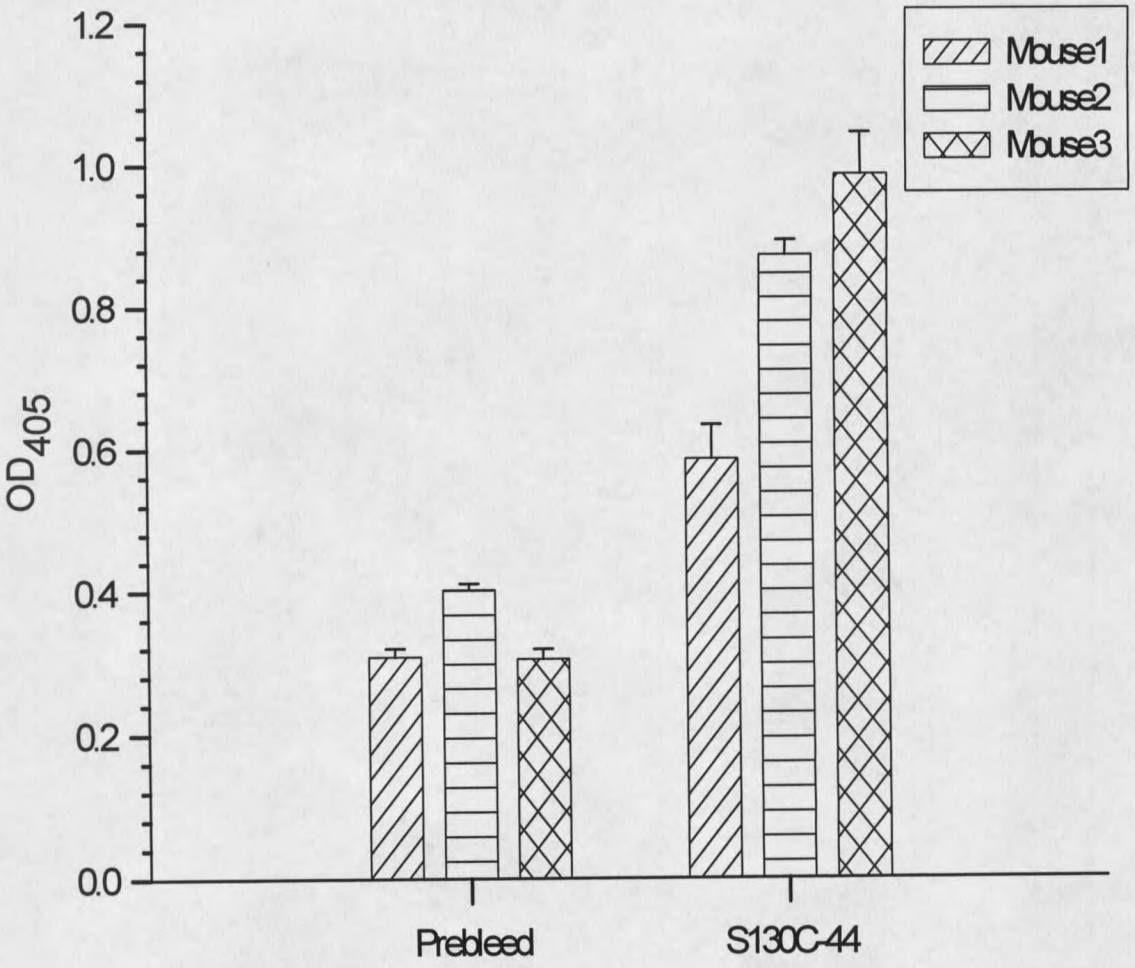


Fig 4.60. Detection of anti-gp120 antibodies in sera from S130C-44F.C immunized mice. Sera at dilution 1:300 were bound to wells coated with 0.1 μg HIV-1 gp120BaL and detected using goat anti-mouse AP conjugate. The binding of pre-immune sera at the same dilution was used as a negative control. Histograms represent the mean OD_{405} value of triplicate samples with SD shown as error bars. Experiment was performed by Pincus group.

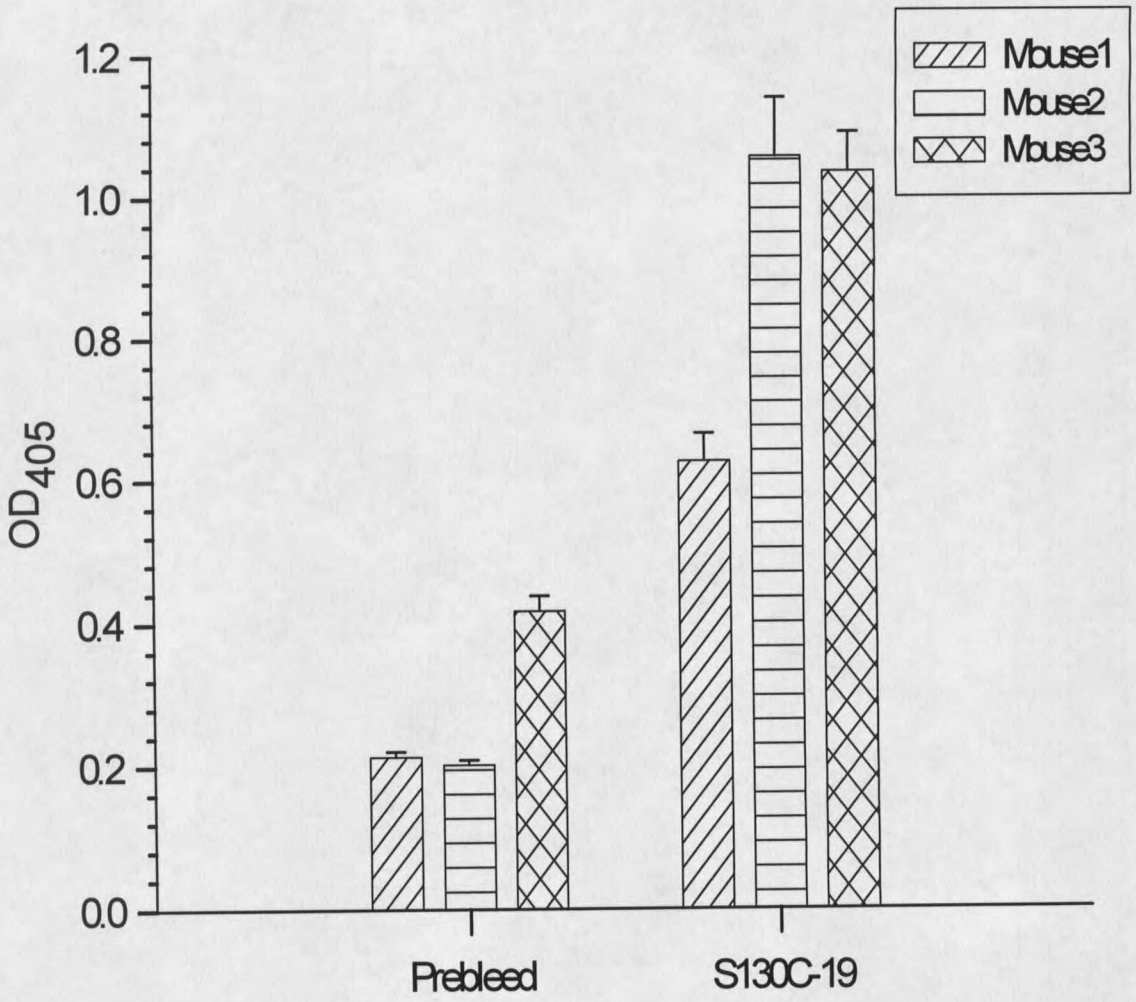


Fig 4.61. Detection of anti-gp120 antibodies in sera from S130C-19A.C immunized mice. Sera at dilution 1:300 were bound to wells coated with 0.1 μg HIV-1 gp120BaL and detected using goat anti-mouse AP conjugate. The binding of pre-immune sera at the same dilution was used as a negative control. Histograms represent the mean OD_{405} value of triplicate samples with SD shown as error bars. Experiment was performed by Pincus group.

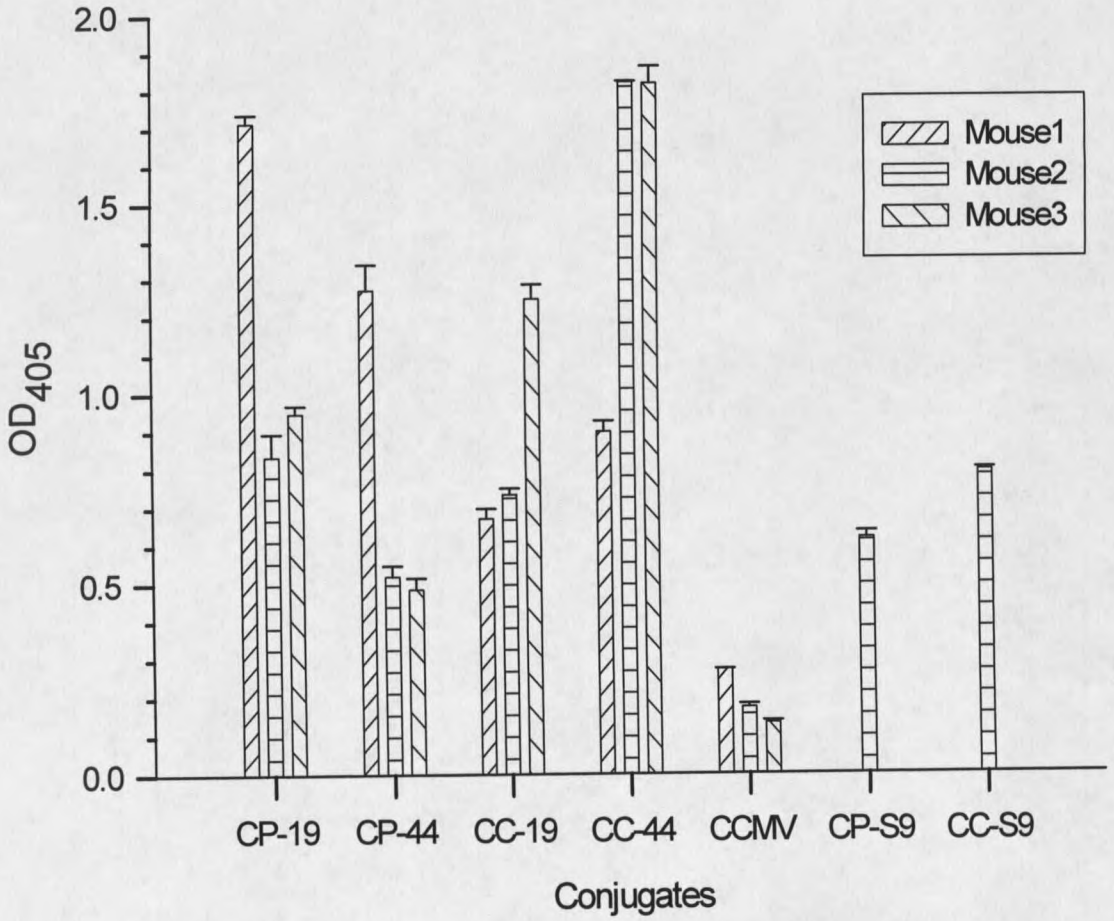


Fig 4.62. Comparison of anti-gp120 antibody level in mice immunized with various virus conjugates. Sera at dilution 1:300 were bound to wells coated with 0.1 μg HIV-1 gp120BaL and detected using goat anti-mouse AP conjugate. The binding of sera to gp120 was compared with the sera from mice immunized with conjugates of an irrelevant peptide, S9, conjugates and of CCMV alone. CC and CV represent CCMV and CPMV, respectively. Histograms represent the mean OD_{405} value of triplicate samples with SD shown as error bars. Experiment was performed by the Pincus group.

CHAPTER FIVE

SUMMARY AND DISCUSSION

Summary and Discussion

Many attempts were made to develop an HIV vaccine based on HIV gp120 sequences at the CD4 receptor binding site, which exhibits a relatively high degree of conservation. Ideally, a carrier molecule would act as a scaffold and constrain the HIV peptide in a stable conformation, presenting it to the immune system and eliciting a range of antibodies that would hopefully cross-react with HIV. The CCMV virus, whose structure has been determined to atomic resolution, was selected as a carrier because it theoretically allowed the design of coat proteins carrying HIV peptides in constrained conformations on the surface of the assembled virion.

In the initial study, different "loop" regions from conserved region 4 and variable region 4 of HIV gp120 that form part of the CD4 binding site were inserted into each of the 4 surface-exposed loops of the CCMV coat protein by means of genetically modifying the viral genome. Presumably, such a chimeric CCMV would carry 180 copies of HIV peptide per virion. However, when the modified CCMV RNAs were inoculated into a plant host, only local lesions on the inoculated leaves appeared and no intact virus particles were formed, suggesting that modification of the coat protein subunit compromised virion assembly in the plant host. There appeared to be a constraint on the size of loops that did not

allow introducing even a moderate-sized foreign fragment of about 10 residues. Expression of chimeric coat proteins was also tried in a yeast system. Many subunit proteins with HIV inserts were produced in yeast; however, most of the protein was found in the yeast pellet after cell lysis, presumably due to mis-folding and/or aggregation of subunit proteins. Furthermore, most of the viral particles found in the cell supernatant were not the proper size and shape for T=3 virus capsids. It was possible that genetic modification of the coat proteins caused their chemical properties to change. When expressed at high levels, chimeric coat proteins might interact with each other inappropriately and cause aggregation. The failure of virus assembly in both plant and yeast systems may have reflected an inflexibility of the CCMV coat protein in protein-protein interactions needed for capsid assembly.

Since the CCMV assembly was so sensitive to genetically introducing a foreign sequence into the coat protein, epitope-presentation systems were developed in which the peptide sequence was chemically attached to an amino acid sidechain residue of the CCMV coat protein on intact viral capsids. The synthetic peptides that were used corresponded to phagotopes selected from a random peptide phage display library by antibodies to the conformationally determined epitopes at the CD4 binding site of HIV gp120. With the aim of inducing a humoral immune response resembling that induced by the original antigen that elicited these antibodies, immunogens were prepared by chemically coupling the synthetic peptide to different carriers (CCMV and CPMV capsids

and KLH) and determining which carrier or linker was better in linking the peptide to the carrier. Furthermore, the peptide conjugates were used in immunizing mice and the anti-peptide antibody titers were measured. It was hypothesized that having more peptide attached to the carriers would induce higher anti-peptide antibody titers.

Heterobifunctional linkers were first used to couple a cysteine sidechain of peptides 44F.C and 19A.C to a lysine sidechain of salt stable (K42R) CCMV capsids isolated from yeast. Comparing the two linkers tried, SPDP acted as efficiently as sulfo-SMCC in coupling to CCMV (data using SPDP as shown here compared to that using sulfo-SMCC performed by R. Pomwised, unpublished). However, the problems with using these linkers in CCMV were low yields of conjugate and viral aggregation. It was expected that if viral aggregation were reduced, more virus surface would be available to attach to a peptide. The fact that CCMV contains three or four reactive lysines on the surface per subunit may have caused unwanted reactions, such as coupling uncontrollable amounts of peptides per subunit. Moreover, if the lysines were close to each other on the CCMV surface a sulfhydryl reactive group of an excess linker molecule may nonspecifically reacted with another lysine sidechain and cause coupling between lysines or reacted with one of the two cysteine residues in the CCMV coat protein. These cysteine residues are "buried" in the CCMV crystal structure, but may in fact be accessible as the protein "breathes", resulting in a loss of peptide coupling sites.

Due to low coupling and high aggregation in CCMV, coupling a peptide to the CPMV capsid protein offered an advantage, because CPMV was reported to contain only one reactive lysine site on the surface per large and small subunit pair. The results from the Scripps group showed that one peptide was linked to the reactive lysine which is located at small subunit of the coat protein (118). In this case, 60 peptides would be attached per viral particle (1 peptide per subunit). However, our results showed more than one peptide attached to each small subunit and also peptide attached to the large subunit. It is possible that the sulfo-SMCC we used in coupling peptide to CPMV was more reactive and less selective than the fluorescein N-hydroxysuccinimide ester they used in their experiments. This notion was supported by the fact that we used less peptide but obtained more linking (we used 20 molar excess of sulfo-SMCC over coat protein subunit, while they used 200 dye molecules to 1 coat protein subunit in order to get 1 dye per subunit). Using both linkers, excess linking reagent remaining in the reaction may have interfered with the peptide coupling reaction and caused viral crosslinking. When the S130C mutant virus containing a single cysteine residue introduced at an optimum site on each subunit was coupled to the peptide using BMH, higher conjugation yields and less viral aggregation were obtained because the cysteine located inside of the doughnut-shape capsomere was not too exposed on the surface where it would easily couple to a cysteine from another virus and not too close to a cysteine on an adjacent subunit, preventing intra-viral crosslinking. Moreover, the excess linker, which was one of

the factors that caused viral aggregation, was also eliminated by purifying the linker-peptide conjugate by HPLC before adding the virus. Thus, peptide 19A.C, which had previously coupled far less than peptide 44F.C to CCMV, became attached equally well to CCMV S130C. It was noteworthy that peptide 19A.C itself had attached well to the SPDP linker by itself in the kinetic assay (Fig. 4.4). Similar to the kinetic assay, good coupling of peptide 19A.C was also observed in the S130C-19A.C conjugate where the peptide was attached first to the linker. In making the CCMV-19A.C and CPMV-19A.C conjugates, the virus carriers were attached to the linker first and then to the peptide. Comparing between the two viruses, peptide 19A.C probably coupled far more to CPMV, because a 60 molar excess was used over CPMV coat protein subunit, while only a 10 molar excess of peptide over CCMV coat protein subunit was used Thus, peptide 19A.C had more chances to attach to CPMV than to CCMV. Comparing attachment of peptides 19A.C and 44F.C to the CCMV, peptide 19A.C may have attached less to CCMV because peptide 19A.C is more hydrophobic. The peptide molecules might bind to each other due to hydrophobic interaction or bind to unexpected sites on the virus, thereby lowering its yield in coupling to the virus.

When we succeeded in getting good coupling of peptides 19A.C and 44F.C to S130C, we anticipated that more peptide per carrier would elicit more anti-peptide antibodies. After CCMV S130C conjugated with peptide (44F.C or 19A.C) was used to immunize mice, anti-peptide antibody titers were compared

to the titer of sera from mice immunized with other conjugates, made by attaching peptides to other carriers, CCMV, CPMV, which had less peptide, as well as to KLH. The ideal carrier should have its own immunogenicity and be capable of presenting the peptide to be recognized by immune system, and thus increase the peptide's immunogenicity. All carriers used in these experiments were immunogenic because the anti-carrier antibody titers were comparable when they were immunized with an adjuvant.

There was some variation in anti-peptide titer between the 3 mice in each group immunized with the same conjugate, because an outbred strain (CD1) was used. However, when comparing the average anti-peptide antibody titer from each group, a conclusion could be drawn that the amount of peptide attached to the carrier was not a factor in determining the anti-peptide antibody titer. The CCMV-19 A.C conjugate, which had far less peptide attached than the CPMV-19A.C conjugate, elicited a higher anti-peptide titer (1:10,000-100,000) versus (1:1,000-5,000). Furthermore, S130C-44F.C and S130C-19A.C, which had higher coupling yields than the CCMV conjugates, produced a lower anti-peptide antibody titers (1:5,000-10,000 and 1:1,000-20,000) than CCMV-44F.C and CCMV-19A.C (1:10,000-50,000 and 1:10,000-100,000). It was possible that the peptides attached to CPMV and S130C might not be exposed as well as on the capsid surface because of the different attachment sites used. Thus, aside from the amount of peptide attached to a carrier, the exposure of peptide on the carrier surface should be taken into account. To determine how well a peptide

exposed on the viral surface, the peptide-virus conjugates could be crystallized and the structures compared to determine whether there is a correlation between which peptide is exposed well on the viral surface and which induces a strong immune response. However, good crystal structure of the peptide-virus conjugate cannot be obtained if the peptides are not uniformly attached to all the viral subunits.

In comparing our results to those of the Pincus group with peptide S9, the anti-peptide antibody titers of our sera from CCMV and CPMV conjugates were lower in spite of getting comparable yields of conjugates (Fig. 4.1 lanes 3 and 5). It was possible that this was due to the fact that a different immunization protocol was used. The Pincus group always immunized mice with equivalent amounts of peptide while we used equivalent amounts of carrier conjugate. Having too much or too little peptide attached to the carrier might induce less immune response or possibly tolerance. Moreover, the route and period of immunization as well as the strain of mice used in our laboratory and theirs were different.

Comparing all the carriers used to immunize mice with an adjuvant, CCMV appeared to be the best carrier in presenting a peptide to the immune response. In spite of less coupling of both peptides to CCMV, conjugates would induce stronger anti-peptide antibody titers than the other conjugates. In vaccine development for humans use, the adjuvant we used would be too toxic. A good carrier should therefore be very immunogenic by itself. The data from the immunizations showed that CCMV S130C was poorly immunogenic by itself,

because only low anti-carrier and no anti-peptide antibody titer were detected when immunizing mice without the adjuvant. Based on the results obtained here, CCMV might not be suitable in the long run for human immunizations, where strong adjuvants should be avoided because of their toxicity. In contrast, KLH was a more immunogenic carrier in the absence of adjuvant, as shown in high anti-carrier titers (above 1:20,000) when immunized without CFA, although anti-peptide titers observed were not as strong as seen with KLH in CFA. However, our results were different from the Pincus group, for whom mice immunized with KLH, CPMV and CCMV conjugates to peptide S9 without CFA had both higher carrier antibody titers and higher anti-peptide antibodies titers than our mice. It may not be appropriate to draw conclusions before following the immunization protocol used in his laboratory with our conjugates, but a follow up experiment using subcutaneous immunizations of balb/c mice with S130-44F.C again showed much lower titers than mice immunized with KLH-44 . IgG isotypes were determined in sera from mice immunized with KLH-44F.C or S130C-44F.C without an adjuvant to investigate whether immunization of mice with S130C-44F.C in the absence of adjuvants may have resulted in tolerance. In the absence of adjuvants, sera from S130-44F.C were predominantly IgG1, indicating a Th-2 type of immune response. This kind of response is usually associated with tolerance rather than immunity. Typically, breaking of tolerance is associated with a Th-1 type of immune response (119). In contrast, KLH induced an immune response that was both Th-1 and Th-2,

where all IgG subtype levels were comparable, which was similar to the results from the Pincus group with peptide S9 conjugates. However, sera from mice immunized with CCMV conjugates in the absence of CFA by the Pincus group had predominantly IgG2a, indicating a Th-1 type response. It was possible that the different peptide sequences used led to different Th polarization.

The results of experiments to detect anti-gp160IIIB and anti-gp120Bal antibodies in sera of mice immunized with peptide conjugates in Freund's adjuvant were inconclusive. Only some mice showed titers significantly above those of the pre-immune sera. There was no anti-gp120 activity in sera from CCMV carrier control mice but those from mice immunized with CCMV and CPMV conjugated to an irrelevant peptide, S9 showed some activities. FACS analysis did not show any significant binding of the immune sera to HIV-infected cells and no neutralization activity was detected. However, the low anti-gp120 antibody titers in the sera might not be sufficient to detect the lower amount of gp120 on HIV-infected cells compared to the ELISA assays. Thus, more experiments need to be performed to determine whether any of the "anti-gp120 activity" observed in sera is due to specific anti-gp120 antibodies. For example, if the peptide, in increasing concentrations, can inhibit the binding of the antibodies in the sera to gp120 or gp160, this would argue that the cross-reactive serum antibody binding observed might be due to specific anti-gp120 or gp160 antibodies.

It was proposed that the peptides corresponding to selected phagotopes could adopt the conformations that mimic the epitopes in HIV gp120 and would be capable of eliciting an immune response similar to that of the original patients who made the antibodies which were used to select the phage (F105 or 5145A), and that therefore these peptides might also be appropriate for developing a vaccine. In the inhibition assays, the synthetic peptides competed with gp120 for binding to the mAbs used in phage selection, indicating that the peptides bound the same antigenic site of the mAb as gp120 (J. Jacobs, unpublished). The binding between the peptide displayed on the phage and the mAb might result from the phage surface constraining the peptide insert in a specific conformation, which facilitated in the binding to the mAb. A study has helped in gaining insight the role of the mimotope carrier in inducing of a specific immune response (120). In this experiment, mice were immunized with phage display peptide sequences, inserted in the N-terminal region of the major coat protein pVIII that had been selected by an anti-HBsAg mAb, which presumably mimicked an epitope of the human hepatitis B surface antigen (HBsAg). The humoral immune response of phagotope-immunized animals was compared with those of a recombinant HBsAg vaccine or with the mimotope sequence on different carrier molecules (phage coat protein pIII, recombinant human H ferritin, HBV core peptide) flanked by a few residues from the pVIII sequence. The results revealed that the phages as originally selected with peptide displayed on (pVIII) are the best form of immunogen in mice, inducing the most reproducible and potent

immunization (120). Unlike pVIII, which is present in 2700 copies per phage, pIII, the protein on which the peptides were displayed in our study, is present in only 3-5 copies per phage particle. Only 10-30% of all the pVIII molecules can display the mimotopes (120), but even so, animals injected with the same amount of phage particle would receive between 50 and 160 times less mimotopes displayed on pIII molecules than those on pVIII. Thus, it would be difficult to immunize with sufficient phage carrying mimotope on pIII molecules in order to get a comparable amount of peptide to the amount used on the pVIII molecule in inducing an immune response. This was a limitation of our study, so finding another good carrier may be the only option. So far, the virus carriers (CCMV and CPMV) as well as the KLH used in these experiments each offer some advantages and disadvantages. It took time to grow and purify the virus, and couple it. However, as CCMV is resistant to low pH, these viruses might be developed for mucosal immunizations such as oral, nasal or genital immunization, which is also the entry route of HIV. KLH is widely used as a carrier but the costs would be high if large amounts were needed.

When our synthetic peptides based on sequence from phage display libraries were coupled to a carrier they showed no reactivity with the mAb (data not shown). When it bound to the corresponding mAb, the free peptide acted as an antigenic mimic because it was flexible and could adopt a conformation that allowed binding to the selecting antibody. Coupling to a carrier, however, may favor different conformations of the same peptide, hence changing its properties

as mimotope. Thus, it may have lost its mimicry to the original antigen and would not be able to elicit cross-reacting antibodies or fail as an immunogenic mimic. Alternatively, the peptide may be an antigenic mimic without being a true structural mimic. Such a peptide would bind the selecting mAb in an entirely different way than does the original authentic epitope. In this case the peptide would be expected to elicit new antibodies that fit it in different ways than the original selecting mAb did.

The linear random peptide phage display library may not be the best source for screening epitopes, especially discontinuous epitopes. Since the length of peptide was so short (≈9 residues), it is difficult to generate enough structural diversity. Moreover, the conformation may have been flexible when one end was free, so the peptide could adopt a range of conformations that might fit the antibody binding sites when screened, but it may have adopt another conformation when linked to a carrier. Thus, the antigenic behavior of the peptides in the conjugates cannot be assumed to be the same as in that in phagotopes. Therefore, it is not unexpected that the antibodies from mice immunized with our peptide conjugates would not show specific reactivity to gp120.

Future Directions

Short peptides do not generally fold into a well-defined three-dimensional structure. However, constraints can be artificially imposed on the peptide in

order to reduce the range of conformations available to it. The most common constraint on displayed peptides is a disulfide bond between two cysteine residues at fixed positions in the sequence. A library of constrained peptides will represent fewer three-dimensional shapes than a library of unconstrained peptides, but those that bind might do so more strongly, because they would not have as large of a decrease in entropy upon binding and this could strengthen binding compared to unconstrained peptide. To address this problem we have started screening a constrained peptide library, which has 10 random residues between two cysteines that are linked by a disulfide bond. Phages from the constrained peptide phage displayed library were selected using Mabs F105, 5145A, and 1125H and sequenced. So far, there are some promising results. Phage clones selected by mAb 5145A and 1125H have consensus sequences and the phage compete with gp120 in binding for the original selecting mAb.

In order to present the peptide in the original conformation that was selected when it was in the context of the phage scaffold, the phage pIII protein bearing the selected peptide at its N-terminal end can be expressed. In this experiment, the DNA from the selected phage coding for the N-terminal domain (D1) including the flanking leader sequence is amplified by PCR, and cloned into an expression vector. The proteins will be expressed in *E.coli* and analyzed to determine whether the protein can bind the original selecting mAb. If so, the entire pIII domain with the peptide can be coupled to a carrier. If it still mimics

the original epitope, it should be expected that it would elicit antibodies like the original selecting mAb.

Additionally, the peptide bound to the original selecting mAb will be crystallized and its 3-D structure analyzed by X-ray crystallography. The information from the 3-D structure can help to design peptide derivative constrained in the proper conformations that mimic the actual true antigenic sites.

REFERECES CITED

1. Girard, M., Habel, A., and Chanel, C. (1999) New prospects for the development of a vaccine against human immunodeficiency virus type1: an overview. *C.R. Acad. Sci. Paris, scienes de la vie/ life science* 322, 959-966.

2. Pantaleo, G., Graziosi, C., and Fauci, A.S. (1993) New concepts in the immunopathogenesis of human immunodeficiency virus infection. *N. Eng. J. Med 328*, 1481-1485.

3. Koup, R.A., Safrit, J.T., Cao, Y., Andrews, C.A., McLeod, G., Borkowsky, W., Farthing, C., and Ho, D.D. (1994) Temporal association of cellular immune responses with the initial control of viremia in primary immunodeficiency virus type 1 syndrome. *J. Virol.* 68, 4650-4655.

4. Sinicco, A., Biglino, A., Sciandra, M., Forno, B., Pollono, A.M., Raiteri, R., and Gioannini, P. (1993) Cytokine network and acute primary HIV-1 infection. *AIDS* 7, 1167-1172.

5. Aukrust, P., Liabakk, N.B., Muller, F., Espevik, T., and Froland, S.S. (1995) Activation of tumor necrosis factor-alpha system in HIV-1 infection: association with markers of immune activation. *Infection* 23: 9-15.

6. Bass, H., Z., Nishanian, P., Hardy, W.D., Mitsuyasu, R.T., Esmail, E., Cumberland, W., and Fahey, J.L. (1992) Immune changes in HIV-1 infection: significant correlations and differences in serum markers and lymphoid phenotype antigens. *Clin. Immunol. Immunopathol.* 64, 63-70.

7. Mahalinggam, M., Peakman, E.T., Davies, E.T., Ozniak, A., McManus, T.J., and Vergani, D. (1993) T cell activation and disease severity in HIV infection. *Clin. Exp. Immunol.* 93, 337-343.

8. Lawn, S.D., Butera, S.T., and Folks, T.M. (2001) Contribution of immune activation to the pathogenesis and transmission of human immunodefiency virus type1 infection. *Clin. Micro. Rev.* 14, 753-777.

9. Bukrinsky, M.I., Stanwick, T.L., Dempsey, M.P., Stevenson, M. (1991) Quiescent T lymphocyte as an inducible virus reservoir in HIV-infection. *Science* 254, 423-427.

10. Levy, J.A. 1998. *HIV and the pathogenesis of AIDS*, Second Edition, ASM Press, Washington D.C.

11. Moore, J.P., Parren, P.W.H.I., and Burton, D.R. (2001) Minireview: Genetic subtypes, humoral immunity, and human immunodeficiency virus type 1 vaccine development. *J. Virol.* 75, 5721-5729.

12. Robenson, D.L., Anderson, J., Bradac, J., Carr, J., Foley, B., Funkhouser, R., Goa, F., Hann, B.H., Kalish, M.L., Kuiken, C., Learn, G.H., Leiter, T., McCutchan, F., Osmanov, S., Peters, M., Pieniazek, D., Salminen, M., Sharp, P. M., Wolinsky, S., and Korber, B. (2000) HIV-1 nomenclature proposal. *Science.* 288, 55-57.

13. McCutchan, F. E. (2000) Understanding the genetic diversity of HIV-1. *AIDS* 14(suppl. 3), S31-S44.

14. Gaschen, B., Taylor, J., Yusim, K., Foley, B., Goa, F., Lang, D., Novitsky, V., Haynes, B., Hahn, B.H., Bhattacharya, T., and Korber, B. (2002) Diversity considerations in HIV-1 vaccine selection. *Science*. 296, 2354-2360.

15. Blackard, J.T., Cohen, D.E., and Mayer, K.H. (2002) Human immunodefiecy virus superinfection and recombinations; current state of knowledge and potential clinical consequences. *Clin.Inf.Dis*. 34, 1108-1114.

16. Jetzt, A.E., Yu, H., Klarmann, G.J. (2000) High rate of recombination throughout the human immunodeficiency virus type 1 genome. *J. Virol.* 74, 1234-1240.

17. Allan, J., Lee, T.H., McLane, M.F., Sodroski, J., Haseltine, W., and Essex, M. (1983) Identification of the major envelope glycoprotein product of HTLV-III. *Science*. 228, 1322-1323.

18. Robey, W.G., Safai, B., Oroszlan, S., Arthur, L., Gonda, M., Gallo, R., and Fischinger, P.J.. (1985) Characterization of envelope and core structural gene products of HTLV-III with sera from AIDS patients. *Science*. 228, 593-595.

19. Souza,M.P.D.,Cairns,J.S, and Plaeger, S.F. (2000) Current evidence and future directions for targeting HIV entry. *JAMA*. 284, 215-221.

20. Follis, K.E., Larson, S.J., Liu, M., and Nunberg, J.H. (2002) Genetic evidence that interhelical packing interactions in the gp41 core are critical for transition of the human immunodeficiency virus type 1 envelope glycoprotein to the fusion-active state. *J. Virol.* 76, 7356-7362.

21. Wyatte, W., and Sodroski, J. (1998) The HIV-1 envelope glycoproteins: fusogens, antigens, and immunogens. *Science.* 280, 1884-1888.

22. Gelderblom, H. R., Hausmann, E. H, Ozel, M., Pauli, G., Koch, M. A. (1987) Fine structure of human immunodeficiency virus (HIV) and immunolocalization of structural proteins. *Virol.* 156, 171-176.

23. Ozel M., Pauli, G., and Gelderblom, H. R. (1987) The organization of the envelope projections on the surface of HIV. *Arch. Virol.* 100, 255-266.

24. Starcich, B. R., Hahn, B.H., Shaw, G.M., McNeely, P.D., Modrow, S., Wolf, H., Parks, E.S., Parks, W.P., Josephs, S.F., Gallo, R.C., and Wong-Staal, F. (1986) Identification and characterization of conserved and variable region in the envelope gene of the HTLV-III/LAV, the retrovirus of AIDS. *Cell.* 45, 637-648.

25. Thali, M., Furman, C., Ho, D.D., Robinson, J., Tilley, S., Pinter, A., and Sodroski, J. (1992) Discontinuous, conserved neutralization epitopes overlapping the CD4 binding region of the HIV-gp120envelope glycoprotein. *J. Virol.* 66, 5635-5641.

26. Janssens, W., Nkengasong, J., Heyndrickx, L., Auwera, G.V.D., Vereecken, K., Coppens, S., Willems, B., Beirnaert, E., Fransen, K., Peeters, M., and Groen, G.V.D. (1999) Intrapatient variability of HIV type 1 group O ANT70 during a 10-year follow-up. *AIDS Res. Hum. Retroviruses.* 15, 1325-1332.

27. Daniel, R.S., Smith, M.H., and Fisher, A.G. (1991) Molecular characterization of biologically diverse envelope variants of human immunodeficiency virus type 1 derived from an individual. *J. Virol.* 65, 5574-5578.

28. Kwong P.D., Wyatt, R., Robinson, J., Sweet, R. W, Sodroski, J., and Hendrickson, W. A. (1998) Structure of an HIV gp120 envelope glycoprotein in complex with the CD4 receptor and a neutralizing human antibody. *Nature.* 393, 648-659.

29. Rizzuto, C. D., Wyatt, R., Hernandez-Ramos, N., Sun, Y., Kwong, P. D., Hendrickson, W.A., and Sodroski, J (1998) A conserved HIV gp120 glycoprotein structure involved in chemokine receptor binding. *Science*. 280, 1949-1953.

30. Deng, H., Liu, R., Ellmeier, W., Choe, S., Unutmaz, D., Burkhart, M., Marzio, P.D., Marmon, S., Sutton, R.E., Hill, C.M., Dauis, C.B., Peiper, S.C., Schall, T.J., Littman, D.R., and Kandau, N.R. (1996) Identification of a major co-receptor for primary isolation of HIV-1. *Nature.* 381, 661-666.

31. Alkhatib, G., Combadiere, C., Broder, C.C., Feng, Y., Kennedy, P.E., Murphy, P.M., and Berger, E.A. (1996) CC CKR 5: Rantes, MIP-1α, MIP-1β receptor as a fusion coreceptor for macrophage-tropic HIV-1. *Science.* 272; 1955-1958.

32 Wu I, Gerard, N.P., Wyatt, R., Choe, H., Parolin, C., Ruffing, N., Borsetti, A., Cardoso, A.A., Desjardin, E., Newman, W., Gerard, C., and Sodroski, J. (1996) CD4-induced interaction of primary HIV-1 gp120 glycoproteins with the chemokine receptor CCR-5. *Nature.* 384,179-183.

33. Liu, R., Paxton, W.A., Choe, S., Ceradini, D., martin, S.R., Horuk, R., macDonald, M.E., Stuhlmann, H., Koup, R.A., and Landau, N.R. (1996). Homozygous defect in HIV-1 accounts for resistance of some multiple exposed individuals to HIV-1 infection. *Cell* . 86, 367-377.

34. Samson, M., Libert, F., Doranz, B.J., Rucker, J., Liesnard, C., Farber, C.M., Saragosti, S., Lapoumeroulie, C., Lognaux, J., Forceille, C., Muyldermans, G., Verhofstede, C., Burtonboy, G., Georges, M., Imai, T., Rana, S., Yi, Y., Smyth, R.J., Collman, R.G., Doms, R.W., Vassart, G., and Parmentier, M. (1996) Resistance to HIV-1 infection in Caucasian individuals bearing mutant alleles of the CCR5 chemokine receptors gene. *Nature.* 382, 722-725.

35. Dean M., Carrington, M., Huttley, G.A., Smith, M.W., Allikmets, R., Geodert, J.J., Buchbinder, S.P., Vittinghoff, E., Gomperts, E., Donfield, S., Vlahor, D., Kaslow, R., Saah, A., Rinaldo, C., and Detels, R. (1996) Genetics restriction of HIV-1 infection and progression to AIDS by a deletion allele of the *CKR5* structural gene. *Science*. 273, 1856-1862.

36. Berger, E.A. (1997) HIV entry and tropism: the chemokine receptor connection *AIDS* 11(suppl. A), S3-S16.

37. Bieniaaz, P.D., and Cullen B.R. (1998) Chemokine receptors and human deficiency virus infection. *Front. Biosci.* 3, 44-58.

38. Dragic, T, Trkola, A., and Morre, J.P. (1997) HIV co-receptors: gateways to the cell. *Adv. Res. Ther.* 7, 2-13.

39. Littman, D.R. (1998) Chemokine receptors: keys to AIDS pathogenesis. *Cell.* 93, 677-680.

40. Hung, C.S., Heyden, N.V.D., and Ratner, L. (1999) Analysis of the critical domain in the V3 loop of human immunodeficiency virus type 1 gp120 involved in CCR5 utilization. *J. Virol.* 73, 8216-8226.

41. Haynes, B.F., Pantaleo, G., and Fauci, A.S.. (1996) Toward an understanding of the correlates of protective immunity to HIV infection. *Science.* 271, 324-328.

42. Walker, C.M., Moody, D.J., Stites, D.P., and Levy, J.A. (1986). CD8+ lymphocytes can control HIV infection in vitro by suppressing virus replication. *Science.* 234, 1563-1566.

43. Koup, R.A., Safrit, J.T., Cao, Y., Andrews, C.A., Mcleod, G., Borkowsky, W., Farthing, C., and Ho, D.D. (1994). Temporal association of cellular immune responses with the initial control of viremia in primary human immunodeficiency virus type-1 syndrome. *J. Virol.* 68, 4650-4655.

44. Borrow, P., Lewicki, H., Hahn, B.H., Shaw, G.M., and Oldstone, M.B.A. (1994). Virus-specific CD8+ cytolytic-T-lymphocyte activity associated with control of viremis in primary human immunodeficiency virus type-1 infection. *J. Virol.* 68, 6103-6110.

45. Pantaleo, G., demarest, J.F., Soudeyns, H., Graziosi, C., Denis, F., Adelsberger, J.W., Borrow, P., Saag, M.S., Shaw, G.M., Sekaly, R.P., and Fauci, A.S. (1994). Major expansion of CD8+ T cells with a predominant Vβ usage during the primary immune response to HIV. *Nature.* 370, 463-467.

46. Ogg, G.S., Jin, X., Bonhoeffer, S., dunbar, P.R., Nowak, M.A., Monard, S., Segal, J.P., Cao, Y., Rowland-Jones, S.L., Carundolo, V., Hurley, A., Markowitz, M., Ho, D.D., Nixon, D.F., and McMichael, A.J.

(1998). Quantification of HIV-1 specific cytotoxic T lymphocytes and plasma load of viral RNA. *Science* 279, 2103-2106.

47. Letvin, N.L., Barouch, D.H., and Montefiori, D.C. (2002) Prospects for vaccine protection against HIV-1 infection and AIDS. *Annu. Rev. Immunol.* 20: 73-99.

48. Kaslow, R.A., Carrington, M., Apple, R., Park, L., Munoz, A., Saah, A.J., Blattner, W., Phair, J., Erlich, H., and Mann, D.L. (1996). Influence of combinations of human major histocompatibilitiy complex genes on the course of HIV-1 infection. *Natl. Med.* 2, 405-411.

49. Carrington, M., Nelson, G.W., Martin, M.P., Kissner, T., Vlahov, D., Goedertt, J.J., Kaslow, R., Buchbinder, S., Hoots, K., O'Briens. (1999). HLA and HIV-1: heterozygote advantage and B*35-CW*04 disadvantage. *Science*. 283, 1748-1752.

50. McMichael, A.J., and Phillips, R.E. (1997). Escape of human immunodeficiency virus from immune control. *Annu. Rev. Immunol.* 15, 271-296.

51. Collinsk, L., Chen, B.K., Kalams, S.A., Walker, B.D., and Battimore, D. (1998). *Nef* protein protects infected primary cells against killing by cytotoxic T lymphocytes. *Nature*. 391, 397-410.

52. Mascola, J.R., Lewis, M.G., Stiergler, G., Harris, D., Vancott, T.C., Hayes, D., Louder, M.K., Brown, C.R., Sapan, C.V., Frankel, S.S., Lu, Y., Robb, M.L., Katinger, H., and Bir, D.C. (1999). Protection of macaques against pathogenic simian/human immunodeficiency virus 89.6 PD by passive transfer of neutralizing antibodies. *J.Virol.* 73, 4009-4018.

53. Ferranteli, F., and Ruprecht, R. M. (2002) Neutralizing antibodies against HIV-back in the major leagues? *Curr.Opin Immuno*. 14, 495-502

54. Moore, J.P., Sattentau, Q.J., Wyatt, R, and Sodroski, J. (1994) Probing the structure of the human immunodeficiency virus surface glycoprotein gp120 with a panel of monoclonal antibodies. *J. Virol.* 68, 469-484.

55. Moore, J.P., and Sodroksi, J. (1996). Antibody cross-competitive analysis of the human immunodeficiency virus type 1 gp120 exterior envelope glycoprotein. *J. Virol.* 70, 1863-1872.

56. Parren, P.W.H.I., Sattentau Q.J., and Burton D.R. (1997). HIV-1 antibody-debris or virion? *Nat. Med.* 3, 366-367.

57. Wyatt, R., and Sodroski, J. (1998). The HIV-1 envelope glycoproteins: fusogens, antigens, and immunogens. *Science*. 280, 1884-1888.

58. Thali, M., Olshevsky, U., Furman, C., Gabuzda, D., Posner, M., and Sodroski, J. (1991). Characterization of a discontinuous human immunodeficiency type-1 gp120 epitope recognized by a broadly reactive neutralizing human monoclonal antibody. *J.Virol.* 65, 6188-6193.

59. Mckeating J., Thali, m., Furman, C., Karwowska, s., Gorny, M.K., Cordell, J., Zolla-Pazner, S., Sodroski, J., and Weiss, R.A. (1992). Amino acid residues of the human immunodeficiency virus type-1 gp120 critical for the binding of rat and human neutralizing antibodies that block the gp120-sCD4 interaction. *Virol.* 190, 134-142.

60. Beassley R.P., Hwang, L., Lee, G.C. (1983). Prevention of perinatally transmitted hepatitis B vaccine. *Lancet* i, 1099-1102

61. Gellin B.G., Greenberg, R.N., Hart, R.H., Bertino, J.S., Stein D.H., Deloria, M.A., Clements-Mann, M.L. (1997) Immunogenicity of two doses of yeast recombinant hepatitis B vaccine in healthy older adults. *J. Infect. Dis.* 175, 1494-1497.

62. Mascola, J. R., Snyder, S. W., Weislo, O.S., Belay, S.M., Belshe, R.B., Schwartz, D.H., Clements, M.L., Dolin, R., Graham, B.S., Gorse, G.J., Keefey, M.C., McElarath, M.J., Walker, K.F., McNeil, J.G., McCutchan, F.G., and Burke, D.S. (1996) Immunization with envelope subunit vaccine products elicits neutralizing antibodies against laboratory-adapted but not primary isolates of human immunodeficiency type 1. *J. Infect. Dis.* 173, 340-348.

63. Connor, B.S., Korber, B.T., Graham, B.S, Hahn, B.H., Ho, D.D., and Wolinsky, S.M. (1998) Immunological and virological analyses of persons infected by human immunodeficiency virus type 1 while participating in trials of recombinant gp120 subunit vaccines. *J. Virol.* 72, 1552-1576.

64. VanCott, T.C., Bethke, F.R., Burke, D.S., Redfield, R.R., and Birx, D.L. (1995) Lack of induction of antibodies specific for conserved, discontinuous epitopes of HIV-1 envelope glycoprotein by candidate AIDS vaccines. *J. Immunol.* 155, 4100-4110.

65. Binley, J.M., Sanders, R.W., Clads B, Schuelke, N., Master, a., Guo, Y., Kajumo, F., anselma, D.J., Maddon, P.J., Olson, W.C., and Moore, J.P. (2000) A recombinant human immunodeficiency virus type 1 envelope glycoprotein complex stabilized by an intermolecular disulfide bond between gp120 and gp41 subunits is an antigenic mimic of the trimeric virion-associated structure. *J. Virol.* 74, 627-643.

66. Reitter, J.M., Means, R.E., and Desrosiers, R.C. (1998) A role for carbohydrates in immune evasion in AIDS. *Nat. Med.* 4, 679-684.

67. Sander, R.W., Schiffner, L, Master, A, Kajumo, F., Guo, Y., Dragic, T., Moore, J.P., and Binley, J.M.. (2000) Variable, loop-deleted variants of the human immunodeficiency virus type 1 envelope glycoprotein can be stabilized by an intermolecular disulfide bond between the gp 120 and gp 41 subunits. *J. Virol.* 74, 5091-5100.

68. Fouts, T., Godfrey, K., Bobb, K., Montefiori, D., Hanson, C., Kalyanaraman, V.S, Devico, A., and Pa, R. I. (2002) Crosslinked HIV-1 envelope-CD4 receptor complexes elicit broadly cross-reactive neutralizing antibodies in rhesus macaques. *Proc.Natl.Acad.Sci USA*. 99, 11842-11847.

69. Hart, M.K., Palker, T.J., matthews, T.J., langlois, A.J., Lerche, N.W., Martin, M.E., Scearce, R.M., McDonal, C., Bolognesi, D.P., and Haynes, B.F. (1990) Synthetic peptides containing T and B cell epitopes from human immunodeficiency virus envelope gp 120 induce anti-HIV proliferative responses and high titers of neutralizing antibodies in rhesus monkeys. *J.Immunol.* 145, 2677-2685.

70. Lu, Y., Ding, J., Xiao, Y., Dierich, M.P., and Chen, Y.H. (2000) Multi-epitope-vaccines intensively increased levels of antibodies recognizing three neutralizing epitopes on HIV-1 envelope protein. *Scan.J.Immunol.* 51, 497-501.

71. Eckert, D.M., Malashkevish, V.N, Hong, L.H, Cow, P.A., and Kim, P.S. (1999) Inhibiting HIV-1 entry: discover of D-peptide inhibitors target the gp41 coiled-colied pocket. *Cell.* 99, 103-115.

72. Sia, S.K., Carr, P.A., Cochran, A. G., Vladimir, V. N., Malashkevich, N., and Kim, P.S. (2002) Short constrained peptides that inhibit HIV-1 entry. *Proc. Natl. acad. Sci USA.* 99, 14664-14669.

73. Chan, D. C., Fass, D., Berger, J.M., and Kim,P.S. (1997). Core structure of gp41 from the HIV envelope glycoprotein. *Cell.* 89, 263-273.

74. Weissenhorn, W., Dessen, A, Harrison, S.C., Skehel, J.J., and Wiley, D.C. (1997). Atomic structure of the ectodomain from HIV-1 gp41. *Nature*. 387, 426-430.

75. Tan, K., Liu, J., Wang, J., Shen, S., and Lu, M. (1997). Atomic structure of a thermostable subdomain of HIV-1 gp41. *Proc. Natl. Sci. USA*. 94, 12303-12308.

76. Chen, C.H., Mathews, J., McDanal, C.B., Bolognesi, D.P., and Greenberg, M.L. (1995). A molecular clasp in the human immunodeficiency virus (HIV) type 1 TM protein determines the anti-HIV activity of gp41 derivatives: implication for viral fusion. *J. Virol.* 69, 3771-3777.

77. Lu, M., Blacklow, S.C., and Kim, P.S. (1995) A trimeric structural domain of the HIV-1 transmembrane glycoprotein. *Nat. struc. Biol.* 2, 1975-1082.

78. Wild, C., Oas, T., Mcdanal, C., Bolognesi, D., and Matthews, T. (1992) a synthetic peptide inhibitor of human immunodeficiency virus replication: correlation between solution structure and viral inhibition. *Proc. Natl. Acad.Sci.* 89, 10537-10541.

79. Bewley, C. A., Louis, J.M., Ghirlando, R., and Clore, G.M. (2002) Design of a novel peptide inhibitor of HIV fusion that disrupts the internal trimeric coiled-coil of gp41. *J.Biol.Chem.* 277, 14238-14245.

80. Excler, J. L., and Plotkin, S.A. (1997) The prime boost concept applied to HIV preventive vaccines. *AIDS* 11 (suppl. A) S127-S137.

81. Sattentau, Q.J., Moulard, M., Brivet, B., Botto, F., Guillemot, J.C., Mondor, I., Poignard, P., and Ugolini, S. (1999) Antibody neutralization of HIV-1 and the potential for vaccine design. *Immuno. Lett.* 66, 143-149.

82. Beddows, S., Louisirirochanakul, S., Cheingson-Popov, R., Easter-brook, P.J., Simmonds, P., and Weber, J.. (1998) Neutralization of primary isolate and T-cell line adapted isolates of human immunodeficiency virus type 1: Role of V3-specific antibodies. *J. Gen. Virol.* 79, 77-82.

83. Wyat, R., Kwong, P.D., Desjardins, E., Sweet, R.W., Robinson, J., Hendrickson, W.A., and Sodroski, J. (1998) The antigenic structure of the HIV gp120 envelope glycoprotein. *Nature*. 393, 705-711.

84. Brand, D., Lemiale, F., Thibault, G., Verrier, B., Lebigot, S., Roingeard, P., Buzelay, L., Brunet, S, and Barin, F. (2000) Antigenic properties of recombinant envelope glycoproteins derived from T-cell-line-adapted isolates or primary human immunodeficiency virus isolates and their relationship to immunogenicity. *Virol.* 271, 350-362.

85. Buratii, E., Tisminetzky, S.G., Scodeller, E.S., and Baralle, F.E.. (1996) Conformational display of two neutralizing epitopes of HIV-1 V3 loop sequence and induces neutralizing antibodies. *Vaccine* 13, 1233-1239.

86. Scodeller, E.A., Tisminetzky, S.G., Porro, F., Schiappacassi, M., De Rossi, A., Chiecco-Bianchi, L. and Baralle, F.E.. (1995) A new epitope presenting system displays a HIV-1 V3 loop sequence and induces neutralizing antibodies. *Vaccine* 13, 1233-1239.

87. Haynes, J., Cunniungham J., Seefried,V, Lennick M, Garvin R, Shen S. (1986) Development of a genetically engineered, candidate polio vaccine employing the self-assembling properties of the tobacco mosaic virus coat protein. *Biotechnology* 4, 637-41.

88. Turpin, T.H., Reini, S.J., Charoenvit, Y., Hoffman, S.L., Fallarme, V., Grill, L.K.. (1995) Maralial epitopes expressed on the surface of a recombinant tobacco mosaic virus. *Bio/Technology* 13, 53-57.

89. Jagadish M., Edwards S., Handen M., Grusivin J., Vandenberg K. (1996) Chimeric potyvirus-like particles as vaccine carriers. *Intervirol* 39, 85-92.

90. Jagadish, M., Hamilton R., Fernandez C., Schoofd P., Davern K. (1993) High level production of hybrid potyvirus-like carrying repetitive copies of foreign antigens in *Escherichia coli*. *Biotechnology* 11, 1166-70.

91. Carla, M., Rizza, P., Lattanzi, L., Mancini, C., Spada, M., Belardelli, F., Benvenuto, E., and Capone, I. (2001) Chimeric plant virus particles as immunogens for inducing murine and human immune responses against human immunodeficiency virus type 1. *J. Virol.* 75, 8434-8439.

92. Yusibov, V., Hooper, D.C., Spitsin, S.V., Fleysh, N., Kean, R.B., Mikheeva, T., Deka, D., Karasev, A., Cox, S., Randall, J., and Koprowski, H.. (2002) Expression in plants and immunogenicity of plant virus-based experimental rabies vaccine. *Vaccine* 20, 3155-3164.

93. Brennan, F.R., Bellaby, T., Helliwell, S.M., Jones, T.D., Kamstrup, S., Dalsgaard, K., Flock, J.I., and Hamilton, W.D. (1999) Chimeric plant virus particles administrated nasally or orally induce systemic and mucosal immune responses in mice. *J. Virol.* 73, 930-938.

94. Mason, H. S., Hag, T.A., Clements, J.D., and Arntzen, C J. (1998) Edible vaccine protects mice against *Escherichia coli* heat-labile enterotoxin (LT): potatoes expressing a synthetic LT-B gene. *Vaccine* 16, 1336-1343.

95. Lehner, T., Bergmeir, L., Wang, Y., Toa, L., and Mitchell E. (1999) a rationale basis for musocal vaccination against HIV infection. *Immunol Rev* 170. 183-196.

96. Allison, R.F., Janda, M., and Ahlquist, P. (1988). Infectious in vitro transcripts from cowpea chlorotic mottle virus cDNA clones and exchange of individual RNA components with brome mosaic virus. *J. Virol.* 62: 3581-3588.

97. Fox, J.M., Wang, G., Speir, J.A., Olson, N.H., Johnson, J.E., Baker, T.S., and Young, M.J. (1998). Comparison of the native CCMV virion with *in vitro* assembled CCMV virions by cryoelectron microscopy and image reconstruction. *Virol* 244, 212-218.

98. Loesch-Fries, L.S., and Hall, T.C. (1980). Synthesis, accumulation, and encapsidation of individual brome mosaic virus RNA components in barely protoplasts. *J. Gen. Virol.* 47, 323-332.

99. Lane, L.C. (1974). The bromoviruss. *Adv. Virus Res.* 19, 151-220.

100. Dasgupla, R., and Kaesberg, P. (1982). Complete nucleotide sequences of coat protein messenger RNAs of bromo mosaic virus and cowpea chlorotic mottle virus. *Nucl. Acids Res.* 10, 703-713.

101. Steven, A.C., Smith, P. R., and Horne, R.W. (1978). Capsid fine structure of cowpea chlorotic mottle virus: From a computer analysis of negatively strained virus arrays. *J. Ultrastruct. Res.* 64, 63-73.

102. Speir, J.A., Munshi, S., Wang, G., Baker, T.S., and Fohnson, J.E. (1995) Structures of the native and swollen forms of cowpea chlorotic mottle virus determined by X-ray crystallography and cryo-electron microscope. *Structure*. 3:1-15.

103. Fox, J.M., Zhoa, X., Speir, J.A., and Young, M.J. (1996) Analysis of a salt stable mutant of cowpea chlorotic mottle virus. *Virol.* 222, 115-122.

104. Zhao, X., Fox, J.M., Olson, N.H., baker, T.S., and Young, M.J. (1995) In vitro assembly chlorotic mottle virus from coat protein expressed in *Escherichia coli* and in vitro-transcribed viral cDNA. *Virol.* 207, 486-494.

105. Johnson, J., Lin, T., and Lomonossoff, G. (1997). Presentation of heterologous peptides on plant viruses: genetics, structure, and function. *Annu. Rev. Phytopathol.* 35, 67-86.

106. Chen, Z., Staufacher, C., and Johnson,J.. (1990) Capsid structure and RNA packing in comovirus. *Semin. Virol.* 1, 453-466.

107. Lomonossoff, G.P., and Johnson, J.E. (1995). Viral expression systems for peptides. *Semin Virol.* 6, 257-267.

108. Usha, R., Rohill, J.B., Spall, V.E., Shanks, M., Maule, A.J., Johnson, J.E., and Lomonossoff, G.P. (1993) Expression of an animal virus antigenic site on the surface of a plant virus particle. *Virol.* 197, 366-374.

109. Porta, C., Spall, V.E., Loveland, J., Johnson, J.E., Barker, P.J., and Lomonossoff, G.P. (1994). Development of cowpea mosaic virus as a high-yielding system for the presentation of foreign peptides. *Virol.* 202, 949-955.

110. Brennan, F.R., Jones, T.D., Longstaff, M., Chapman, S., Bellaby, T., Smith, H., Xu, F., Hamilton, W.D.O., and Flock, J.I. (1999). Immunogenicity of peptides derived from a fibronectin-binding protein of *S. aureus* expressed on two different –plant viruses. *Vaccine* 17, 1846-1857.

111. Manufacturer's instructions for the "EasySelect™ *Pichia* Expression Kit" (Invitrogen)

112. Pierce catalogue, page 297, BMH, product number 22330.

113. Pierce catalogue, page 322, SPDP, product number 21857.

114. Pierce cataloque, page 329, sulfo-SMCC, product number 22322

115. Sambrook, J., Fritsch, E.F., and Maniatis, T. (1989). "Molecular cloning: a laboratory manual," 2nd ed. Cold spring habor Laboratory Press, Cold spring harbor.

116. Linder, S., Schliwa, M., and Kube-Granderath, E. (1996). Direct PCR screening of *Pichia pastoris* clones. *BioTechniques* 20, 980-982.

117. Harlow, E. and Lane,D. (1988). Antibodies: a laboratory manual. Cold Spring Habor Laboratory Press, Cold spring harbor.

118. Wang, Q., Kaltgrad, E., Lin, T., Johnson, J.E., and Finn, M.G. (2002) Natural supramolecular building blocks: wild-type cowpea mosaic virus. *Chem. Biol.* 9, 805-811.

119. Czerkinsky, C., Anjuere, F., McGhee, J.R., George-Chandy, A., Holmgren, J., Kieny, M.P., Fujiyashi, K., Mestecky, J.F., Pierrefite-Carle, V., Rask, C., and Sun, J.B. (1999) Mucosal immunity and tolerance: relevance to vaccine development. *Immunol Rev.* 170, 197-222.

120. Meola, A., Delmastro, P., Monaci, P., Luzzago, A., Nicosai, A., Felici, F., Cortese, and Galfre, G. (1995) Derivation of vaccines from mimotopes. *J.Immunol.* 154, 3162-3172.

MONTANA STATE UNIVERSITY - BOZEMAN
3 1762 10391955 9